International Journal on Advances in Systems and Measurements

2023 vol. 16 nr. 3&4

The *International Journal on Advances in Systems and Measurements* is published by IARIA.
ISSN: 1942-261x
journals site: http://www.iariajournals.org
contact: petre@iaria.org

Sponsored by IARIA
www.iaria.org

International Journal on Advances in Systems and Measurements
Volume 16, Number 3 & 4, 2023

Jaime Calvo-Gallego, University of Salamanca, Spain
Maria-Dolores Cano Baños, Universidad Politécnica de Cartagena,Spain
Juan-Vicente Capella-Hernández, Universitat Politècnica de València, Spain
Vítor Carvalho, Minho University & IPCA, Portugal
Irinela Chilibon, National Institute of Research and Development for Optoelectronics, Romania
Soolyeon Cho, North Carolina State University, USA
Hugo Coll Ferri, Polytechnic University of Valencia, Spain
Denis Collange, Orange Labs, France
Noelia Correia, Universidade do Algarve, Portugal
Pierre-Jean Cottinet, INSA de Lyon - LGEF, France
Paulo Estevao Cruvinel, Embrapa Instrumentation Centre - São Carlos, Brazil
Marc Daumas, University of Perpignan, France
Jianguo Ding, University of Luxembourg, Luxembourg
António Dourado, University of Coimbra, Portugal
Daniela Dragomirescu, LAAS-CNRS / University of Toulouse, France
Matthew Dunlop, Virginia Tech, USA
Mohamed Eltoweissy, Pacific Northwest National Laboratory / Virginia Tech, USA
Paulo Felisberto, LARSyS, University of Algarve, Portugal
Javad Foroughi, University of Wollongong, Australia
Miguel Franklin de Castro, Federal University of Ceará, Brazil
Mounir Gaidi, Centre de Recherches et des Technologies de l'Energie (CRTEn), Tunisie
Eva Gescheidtova, Brno University of Technology, Czech Republic
Tejas R. Gandhi, Virtua Health-Marlton, USA
Teodor Ghetiu, University of York, UK
Franca Giannini, IMATI - Consiglio Nazionale delle Ricerche - Genova, Italy
Gonçalo Gomes, Nokia Siemens Networks, Portugal
Luis Gomes, Universidade Nova Lisboa, Portugal
Antonio Luis Gomes Valente, University of Trás-os-Montes and Alto Douro, Portugal
Genady Grabarnik,CUNY - New York, USA
Stefanos Gritzalis, University of the Aegean, Greece
Richard Gunstone, Bournemouth University, UK
Jianlin Guo, Mitsubishi Electric Research Laboratories, USA
Mohammad Hammoudeh, Manchester Metropolitan University, UK
Petr Hanáček, Brno University of Technology, Czech Republic
Go Hasegawa, Osaka University, Japan
Henning Heuer, Fraunhofer Institut Zerstörungsfreie Prüfverfahren (FhG-IZFP-D), Germany
Paloma R. Horche, Universidad Politécnica de Madrid, Spain
Vincent Huang, Ericsson Research, Sweden
Friedrich Hülsmann, Gottfried Wilhelm Leibniz Bibliothek - Hannover, Germany
Travis Humble, Oak Ridge National Laboratory, USA
Florentin Ipate, University of Pitesti, Romania
Imad Jawhar, United Arab Emirates University, UAE
Terje Jensen, Telenor Group Industrial Development, Norway
Liudi Jiang, University of Southampton, UK
Kenneth B. Kent, University of New Brunswick, Canada
Fotis Kerasiotis, University of Patras, Greece

Andrei Khrennikov, Linnaeus University, Sweden
Alexander Klaus, Fraunhofer Institute for Experimental Software Engineering (IESE), Germany
Andrew Kusiak, The University of Iowa, USA
Vladimir Laukhin, Institució Catalana de Recerca i Estudis Avançats (ICREA) / Institut de Ciencia de Materials de Barcelona (ICMAB-CSIC), Spain
Kevin Lee, Murdoch University, Australia
Wolfgang Leister, Norsk Regnesentral (Norwegian Computing Center), Norway
Andreas Löf, University of Waikato, New Zealand
Jerzy P. Lukaszewicz, Nicholas Copernicus University - Torun, Poland
Zoubir Mammeri, IRIT - Paul Sabatier University - Toulouse, France
Sathiamoorthy Manoharan, University of Auckland, New Zealand
Stefano Mariani, Politecnico di Milano, Italy
Paulo Martins Pedro, Chaminade University, USA / Unicamp, Brazil
Don McNickle, University of Canterbury, New Zealand
Mahmoud Meribout, The Petroleum Institute - Abu Dhabi, UAE
Luca Mesin, Politecnico di Torino, Italy
Marco Mevius, HTWG Konstanz, Germany
Marek Miskowicz, AGH University of Science and Technology, Poland
Jean-Henry Morin, University of Geneva, Switzerland
Fabrice Mourlin, Paris 12th University, France
Adrian Muscat, University of Malta, Malta
Arnaldo S. R. Oliveira, Universidade de Aveiro-DETI / Instituto de Telecomunicações, Portugal
Aida Omerovic, SINTEF ICT, Norway
Victor Ovchinnikov, Aalto University, Finland
Telhat Özdoğan, Amasya University - Amasya, Turkey
Gurkan Ozhan, Middle East Technical University, Turkey
Constantin Paleologu, University Politehnica of Bucharest, Romania
Matteo G A Paris, Universita` degli Studi di Milano,Italy
Vittorio M.N. Passaro, Politecnico di Bari, Italy
Giuseppe Patanè, CNR-IMATI, Italy
Marek Penhaker, VSB- Technical University of Ostrava, Czech Republic
Juho Perälä, Bitfactor Oy, Finland
Florian Pinel, T.J.Watson Research Center, IBM, USA
Ana-Catalina Plesa, German Aerospace Center, Germany
Miodrag Potkonjak, University of California - Los Angeles, USA
Alessandro Pozzebon, University of Siena, Italy
Vladimir Privman, Clarkson University, USA
Mohammed Rajabali Nejad, Universiteit Twente, the Netherlands
Konandur Rajanna, Indian Institute of Science, India
Nageswara Rao, Oak Ridge National Laboratory, USA
Stefan Rass, Universität Klagenfurt, Austria
Candid Reig, University of Valencia, Spain
Teresa Restivo, University of Porto, Portugal
Leon Reznik, Rochester Institute of Technology, USA
Gerasimos Rigatos, Harper-Adams University College, UK
Luis Roa Oppliger, Universidad de Concepción, Chile

Ivan Rodero, Rutgers University - Piscataway, USA
Lorenzo Rubio Arjona, Universitat Politècnica de València, Spain
Claus-Peter Rückemann, Universität Münster / DIMF / Leibniz Universität Hannover, Germany
Subhash Saini, NASA, USA
Mikko Sallinen, University of Oulu, Finland
Christian Schanes, Vienna University of Technology, Austria
Cristina Seceleanu, Mälardalen University, Sweden
Guodong Shao, National Institute of Standards and Technology (NIST), USA
Dongwan Shin, New Mexico Tech, USA
Larisa Shwartz, T.J. Watson Research Center, IBM, USA
Simone Silvestri, University of Rome "La Sapienza", Italy
Diglio A. Simoni, RTI International, USA
Radosveta Sokullu, Ege University, Turkey
Junho Song, Sunnybrook Health Science Centre - Toronto, Canada
Leonel Sousa, INESC-ID/IST, TU-Lisbon, Portugal
Arvind K. Srivastav, NanoSonix Inc., USA
Grigore Stamatescu, University Politehnica of Bucharest, Romania
Raluca-Ioana Stefan-van Staden, National Institute of Research for Electrochemistry and Condensed Matter, Romania
Pavel Šteffan, Brno University of Technology, Czech Republic
Chelakara S. Subramanian, Florida Institute of Technology, USA
Sofiene Tahar, Concordia University, Canada
Muhammad Tariq, Waseda University, Japan
Roald Taymanov, D.I.Mendeleyev Institute for Metrology, St.Petersburg, Russia
Francesco Tiezzi, IMT Institute for Advanced Studies Lucca, Italy
Wilfried Uhring, University of Strasbourg // CNRS, France
Guillaume Valadon, French Network and Information and Security Agency, France
Eloisa Vargiu, Barcelona Digital - Barcelona, Spain
Miroslav Velev, Aries Design Automation, USA
Dario Vieira, EFREI, France
Stephen White, University of Huddersfield, UK
Shengnan Wu, American Airlines, USA
Qingsong Xu, University of Macau, Macau, China
Xiaodong Xu, Beijing University of Posts & Telecommunications, China
Ravi M. Yadahalli, PES Institute of Technology and Management, India
Yanyan (Linda) Yang, University of Portsmouth, UK
Shigeru Yamashita, Ritsumeikan University, Japan
Patrick Meumeu Yomsi, INRIA Nancy-Grand Est, France
Alberto Yúfera, Centro Nacional de Microelectronica (CNM-CSIC) - Sevilla, Spain
Sergey Y. Yurish, IFSA, Spain
David Zammit-Mangion, University of Malta, Malta
Guigen Zhang, Clemson University, USA
Weiping Zhang, Shanghai Jiao Tong University, P. R. China

International Journal on Advances in Systems and Measurements
Volume 16, Numbers 3 & 4, 2023

CONTENTS

The Social Accumulator as a Concept to Manage Social Energy in the Age of Digital Transformation

An Explanation Model for Digital Interaction among Human Actors

Karsten Böhm
FH Kufstein Tirol – University of Applied Sciences
Kufstein, Austria
e-mail: karsten.boehm@fh-kufstein.ac.at

Jürgen Sammet, Joel Schmidt
HAM – University of Applied Management
Ismaning, Germany
e-mail: {juergen.sammet|joel.schmidt}@fham.de

***Abstract*—The increasing intensity of digital supported interaction and communication stimulated by the COVID19 pandemic over a period of roughly two years has changed the perception and experiences with those new forms of interaction by human actors. While not being completely new, the massive use of the technologies made a difference for the users that lead to different socio-technical effects. As a result, the concept of the Social Accumulator (SOAC) is introduced in this paper and related to known concepts like Social Energy. It builds on the experiences from the intensified digital interactions both in academia and business life and should serve as an explanation model for the effects of digital interaction that is easy to understand and to apply. The SOAC should help to understand the processes of Knowledge Creation and Knowledge Sharing when being driven by digital tools, which becomes increasingly important in a world that transforms education and businesses towards a highly digitized world.**

Keywords—Digital Transformation; Social Interaction; Social Energy; Higher Education; Digital Interaction; CSCW; Communication; Collaboration.

I. INTRODUCTION

In recent years, digitization and digital transformation of the economy and society have emerged as central topics. Furthermore, the global COVID-19 pandemic has acted as a catalyst for rapid digital transformation in many economies. Austria and Germany witnessed a significant real-world application of fully digital work experiences during this period, representing a large-scale implementation. In contrast, countries such as Sweden, Denmark, and Estonia had already gained extensive experience with digital transformation on a broad scale. These varied experiences underscore the need for support in navigating digital shifts and the lack of simple, effective frameworks for understanding the effects of digital transformation on cognition and social interaction.

This paper builds on Böhm's [1] contribution at the 2022 eKNOW conference held in Porto, Portugal, making several valuable contributions extending the original content: 1) an expanded time-frame including 2023 promotes a shift of focus to post-pandemic conditions reflecting the current movement of organizations to use digitally supported communication; 2) an increased depth and breadth of theoretical foundations, as the SOAC concept is embedded within the theory of social energy, providing new insights and understanding of relationships between these two concepts; 3) an extension of potential applications of the SOAC concept in three areas.

In terms of knowledge management, the pandemic situation offers a unique context for the use of information technology in developing knowledge intensive businesses and activities. Much can be gained by reflecting on experiences during the pandemic from the perspective of knowledge management considering the interactions among human users (mostly) using digital channels.

Initially, during early stages of the pandemic the technical challenges dominating the agendas of businesses, organizations and academia included improvement of infrastructure, availability of software systems and the development of necessary skills. Yet surprisingly, the challenges that were at first considered major barriers to technology adoption within the knowledge management community were resolved rather quickly. For example, collaboration challenges in the digital world were solved with new tools and strategies, which gained almost immediate acceptance, becoming the "new normal" of online interaction. As the duration of the pandemic extended into the second year, it became increasingly apparent that the new mode of digital interaction had unique properties resulting in both advantages and disadvantages. Advantages included the ability to establish immediate connections between colleagues and peers; communication and collaboration between individuals and groups of all sizes was facilitated by a wide range of useful tools that were developed on demand as new needs, requirements and features were identified. Geographic distance and location were no longer impediments, meaning frustrations with travel times were non-existent. The transition from paper to digital in office settings became a reality, and its implementation lead to easier and more efficient ways of knowledge sharing among office staff. Disadvantages included the difficulties in differentiation between working time and free time as boundaries became much more blurred; the significant increase in frequency and duration of digital meetings; and the shrinking availability of time slots for concentrated work. Despite massive use of digital communication tools, the individual feelings of loneliness and isolation increased, as informal conversation or communication became more difficult or simply did not occur. This has hindered informal knowledge exchange and will

continue to have a negative impact on human health and well-being. The long-term negative effects led to a unique form of tiredness and exhaustion, which became known as “Zoom fatigue” [2]. Recent research has validated this effect in a study carried out in Germany [3].

Channel reduction theory (from the German "Kanalreduktionstheorie") [4] assumes that remote communication generally has deficits. Recent studies identify a shift in relationships between communication partners. At the same time, new phenomenon starts to emerge: 1) Intimacy between communication partners can be even higher in an online setting, because the situation leads to a higher readiness of self-revelation (phenomenon: “talking to a stranger”); and 2) digital settings often focus only on the factual level. These new developments are positively received as communication is more efficient and less status oriented, referring to the disentrainment hyperpersonal model of computer mediated communication [5].

Based on the situation described above, “this rapid and large-scale switch from in-person to remote interactions”, had already been identified in the literature as remote living or “Telelife” [6], which emphasizes that people will collaborate more remotely. Given these observations, it is clear that the massive application of technology mediated communication and collaboration does not only have benefits and positive effects, but also drawbacks – which is to be expected in massive use of any technology. Therefore, the right balance between digital interaction and direct interaction of human actors is of critical importance and warrants more in-depth exploration and consideration.

Direct interaction between human and digital interaction, in which technical means are used for the communication (e.g., a phone call, a chat or a video conference call) are perceived differently in terms of richness and cognitive load, as well as towards trust building and perceived interactivity. As this might simply be due to the fact that the channels are less rich [7], [8], both channels will be included in this current analysis. In essence, most users perceive direct interactions as more attractive and easier to use than digital interactions. This became increasingly clear during the COVID19-pandemic with the switch to solely digital interaction for an extended period of time. With this understanding in mind, it is important to address the questions of when and how: When to use each channel? How to more effectively interweave the two channels?

This paper introduces the concept of the Social Accumulator (SOAC) as an explanation model for the digital interaction of human actors, focusing on both positive and negative effects of computer supported collaborative work (CSCW). By emphasizing different factors in a simple conceptual model, the SOAC supports the interweaving of digital and in-person channels during communication and collaboration activities.

The paper is structured as follows: Section II provides an overview of the concepts of social energy; Section III introduces the concept of SOAC; Section IV provides an illustration of positive and negative characteristics effecting the SOAC of human actors; Section V presents application areas of the model, including challenges for implementation. The paper concludes in Section VI with a summary and an outlook for future research.

II. Social Energy

The concept of energy is a crucial element in understanding psychological well-being, yet there is no standard definition of energy in the body of relevant literature. According to Lavrusheva [9] it is often linked with vitality, vigor, and overall well-being. Lavrusheva has identified five characteristics of vitality, which are also applicable to the energy concept. First, vitality is subjective, reflecting the feeling of aliveness and energy of an individual. Therefore, assessing energetic or vital states depends on self-reported evaluations, resulting in various interpretations. Second, vitality is deeply tied to positivity, involving a positive sensation of energy [10]. This means that energy is frequently associated with positive experiences. Third, vitality is in an ongoing state of fluctuation, as it becomes depleted and replenished, which encourages comparison to a renewable resource [11], [12]. Fourth, vitality can be regulated and managed by individuals, which can assist in dealing effectively with life's challenges and improving performance at work [13]. Fifth, vitality includes both physical and psychological aspects, underscoring its comprehensive nature [9].

Klijn and colleagues [14] have also outlined four dimensions of “personal energy”, namely physical, emotional, mental and spiritual. The *physical* dimension pertains to nutrition, exercise, sleep, and overall physical health. *Emotional* energy involves positive emotions and the avoidance of negative emotions, contributing to feeling “energized”. The *mental* energy dimension emphasizes cognitive focus and maintaining a peaceful mind, similar to Csiksentmihalyi's flow [15]. Lastly, *spiritual* energy relates to beliefs and personal values, where feelings of meaningfulness lead to an energized state.

Among the various theoretical frameworks that have been applied to the study of vitality, self-determination theory (SDT) is one that is most commonly [9]. Developed by Deci and Ryan in the early 1970s [10], SDT argues that individuals have inherent psychological needs for autonomy, competence, and relatedness. As explained by Ryan and Frederick [10], when these needs are fulfilled, individuals experience an increase in vitality. Autonomy involves a sense of self-directed behavior and volition, leading to greater satisfaction, intrinsic motivation, and authenticity. Competence refers to the desire for skill development, aligning with personal values and interests, fostering a sense of achievement and self-efficacy. And finally, relatedness emphasizes the importance of social connections and a sense of belonging, fulfilling the inherent need for meaningful relationships and emotional support.

In conclusion, the exploration of "energy" and "vitality" in psychological well-being reveals the multi-dimensional nature of these constructs and their interplay with individual and social factors. An aspect that is particularly interesting from the standpoint of social energy is the need for relatedness.

Social interactions have long been recognized as energy-consuming processes, as posited in the communicate bond, belong (CBB) theory, which is based on human energy management (HEM) [16]. HEM is guided by two principles: energy conservation (where individuals seek to minimize energy expenditure) and energy investment (where individuals invest energy to achieve valued goals, often with the intention of conserving energy in the long run) [17]. One of the valued goals in energy investment is the "need to belong" [18], which drives individuals to invest social energy in interactions to fulfill the desire for connection and avoid disconnection, ultimately resulting in feeling energized.

One current definition of *social energy*, is put forward by Hall and Merolla who define it "as the behavioral, perceptual, emotional, and cognitive tasks required for engaging in social interactions" [19], where the level of social energy plays a significant role in determining the outcomes of these interactions. Both connecting and disconnecting socially demand substantial energy expenditures [20]. Interestingly, research has shown that individuals who feel more connected after a social interaction are more likely to seek solitude later in the same day, suggesting a need for energy recovery [20]. It has also been shown that repeated social interactions lead to the investment of more energy in relationships, resulting in reduced energy requirements during future interactions [21]. These findings support the CBB model as it maintains that energy recovery takes place during periods of solitude.

Various factors influence the level of social energy expended during interactions. Topics of communication, personal interests, and characteristics of conversation partners all play a crucial role [20]. Interaction length also affects energy expenditure.

In a separate study, Hall et al. investigated which communication media is most suitable to satisfy the need to belong [22]. Face-to-face interactions were found to have a primacy for promoting connection and avoiding disconnection. However, the results for video-calls were inconclusive, with mixed evidence for their ability to foster connecting and avoid disconnecting.

In conclusion, the SOAC model, especially its focus on the need for relatedness, provides valuable insights into human energy management during social interactions. Understanding the dynamics of energy expenditure and recovery in social settings contributes to a deeper understanding of human behavior and well-being.

As noted, the medium in which interaction occurs plays a significant role in determining the amount of social energy that must be expended to satisfy the need to belong (CBB) or the need for relatedness (SDT). The COVID-19 pandemic has popularized videoconferencing in unprecedented ways (both in terms of frequency of use and length of use). At the same time, there are indications that videoconferencing can be exhausting and often results in the opposite of feeling energized, culminating in the phenomenon of "Zoom fatigue". Shockley et al. [23] determined that one major cause of fatigue lies in the way individuals present themselves through the camera. Self-presentation is fundamental to any form of interaction [24] as individuals strive to appear in a positive light. Self-presentation requires a high level of self-regulation and monitoring. Thus, it is an activity that consumes energy. When a person sees their own image on the screen, it leads to an increased use of self-evaluation [25]. Simultaneously, uncertainty grows, as only a small video clip is visible. Users continuously receive non-verbal cues that are incomprehensible due to the limited video frame. Perception of the images is only possible in 2D, and the other three senses are not directly engaged. Furthermore, reciprocal eye contact is not possible, affecting perception [26]. This results in uncertainty along with further increased use of self-monitoring [27]. The use of the camera is tiring, but Bennett et al. [28] describe various ways to reduce this fatigue or even reverse it. Indeed, their research asserts that video conferencing can be a good way to satisfy the need to belong. Bennett and colleagues identified seven recommendations for reducing fatigue and increasing energy:

1. Holding meetings earlier in the day can help to reduce fatigue, since they would be scheduled when employees are generally less tired, according to Hülsheger et al. [29]. Consequently, meetings as emotionally charged events [30] could even have a positive impact on the energy curve of the day [30].
2. Enhancing group cohesion helps to reduce fatigue by making participants feel more connected with each other and increasing interest in participating in meetings, thereby minimizing attention-demanding efforts and associated fatigue, as shown by Kaplan and Berman [31].
3. Muting the microphone during a meeting when not speaking can help to reduce attention and thereby fatigue, as proposed by Kaplan [32], since it minimizes distractions from background noise, lowering the mental effort required to maintain a quiet environment during the meeting.
4. Turning the video camera on during a meeting can affect the sense of group belonging, as it helps a person to feel more connected with the other participants, which could reduce fatigue.
5. Turning the video camera off during a meeting helps to reduce the number of visual stimuli on the screen, which could decrease fatigue. With the video camera turned off it helps a person to spend less time worrying about their appearance or what is happening in the background while enhancing the sense of group belonging.
6. Breaks during and between video conferences are an effective way to reduce fatigue, according to Kaplan

[32]. These breaks provide participants with the opportunity to mentally disengage and switch off, which is of critical importance when there are no natural breaks occurring between meetings.

7. Establishing group norms can reduce fatigue, as they eliminate uncertainties about acceptable behavior, thereby reducing the mental effort required by participants [32], [33]. Additionally, strong norms could enhance the sense of group belonging, helping to increase interest and participation in meetings, which could further reduce fatigue.

To summarize, it can be concluded that the concept of social energy is a broadly researched topic that has gained new attention within the context of the pandemic situation and the massive use of digital communication channels, and has had a lasting impact on the way people communicate and collaborate with each other in both enterprise settings and educational settings. The ideas presented in this paper provide insight into the current evolution of the workplace of the future (often referred to as "New Work") that is only just beginning. This evolution will be driven by (positive) social energy as it achieves an interactive and long-lasting change process [34]. An explanation model that makes the changes brought about by social energy more visible, would be a valuable contribution to this context of evolution and change.

III. THE CONCEPT OF THE SOCIAL ACCUMULATOR

The main contribution of this paper is the concept of the SOAC, which serves as an *explanation model for the characteristics of (intensified) digital interaction*. The authors perceive a need for deeper understanding of the positive and negative effects of digital interaction in a simplified form in order to plan, facilitate and execute digital communication and other forms of direct communication in the most effective way, without needing to be an expert in that research field. The concept of the SOAC provides insight and guidance in achieving the right balance between traditional and digital communication and interaction in an increasingly digital world. The SOAC concept is also very relevant, offering valuable contributions in the discussion about the future workplace [35] and post pandemic education models [36].

The SOAC builds on the analogy of an electric accumulator that stores electric energy, transformed to the aspect of interaction between human actors. Recharging activities are providing an energizing element and feel good for the humans interacting with each other. However, there are also draining activities which are perceived by the human actors as taking energy from them. These positive/negative or charging/draining aspects with the perceived social or personal energy have also been identified by other models, as elaborated in Section II, but the SOAC incorporates those observations and bundles them together by using a metaphor that is easy to understand for non-experts, as it draws from our everyday experiences with rechargeable batteries. This approach of connecting to everyday experience is also supported by [37] who investigated the appropriateness of a battery shaped icon scales to represent energy levels. Figure 1 illustrates the concept of a SOAC.

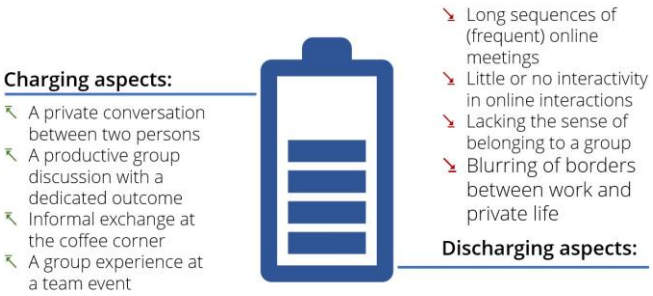

Figure 1. The social accumulator (SOAC) concept with examples of charging and discharging aspects.

The term social accumulator is not a common term, although it is briefly mentioned over ten years ago in [38], albeit within a very different context, namely the social status of youth.

A related concept to the SOAC is the term "social battery", which is not a medical concept, but rather a "metaphor for explaining how much energy a person has for socializing" [39]. This metaphor relates to the SOAC in terms of conceptualizing the limited capacity that each individual has for engaging with others ("socializing"). This limited capacity depends on individual aspects, such as personality (e.g., being more introverted or more extroverted), as well as social interaction (which can lead to feeling either drained or recharged, depending on one's personality) [39], [40]. In addition, a number of aspects have been identified that deplete the social battery (for instance, a person's social network, the type of interaction, the size of the group, to name a few), but there is no mention of the digital channel or digital tools as a potential cause for depletion. Therefore, the social battery concept differs from the concept of the SOAC, which has a special focus on digital channels and the use of digital tools, in order to effectively balance draining and charging aspects. The concept of a social battery is mostly used by youth in the generation Z, and is often related to social media settings [40]. Research is still lacking on the term and concept, but it is interesting to note that there is an awareness about limited capacity, including charging and discharging aspects of social interaction, especially in younger generations that might even lead to consequences like social burnout [41]. Relating to the observations of social energy in Section II, there are similar characteristics found in a number of models. The authors interpret these similarities to mean that the existence of social energy can be viewed as a valuable and finite resource, a viewpoint common in younger generations who are intuitively aware of both benefits and limitations as they monitor their interactions more or less closely. Digital technologies (especially in the domain of social media) may amplify these

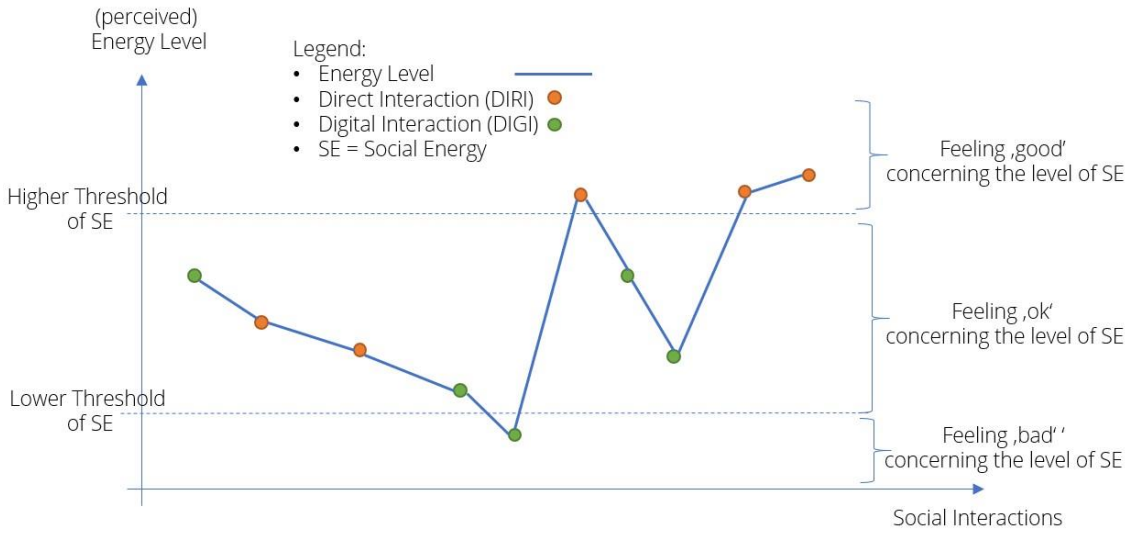

Figure 2. Changes in the SOAC charging stage influenced by direct interactions and digital interactions over time.

effects, which contributes to the awareness and the potential negative effects (e.g., affecting the "need to belong" [18], both in a positive or a negative way).

For the sake of completeness, it should be noted, that the term social battery is misleading in terms of the analogy to the technical concept of a battery: an ordinary battery cannot be recharged without damaging it, whereas an accumulator can be recharged multiple times. The authors therefore prefer to use the term *accumulator*.

Furthermore, the authors are convinced that the metaphor of a battery charging or discharging enables the intuitive perception of comparison with communication or cooperation activities. In terms of digital interaction, it is important to consider the general observation that a direct conversation between human actors ("face to face") is perceived as richer and more satisfying than a digital interaction. Therefore, the SOAC concept identifies in-person types of interactions as positive (charging) activities, while extensive digital interactions are identified as negative (discharging) activities, in line with the concept of zoom fatigue.

Based on these observations the concept of a SOAC is "charged" in (most) direct face-to-face interactions of human users and "discharged" in (many) digital interactions. Recent research [42] has found that a low level of interaction between participants in a digital domain might also lead to the perception of fatigue. However, the involvement of all stakeholders in a digital communication is important, which can be easily overlooked in this context. When balanced correctly a viable amount of social energy is available for the human user, and the interaction is perceived as sufficient. If the level drops below a certain level, this becomes a (perceived) problem, affecting the well-being of the user, especially if the situation continues over a longer timeframe (which explains observations from the longer COVID19 periods). If the level substantially exceeds the average energy level, then the interaction is perceived as a valuable interaction (e.g., users refer to a good chat as being inspirational). If this excessive level situation occurs more often, then the context of the interaction is positively perceived (e.g., an inspirational workplace or motivating group). Figure 2 illustrates the process on a schematic level.

It is important to note that neither digital nor direct interaction are inherently negative (discharging) or positive (charging), but that with the right balance or orchestration, both charging and discharging effects are important for a functioning communication relationship between the participants. In the context of active management of social energy of individuals and groups, it is important to monitor and influence the levels in such a way that they remain above the lower threshold and at times exceed the higher threshold in order to achieve "inspirational peaks" in individual or group collaboration. Due to the greater importance of digital interaction and the limitations of digital channels in terms of richness for all senses, social energy management in this area is even more important. In this case, awareness of the SOAC charging level for individuals or groups can be used as a management objective.

The level of social energy available to human actors has a strong influence on the ability to create and share knowledge, and could also affect levels of creativity and innovation [40], thereby resulting in a strong impact on knowledge intensive activities (e.g., in companies or in educational institutions).

The relationship between social energy and communication is not adequately defined and described only informally in the literature [43]. In the context of this paper, social energy is defined as the individual and subjectively perceived energy level of a human actor in terms of their capability or willingness to participate in or contribute to a physical or digital conversation.

As discussed in Section II, the concept of social energy has multiple dimensions, leading to many different effects. Figure 3 presents the most important dimensions of social energy, personal energy, and the effects of digital communication. A special emphasis is placed upon digital communication, which is influenced by the other two dimensions. For example, the level of personal energy at a specific time of day may impact the perceived energy level of the SOAC (which might not relate to the digital communication channel, but rather to personal circumstances). An assessment of the individual SOAC level should also consider other dimensions as contextual parameters.

As an immediate result of the charging and discharging effects, social energy has a strong impact on knowledge related activities, such as knowledge creation, knowledge sharing, knowledge use and knowledge transfer. Social energy changes over time and even during a conversation. Parallel to this, the management of social energy is not usually the main focus of the interacting users, and consequently, may not be noticed early enough to intervene before the primary activity is harmed or influenced.

The *awareness* created by the SOAC model enables reflection on a person's communication and collaboration situation, making it possible for the actor to take appropriate and effective action.

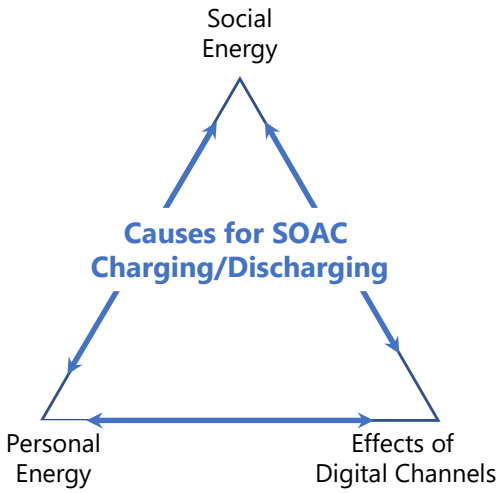

Figure 3. The different influences on charging and discharging effects of SOAC, with an emphasis on the effects of digital channels

Assessing the current situation provides a starting point in becoming more aware of the SOAC charging state, and with reflection can lead to a change of the communication mode (e.g., from digital interaction to direct interaction). Possible next steps taken by a human actor could involve tracking social energy over time to learn more about positive and negative aspects on digital interaction from their individual perspective.

The intent of the authors is to use this model to explain the dichotomy of direct vs. digital communication. The focus is placed on the channel and its methods and characteristics. It is clear that human interaction is also largely influenced by the topic of the communication, along with the opinions and general feelings of human actors. These aspects have positive and negative aspects, requiring specific and appropriate responses (e.g., conflict resolution). However, these responses are not dealt with in detail within this paper.

IV. CHARGING AND DISCHARGING THE SOAC

The aspects and characteristics of both digital and direct communication channels can be considered in terms of their charging effects (adding social energy to the SOAC) and the discharging effects (taking social energy from the SOAC), which will also be a subject for detailed future research. Some general observations regarding "Zoom fatigue" have already been illustrated in Section II. In order to examine the effects on digital channels and direct interaction in greater detail, some examples of both categories will be described in the following subsections.

A. Positive aspects charging the SOAC

To illustrate the positive (charging) aspects that increase social energy some examples are described below in more detail:

1. *A fruitful conversation*: between two human actors that evolves into interesting and sometimes unexpected results is a good example of a charging activity. Very often it is not only the exchange of information, but the overall situation, including gestures and mutual empathy that makes a positive impact. As an important side effect psychological safety is created in such situations.
2. *An informal talk*: at a coffee corner or similar place is a form of latent communication that happens as a by-product of another activity (e.g., taking a coffee). This often leads to the exchange of interesting information, knowledge sharing and even the creation of new knowledge stimulated by the situation. The main characteristic is spontaneity that it is unplanned, but not unlikely. These events happen less frequently in digital interactions. A possible explanation for this could be that interactions in digital environments are less frequent and less original.
3. *A team experience*: almost always requires a presence setting to allow for the emergence of team spirit while working on a common goal or being submerged in a joint activity. Very often these activities serve as trust building entities for new groups or are reassessing mutual trust levels for an existing team charging the SOACs of the participants. Such settings can create transparency within the group as an important side-effect that fuels the positive perception of the group-members.

4. *A collaborative activity*: working together within the same time and space toward a common aim can contribute to the sense of belonging and might even stimulate a mutual learning from the observations and activities of the people involved. The joint goal and making contributions to it provides opportunities for charging effects for the SOAC. When working together on the same physical object (e.g., a shared physical whiteboard or similar collaboration space) the perception of joint work might also be intensified.

B. Negative aspects discharging the SOAC

To illustrate the negative (discharging) aspects that decrease social energy some examples are described below in more detail:

1. *A high frequency and/or long duration of digital interactions*: might be considered as tiring to the human actors. This fact has been reported in a number of studies and it is important to clarify that this could also occur in situations in which only one of the human actors is under such a high load of digital interaction leading to a communication setting which is perceived very different by the participants (e.g., a team lead that is connecting to its peers in a 1:1 session).
2. *Few interactions during a digital interaction:* are another impact factor that is adding cognitive load to the human user, especially if the video setting is static, which requires additional effort for the human brain to remain focused. When presentation settings are transferred 1:1 from an in-person setting, they are often perceived as more demanding in the digital communication and take more time or include more interactions to retain the attention of the audience.
3. *The perception of constant availability*: for human actors also adds to the perceived stress level. The lowered barrier of getting in contact with the other participants in a synchronous interaction might impact the current working process. The cultural assumption within the organization that everyone is expected to be almost always available and instantly can lead to less efficiency in the working tasks and a high level of engagement at the same time.
4. *An imbalance of the presence for different users*: When different means of participating in the digital communication are used with different levels of channel richness (e.g., video on/off, different audio quality) the perception of direct engagement and involvement might vary among the users, leading to a discharging effect on human users, independent of their role in the setting (active/passive). It is a challenging situation for presenters if they cannot "perceive" their audience because the cameras are turned off and the level of interaction is limited.

V. Potential Application areas of SOAC

In this section potential application areas for the SOAC will be explained in detail. It is interesting to note that the SOAC can serve different purposes in diverse application areas. From a knowledge management perspective, the charging and discharging aspects of the SOAC are helpful to identify barriers in the related fields of knowledge (co)-creation, knowledge sharing and knowledge use among the different actors in the application settings that are described below. The concept of the SOAC can also contribute to achieving the right balance of in-person activities and online activities in the post-pandemic era, in which almost all sectors are reconfiguring their mode of operation in order to anticipate the experience from the past two years, along with the challenges and expectations for the future of the new work(place) [44].

A. The context of higher education

The effects of the COVID19 pandemic and the intensified use of distant teaching has transformed how higher education of the future is seen by students and lecturers alike. Initial studies after the pandemic show that the fast transition to distant teaching had a massive impact, as [43] reported for the medical domain. Although focused on a specific sector, the results could be similar in other areas, especially those where more intensive communication and collaboration is as important as experience and applicable knowledge for (complex and diverse) problems. Learning from these experiences is important not only to be better prepared for similar situations in the future, but also to strike a balance between face-to-face and distance learning (sometimes referred to as hybrid learning) in academic institutions.

Due to those experiences higher education institutions (HEI) will have to reflect on how to modernize the education in post-pandemic age with a mixture of in-person and distance teaching activities. It is very likely that even education programs that in the past have relied solely on in-person teaching will (have to) include some form of distance learning elements into their curricula, also due to expectations of Generation Z [45]. Even hybrid settings where in-person teaching and distance teaching occur simultaneously might be a valid scenario for the future.

It is obvious, that some topics are more suitable for distance teaching than others (e.g., labs and exercises), yet some students will favor digital interactions, while others will prefer a more direct interaction. Balancing those two forms of interaction between lecturer and students in the right way (in terms of didactic requirements and individual preferences), will retain a competitive advantage for an HEI in a market that is constantly becoming more competitive and globalized, due to extension into the digital domain by market participants (e.g., Coursera, Udacity and others). Additionally, a generation issue is currently felt in this area as the behavior and expectations of lecturers (often members of Generation X or Y) and students (often members of Generation Z) differ substantially, as [46] reported.

From a post-pandemic perspective, it is interesting to recognize the initial movement away from online teaching and the return to in-person teaching, on the student side as well as on the lecturers/HEI side. With the model of the SOAC in mind, this shift can be explained by a reaction on the number of discharging effects given the massive use of digital channels that needed to be compensated by social interactions (charging the SOAC). For some groups this effect has already been mitigated, since the positive aspects of distance learning, such as time and location independence gained focus again, which has led to requesting more digital channels. From a SOAC perspective, this development can be explained in a fully recharged state (by direct interaction) that provides enough energy for a set of digital interactions. In the long-term, it will be important for HEI to understand the duality of in-person and online teaching, and to *use both modes in a systematic and planned ways* that helps lecturers and learners to plan the different activities in the most efficient way. The SOAC model might support this development of understanding in this context as a balancing device. Otherwise important experiences and knowledge gains within the HEI are in danger to be lost as initiatives of individuals may not be valued and recognized, and investments in technology might not be used as planned, which will prevent their maintenance and iterative development.

The SOAC helps instructors to derive a measurement system during planning and execution of their teaching to find the right mix of direct and digital interaction. For students SOAC can function as a tool for self-reflection on individual learning preferences, in terms of their preferred form of communication, helping them to adapt accordingly by becoming aware of the advantages and drawbacks of digital interaction.

B. The context of professional trainings

For professional training in workplace settings and as part of lifelong learning, the results of the COVID19 pandemic revealed to companies and trainers that digital training can be effective and efficient. The requirement of traveling to a training became less of a demand and the integration into everyday work schedules was much easier for digital training, leading to a higher acceptance rate for training in general and budget saving aspects (no travel and accommodation costs). However, the focus on the training itself in an in-person training, along with the direct and valuable exchange between participants and towards the trainer, had been assigned a new value due to the drawbacks of digital trainings. Overall, it can be expected that the market for professional trainings will change, due to the results of the pandemic. Yet it still remains to be seen what exactly the long-term effects will be.

The SOAC can be helpful in two distinct ways. First, in many organizations, training is still understood as mostly a passive transmission of knowledge, with the focus primarily on content. Aspects of relationship building and interaction are often neglected in this approach. In this context, the SOAC can assist by creating an awareness of the social aspects of learning, emphasizing the importance of collaboration, communication, and engagement in the learning process.

Second, the SOAC can help trainers design interaction with the participants more effectively by mixing direct and digital interactions so that participants receive optimal benefit from the training. Being aware of the characteristics of the charging and discharging effects helps to establish a level of social interaction that is common in a direct training, and also in a digital setting. The SOAC is not merely another plea for the well-known concept of blended learning, but rather goes a level deeper. It recognizes that the different mix of various learning formats, such as online training, peer-learning, classroom training, self-study, and more, serves not only the design of the content level of the learning process, but also the social energy levels. Unlike traditional models that primarily focus on content, the SOAC emphasizes a more holistic approach. In the SOAC model, content learning objectives are supplemented by "social energy objectives." This shift recognizes the importance of human interaction, collaboration, and engagement as essential elements of the learning experience. Rather than simply transferring information, the emphasis is on creating a dynamic and interactive learning environment where participants can energize and motivate each other.

SOAC helps to incorporate education in professional job settings, achieving a match to the individual requirements, thereby providing a framework for the trainer to derive and monitor the charging state of the participants. The concepts of SOAC can also be combined with more agile approaches in delivering the teaching practices. By emphasizing the human and interactive dimensions of training, the SOAC framework enables a more effective, responsive, and learner-centered approach, which is essential in the ever-evolving landscape of professional learning

C. The context of companies and digital business

The third application area highlighting the benefits of SOAC is the digitization process within companies, which have also been accelerated by the pandemic situation. Here, the concept of “New Work” [46][47] became a reality through the perception and evolving work models of many organizations, who had previously resisted such changes. This significant and ongoing change in the organization of companies often leads to more distributed or even virtualized companies, especially in the IT-domain. While it is a common pattern in northern European countries, this is relatively new in the DACH area.

In the post-pandemic context in 2023 a re-evaluation of the office and mobile work (home office) environment is being carried out in many organizations, often moving towards one of the extremes: either (fully) back to the office or (fully) remote work. Some initial studies, such as [49] [35] indicate that there are different perspectives, including the organization, the employer, and also the regulatory side with laws and rules that create a framework. Apart from setting up the rules [49] this perspective emphasizes the need to

communicate an organizational decision to move back to the office, which represents at least one aspect where the SOAC model can be useful as an explanation model (e.g., to (re)build a team spirit within an otherwise distributed team).

The influence of the pandemic can also have future impacts on the workplace based on the experiences and expectations of the new workforce (Generation Z), who demand more remote work possibilities wherever possible, addressing their need for autonomy and freedom. This means the attractiveness of the workplace will also be measured in the dimension of flexibility between working remotely and on-site, which directly relates to direct and digital communication channels and the effects on the SOAC. Some sectors will be more affected by this movement than others; the IT-sector might be a good example as it is an employee-market in the DACH-region (there is more demand than supply for employees) and since the work context is already digital and predominantly digitized.

From a managerial point of view this change creates new challenges for managing teams and projects due to the fact of (perceived) fewer social interactions. From the perspective of digital leadership, these aspects were already being discussed even before the pandemic. Digital leadership refers to both the restructuring of organizational and infrastructural frameworks, as well as the design of new working methods and styles that positively embrace digital transformation. Consequently, it affects both corporate management (including both strategic and operational levels), and personnel leadership. Similar to professional trainings, the focus in many organizations has been less on social aspects and more on technical, strategic, and organizational factors.

Many studies have found that only a few leaders possess the competencies of a digital leader. In a rapidly changing digital landscape, leadership must go beyond merely understanding technology; it requires a blend of strategic insight, adaptability, and a keen awareness of the human factors that drive innovation and change.

In this context, the SOAC can create an easily understandable framework to shift the awareness towards the social aspects of interaction. By placing an emphasis on the relational and interactive elements of leadership, it complements the technical and strategic components. The SOAC underscores the importance of empathy, collaboration, and social engagement in leading a modern organization, particularly in an era where digital transformation is paramount.

The SOAC as a managerial concept will help managers and team leaders to better understand the needs of their colleagues and team mates, and to act according to their (individual) needs, since they are able to sense and classify the charging and discharging activities during the digital and direct interactions. For employees the SOAC functions as a model that helps them to become aware and to voice their needs in terms of communication and interaction over the various channels.

Monitoring the social energy of the members of a group has always been an important task for leaders. However, in a hybrid working environment with a large amount of digital interaction it will be more important to monitor the social energy of the team members and to recharge their SOACs early enough to prevent "outages" that might affect team motivation and performance. The concept of SOAC can help to manage team social energy more actively.

D. Challenges for the application of SOAC

Applying the mental model of a SOAC has its challenges, which are a subject for future research. Some of the foreseen challenges are briefly mentioned in order to provide some hints for the application in the settings described above.

It will be important to retain the simplicity of the concept and to stay as close to the accumulator metaphor as possible in order to make application simple and intuitive for the human actors in the communication process. The notion of the social battery that is familiar to the younger generation might help to introduce the concept.

Likewise, it will be important and challenging to make the current social energy visible for the individual and for the group in order to *create awareness* and the opportunity to appropriately *act on critical states* of the SOAC. A promising approach for teams could be the use of retrospectives as a method from the agile software development for groups [50]. An adapted and simplified version might even work for the individual as a form of self-retrospective that can be mapped to the communication events in the recent period to plot the social energy levels over time. Integration in already established routines will be a key factor in this context, and feedback activities of all sorts might be a promising candidate for integrating SOAC.

Finally, charging and discharging factors will overlay each other and communication setting (in-person or digital) might not be directly related to the social energy level or being conscious for the human users in every situation. Therefore, the identification of relevant communication events and their contribution to the social energy level in a precise way is going to be another challenge. As indicated in Figure 3, personal energy and social energy may also influence the SOAC concept as it focusses on digital versus direct communication and collaboration; therefore, these aspects should be considered as contextual factors. Furthermore, the capacity and the loading/unloading events are highly individual and subjective by nature, which makes a comparison of SOACs of different persons challenging, the observation of an individual SOAC charging state over time might be more promising.

VI. CONCLUSIONS & FUTURE RESEARCH

The main contribution of this paper is the introduction of the SOAC as a mental concept that serves as a simple explanation model depicting the social energy level of an individual or a group, along with the perceived differences of direct and digital interactions. The SOAC concept supports understanding and the interplay between the different forms of interaction and thus enables the improvement of the overall interaction between human users, as both forms are and

continue to be present in our daily professional life. In addition, the paper helps to identify various individual aspects that need to be considered when planning and orchestrating the various forms of interaction. This is exemplified by using application examples from three different fields. The embedding of the concept in the field of social energy clarifies the current state of the art in this domain and explains the contribution of the SOAC concept with its focus on the alternation between direct and digital communication and collaboration.

A limitation of the research is the current focus on the conceptual level. There is a lack of empirical data, the collection of which is the subject of further research in the various usage scenarios mentioned above. This next step will also serve to gather responses from the human actors in the interaction process regarding the understanding and usefulness of the mental model of a SOAC.

ACKNOWLEDGMENTS

The authors would like to thank the Tyrolean Science Fund ("Tiroler Wissenschaftsförderung"), which supported this research under grant number F.33280/6-202 and the colleagues and reviewers which helped to improve it.

REFERENCES

[1] K. Böhm, 'The Social Accumulator (SOAC) An explanation model for digital interaction among human actors', *Proc. EKNOW 2022 - Fourteenth Int. Conf. Inf. Process Knowl. Manag.*, pp. 69–74, 2022.

[2] G. Fauville, M. Luo, A. C. Muller Queiroz, J. N. Bailenson, and J. Hancock, 'Zoom Exhaustion & Fatigue Scale', Social Science Research Network, Rochester, NY, SSRN Scholarly Paper ID 3786329, Feb. 2021. doi: 10.2139/ssrn.3786329.

[3] J. Rump and M. Brandt, 'Zoom-Fatigue'. Accessed: Mar. 27, 2022. [Online]. Available: https://www.ibe-ludwigshafen.de/zoom_fatigue/

[4] N. Döring, *Social Psychology of the Internet. The importance of the Internet for communication processes, identities, social relations and groups.*, 2nd ed. Göttingen Bern: Hogrefe Verlag, 2003.

[5] J. Walther, 'The Effect of Feedback on Identity Shift', *Comput.-Mediat. Commun. Media Psychol.*, vol. Vol. 14, no. Issue 1, pp. 1–26, 2011.

[6] J. Orlosky *et al.*, 'Telelife: The Future of Remote Living', *ArXiv210702965 Cs*, Jul. 2021, Accessed: Jul. 10, 2021. [Online]. Available: http://arxiv.org/abs/2107.02965

[7] K. Ishii, M. M. Lyons, and S. A. Carr, 'Revisiting media richness theory for today and future', *Hum. Behav. Emerg. Technol.*, vol. 1, no. 2, pp. 124–131, 2019, doi: 10.1002/hbe2.138.

[8] A. M. Johnson and A. L. Lederer, 'The Effect of Communication Frequency and Channel Richness on the Convergence Between Chief Executive and Chief Information Officers', *J. Manag. Inf. Syst.*, vol. 22, no. 2, pp. 227–252, Nov. 2005, doi: 10.1080/07421222.2005.11045842.

[9] O. Lavrusheva, 'The concept of vitality. Review of the vitality-related research domain', *New Ideas Psychol.*, vol. 56, p. 100752, Jan. 2020, doi: 10.1016/j.newideapsych.2019.100752.

[10] R. M. Ryan and C. Frederick, 'On energy, personality, and health: Subjective vitality as a dynamic reflection of well-being', *J. Pers.*, vol. 65, no. 3, pp. 529–565, 1997, doi: 10.1111/j.1467-6494.1997.tb00326.x.

[11] A. Rozanski, J. A. Blumenthal, K. W. Davidson, P. G. Saab, and L. Kubzansky, 'The epidemiology, pathophysiology, and management of psychosocial risk factors in cardiac practice: the emerging field of behavioral cardiology', *J. Am. Coll. Cardiol.*, vol. 45, no. 5, pp. 637–651, Mar. 2005, doi: 10.1016/j.jacc.2004.12.005.

[12] G. A. Nix, R. M. Ryan, J. B. Manly, and E. L. Deci, 'Revitalization through self-regulation: The effects of autonomous and controlled motivation on happiness and vitality', *J. Exp. Soc. Psychol.*, vol. 35, no. 3, pp. 266–284, 1999, doi: 10.1006/jesp.1999.1382.

[13] P. Dubreuil, J. Forest, and F. Courcy, 'From strengths use to work performance: The role of harmonious passion, subjective vitality and concentration', *J. Posit. Psychol.*, vol. 9, pp. 1–15, Apr. 2014, doi: 10.1080/17439760.2014.898318.

[14] A. Klijn, M. Tims, E. Lysova, and S. Khapova, 'Personal Energy at Work: A Systematic Review', *Sustainability*, vol. 13, p. 13490, Dec. 2021, doi: 10.3390/su132313490.

[15] M. Csikszentmihalyi, *Beyond boredom and anxiety*, 1st ed. San Francisco: Jossey-Bass Publishers, 1975.

[16] J. A. Hall and D. C. Davis, 'Proposing the Communicate Bond Belong Theory: Evolutionary Intersections With Episodic Interpersonal Communication', *Commun. Theory*, vol. 27, no. 1, pp. 21–47, 2017, doi: 10.1111/comt.12106.

[17] D. C. Davis, 'Development and initial tests of a human energy management theory of communication - ProQuest'. Accessed: Jul. 27, 2023. [Online]. Available: https://www.proquest.com/openview/871024fddd3185b82078b958050d1e5d/1?pq-origsite=gscholar&cbl=18750&diss=y

[18] R. F. Baumeister and M. R. Leary, 'The need to belong: desire for interpersonal attachments as a fundamental human motivation', *Psychol. Bull.*, vol. 117, no. 3, pp. 497–529, May 1995.

[19] J. A. Hall and A. J. Merolla, 'Connecting Everyday Talk and Time Alone to Global Well-Being', *Hum. Commun. Res.*, vol. 46, no. 1, pp. 86–111, Jan. 2020, doi: 10.1093/hcr/hqz014.

[20] J. A. Hall, 'Energy, Episode, and Relationship: A Test of Communicate Bond Belong Theory', *Commun. Q.*, vol. 66, no. 4, pp. 380–402, Aug. 2018, doi: 10.1080/01463373.2017.1411377.

[21] J. Dominguez, S. Bowman, J. A. Hall, and A. Merolla, 'Working hard to make a good impression: the relational consequences of effortful self-presentation', *Commun. Res. Rep.*, vol. 37, no. 5, pp. 276–285, Oct. 2020, doi: 10.1080/08824096.2020.1846511.

[22] J. A. Hall, N. Pennington, and A. J. Merolla, 'Which mediated social interactions satisfy the need to belong?', *J. Comput.-Mediat. Commun.*, vol. 28, no. 1, p. zmac026, Jan. 2023, doi: 10.1093/jcmc/zmac026.

[23] K. M. Shockley, M. A. Clark, H. Dodd, and E. B. King, 'Work-Family Strategies During COVID-19: Examining Gender Dynamics Among Dual-Earner Couples With Young Children', *J. Appl. Psychol.*, no. 106(1), pp. 15–28, doi: https://doi.org/10.1037/apl0000857.

[24] A. C. Klotz, W. He, K. C. Yam, M. C. Bolino, W. Wei, and L. Houston III, 'Good actors but bad apples: Deviant consequences of daily impression management at work', *J. Appl. Psychol.*, vol. 103, no. 10, pp. 1145–1154, 2018, doi: 10.1037/apl0000335.

[25] A. L. Gonzales and J. T. Hancock, 'Mirror, Mirror on my Facebook Wall: Effects of Exposure to Facebook on Self-Esteem', *Cyberpsychology Behav. Soc. Netw.*, vol. 14, no. 1–2, pp. 79–83, Jan. 2011, doi: 10.1089/cyber.2009.0411.

[26] E. Berninger-Schäfer, *Online Coaching*. Wiesbaden: Springer Fachmedien, 2022. doi: 10.1007/978-3-658-39133-1.

[27] J. N. Bailenson, 'Nonverbal Overload: A Theoretical Argument for the Causes of Zoom Fatigue', *Technol. Mind Behav.*, vol. 2, no. 1, Feb. 2021, doi: 10.1037/tmb0000030.

[28] A. A. Bennett, E. D. Campion, K. R. Keeler, and S. K. Keener, 'Videoconference fatigue? Exploring changes in fatigue after videoconference meetings during COVID-19.', *J. Appl. Psychol.*, vol. 106, no. 3, pp. 330–344, Mar. 2021, doi: 10.1037/apl0000906.

[29] U. R. Hülsheger, 'From dawn till dusk: Shedding light on the recovery process by investigating daily change patterns in fatigue.', *J. Appl. Psychol.*, vol. 101, no. 6, pp. 905–914, 2016, doi: 10.1037/apl0000104.

[30] S. G. Rogelberg, J. A. Allen, L. Shanock, C. Scott, and M. Shuffler, 'Employee satisfaction with meetings: A contemporary facet of job satisfaction', *Hum. Resour. Manage.*, vol. 49, no. 2, pp. 149–172, Mar. 2010, doi: 10.1002/hrm.20339.

[31] S. Kaplan and M. G. Berman, 'Directed Attention as a Common Resource for Executive Functioning and Self-Regulation', *Perspect. Psychol. Sci.*, vol. 5, no. 1, pp. 43–57, Jan. 2010, doi: 10.1177/1745691609356784.

[32] S. Kaplan, 'The restorative benefits of nature: Toward an integrative framework', *J. Environ. Psychol.*, vol. 15, no. 3, pp. 169–182, Sep. 1995, doi: 10.1016/0272-4944(95)90001-2.

[33] J. R. Hackman, 'Group influences on individuals in organizations', in *Handbook of industrial and organizational psychology, Vol. 3, 2nd ed*, Palo Alto, CA, US: Consulting Psychologists Press, 1992, pp. 199–267.

[34] U. Brandes, *Social Energy*. Campus Verlag, 2018. [Online]. Available: https://www.campus.de/buecher-campus-verlag/business/fuehrung/social_energy-10867.html

[35] D. Smite, N. B. Moe, J. Hildrum, J. G. Huerta, and D. Mendez, 'Work-From-Home is Here to Stay: Call for Flexibility in Post-Pandemic Work Policies', *ArXiv220311136 Cs*, Mar. 2022, Accessed: Apr. 29, 2022. [Online]. Available: http://arxiv.org/abs/2203.11136

[36] L. Bayerlein, M. T. Hora, B. A. Dean, and S. Perkiss, 'Developing skills in higher education for post-pandemic work', *Labour Ind.*, vol. 31, no. 4, pp. 418–429, Oct. 2021, doi: 10.1080/10301763.2021.1966292.

[37] O. Weigelt *et al.*, 'Time to recharge batteries – development and validation of a pictorial scale of human energy', *Eur. J. Work Organ. Psychol.*, vol. 31, no. 5, pp. 781–798, Sep. 2022, doi: 10.1080/1359432X.2022.2050218.

[38] D. V. Lepeshev and A. N. Teslenko, 'Social status of scientific activity in the minds of the youth of Kazakhstani', *Eur. Sci. J. ESJ*, vol. 10, no. 17, Art. no. 17, Jun. 2014, doi: 10.19044/esj.2014.v10n17p%p.

[39] 'Social battery: What it is and how to recharge it'. Accessed: Jul. 25, 2023. [Online]. Available: https://www.medicalnewstoday.com/articles/social-battery

[40] '7 Ways to Recharge When You're Feeling Drained of Social Energy', Andy Mort. Accessed: Apr. 29, 2022. [Online]. Available: https://www.andymort.com/social-energy/

[41] 'How to Take Care of Your "Social Battery" - Preventing Social Burnout'. Accessed: Jul. 25, 2023. [Online]. Available: https://www.mindtools.com/at5m4h1/social-battery

[42] N. Nurmi and S. Pakarinen, 'Virtual meeting fatigue: Exploring the impact of virtual meetings on cognitive performance and active versus passive fatigue.', *J. Occup. Health Psychol.*, Oct. 2023, doi: 10.1037/ocp0000362.

[43] B. Vaca-Cartagena, E. Quishpe, H. Ulloa, and P. Estévez, 'Differences in medical education before, during, and in the post-peak period of the COVID-19 pandemic—exploring senior medical students' attitudes', *BMC Med. Educ.*, vol. 23, Jul. 2023, doi: 10.1186/s12909-023-04489-6.

[44] J. Kamis, Z. Rahim, Y. Yusoff, N. A. Husin, and R. Yuliviona, 'A Review on Hybrid Work and Work Performance During Post-Pandemic', *KnE Soc. Sci.*, Jul. 2023, doi: 10.18502/kss.v8i13.13756.

[45] M. Kumar and P. Mamgain, 'Generation-Z Student Video-Based Learning Pedagogy Preference and

Teaching Challenges', 2023, pp. 155–167. doi: 10.1002/9781119867647.ch9.

[46] W. Elshami, M. Taha, M. E. Abdalla, M. Abuzaid, and S. Kawas, 'Bridging the Gap in Online Learning Anxiety Generation X teaching Millennial and Z generations', *Sultan Qaboos Univ. Med. J.*, vol. 21, Apr. 2021, doi: 10.18295/squmj.4.2021.040.

[47] R. C. Barnett, 'A New Work-Life Model for the Twenty-First Century', *Ann. Am. Acad. Pol. Soc. Sci.*, vol. 562, no. 1, pp. 143–158, Mar. 1999, doi: 10.1177/000271629956200110.

[48] M. Helmold, 'Culture Change Towards New Work Concepts', in *New Work, Transformational and Virtual Leadership: Lessons from COVID-19 and Other Crises*, M. Helmold, Ed., in Management for Professionals. , Cham: Springer International Publishing, 2021, pp. 45–54. doi: 10.1007/978-3-030-63315-8_4.

[49] J. Koenig, 'Home Office: Before, During and after Corona', Aug. 2022.

[50] Y. Andriyani, R. Hoda, and R. Amor, 'Reflection in Agile Retrospectives', in *Agile Processes in Software Engineering and Extreme Programming*, H. Baumeister, H. Lichter, and M. Riebisch, Eds., in Lecture Notes in Business Information Processing. Cham: Springer International Publishing, 2017, pp. 3–19. doi: 10.1007/978-3-319-57633-6_1.

VR-V&V: Immersive Verification and Validation Support for Traceability Exemplified with ReqIF, ArchiMate, and Test Coverage

Roy Oberhauser[0000-0002-7606-8226]
Computer Science Dept.
Aalen University
Aalen, Germany
e-mail: roy.oberhauser@hs-aalen.de

Abstract – **To build quality into a software (SW) system necessitates supporting quality-related lifecycle activities during the software development. In software engineering, software Verification and Validation (V&V) processes constitute an inherent part of Software Quality Assurance (SQA) processes. A subset of the V&V activities involved are: 1) bidirectional traceability analysis of requirements to design model elements, and 2) software testing. Yet the complex nature of large SW systems and the dependencies involved in both design models and testing present a challenge to current V&V tools and methods regarding support for trace analysis. One of software's essential challenges remains its invisibility, which also affects V&V activities. This paper contributes VR-V&V, a Virtual Reality (VR) solution concept towards supporting immersive V&V activities. By visualizing requirements, models, and testing artifacts with dependencies and trace relations immersively, they are intuitively accessible to a larger stakeholder audience such as SQA personnel while supporting digital cognition. Our prototype realization shows the feasibility of supporting immersive bidirectional traceability as well as immersive software test coverage and analysis. The evaluation results are based on a case study demonstrating its capabilities, in particular traceability support was performed with ReqIF, ArchiMate models, test results, test coverage, and test source to test target dependencies.**

Keywords – Virtual reality; visualization; software verification and validation; software requirements traceability; software test traceability; software test coverage; code coverage; software testing; ReqIF; ArchiMate.

I. INTRODUCTION

This paper extends out Virtual Reality (VR)-based immersive test coverage capability presented in VR-TestCoverage [1], extending its scope to support software (SW) Verification and Validation (V&V) activities in VR, in particular support for immersive trace analysis of dependencies between requirements, design models such as ArchiMate, test results, test coverage, and test source to test target dependencies.

The IEEE 730-2014 Standard for Software Quality Assurance Processes [2] includes evaluation tasks that specifically include the terms *verify* and *validate*, otherwise known as V&V. During the development lifecycle, software validation is the technical process that evaluates and provides evidence about software satisfying requirements, intended usage, and user needs [3]. During the software development lifecycle, software verification is the technical process of evaluating the software or component and associated artifacts for objective evidence that activities performed during each development process satisfy the criteria for that lifecycle activity [3]. The stated intention of V&V is to support an organization in building quality into the software during its development life cycle [4]. V&V does so by ensuring that requirements meet certain quality criteria (e.g., complete, correct, consistent, accurate). Conformance with an activity's requirements and the product's requirements is determined by assessing, analyzing, reviewing, inspecting, and *testing* products and processes [4]. Depending on the required integrity level, SW testing varies in the types, degree, and scope performed to support V&V at various levels, e.g., construction verification via unit testing, integration testing, or system testing. Furthermore, in Annex E of [2] for Industry-specific guidance for applying IEEE 730-2014, the definition of software verification for the medical device industry includes: "Software testing is one of many verification activities intended to confirm that software development output meets its input requirements." Indeed, without executing SW dynamically via SW testing, one would be hard pressed to confirm its requirements are satisfied. Traceability analysis involving bidirectional tracing between elements is a common task specified in many V&V activities. tracing between (product/system or process) requirements, design, construction, test, and other elements to check of correctness, completeness, and consistency [4]. Thus, tracing (dependent on traceability) and testing (either reviewing thereof or performing) are inherent tasks accompanying V&V.

Despite the apparent importance of traceability, the software industry lacks explicit support for bidirectional traceability across software artefacts, e.g., via international specifications, formats, automation, or non-proprietary popular tools. This situation often results in traceability being a manual effort documented utilizing spreadsheets or text documents as exemplified in [5] and [6]. Confounding the traceability issues for V&V are the inherent properties and essential difficulties of software according to Brooks [7]: its complexity, conformity, changeability, and invisibility. Brooks stated that the invisibility of software is an essential difficulty of software construction because the reality of software is not embedded in space. With regard to V&V and traceability support for larger SW systems, comprehension challenges emerge for stakeholders due to two main aspects: as the quantity and granularity of elements and related

artifacts increase, the inter- and intra-dependencies that traceability considers exacerbate the *complexity*. Furthermore, the *invisibility* of these "implicit" relations in current tooling diminishes comprehension due to a lack of visualization capability that can extend across artifacts, model, and heterogeneous tool elements.

As a powerful visualization capability, Virtual Reality (VR) could potentially address aspects of both: 1) invisibility, due to its digital nature and ability to portray artificial constructs, and 2) complexity, due to its unlimited immersive space. VR thus provides an unlimited immersive space for visualizing and analyzing 3D spatial structures viewable from different perspectives. Müller et al. [8] compared VR vs. 2D for a software analysis task, finding that VR does not significantly decrease comprehension and analysis time nor significantly improve correctness (although fewer errors were made). While interaction time was less efficient, VR improved the user experience, was more motivating, less demanding, more inventive/innovative, and more clearly structured. Via its unique visualization and immersive capability, VR can support V&V trace visualization and analysis while providing a motivational benefit.

As to our prior work, with regard to modeling in VR, VR-UML [9] and VR-SysML [10] provide VR-based visualization of Unified Modeling Language (UML) [11] and System Modeling Language (SysML) [12] diagrams respectively, with VR-EA [13] supporting immersive ArchiMate [14] EA models. VR-SysML+Traceability [15] investigated SysML-centric traceability support in VR via automated extraction of manually placed requirement ID annotations in code and test files referencing requirements modeled in SysML and depicting test pass rates; yet it did not address ReqIF [16] sources, ArchiMate, nor automated test coverage nor test dependency aspects.

Extending the immersive test coverage and tracing capability of VR-TestCoverage [1], this paper contributes the solution concept VR-V&V towards supporting immersive V&V activities. It visualizes requirements extracted from ReqIF together with design models and testing artifacts, showing dependencies and trace relations immersively to address invisibility and complexity issues. Thus, comprehension for V&V tracing can be improved while being intuitively accessible to a larger stakeholder audience (such as SQA personnel). Our prototype realization shows its feasibility. The case-based evaluation provides insights into its capabilities, in particular traceability support with ReqIF, ArchiMate models, test results, test coverage, and test source to test target dependencies

The remainder of this paper is structured as follows: Section II discusses related work. In Section III, the solution concept is described. Section IV provides details about the realization. The evaluation is described in Section V and is followed by a conclusion.

II. Related Work

In work related to requirements traceability visualization, Li & Maalej [17] found traceability matrices and graphs preferrable for management tasks. Graphs were preferred for navigating linked artifacts, while matrices were preferred for an overview. Users were not always capable of choosing the most suitable visualization. Abad et al. [18] performed a systematic literature review on requirements engineering visualization. Madaki & Zainon [19] performed a review on tools and techniques for visualizing SW requirement traceability. In none of the above literature were immersive or VR techniques mentioned, nor was our own literature search able to find similar work. Some software tool vendors provide proprietary product solutions to support some aspects of traceability, e.g., IBM Engineering Requirements Management DOORS Next [20], Perforce Helix ALM [21], Sparx Systems Enterprise Architect [22], etc. Yet these typically do not address heterogenous design models, cross-diagram dependencies, integration with ReqIF requirements, and test coverage and test target dependencies. In any case, they do not support the display of such trace dependencies in 3D or VR.

Furthermore, our literature search found no other VR work directly addressing test coverage (or code coverage). VR-related work regarding software analysis includes VR City [23], which applies a 3D city metaphor. While it briefly mentions that its work might be used for test coverage, it shows no actual results in this regard and in this regard only a trace mode visualization is depicted.

Non-VR work on structural testing or code coverage includes Dreef et al. [24], which applies a global overview test-matrix visualization. Rahmani et al. [25] incorporates JaCoCo to process coverage metrics and TRGeneration to visualize a control flow graph and assist the tester in determining the test input requirements to increase coverage. VIRTuM [26] is an IntelliJ JetBrains plugin that provides static and dynamic test-related metrics. Alemerien and Magel [27] list various coverage tools they assess in their study, determining that there is a wide range of differences in how the metrics are calculated. Open Code Coverage Framework (OCCF) [28] proposes a framework to unify code coverage across many programming languages.

In contrast, our solution is VR-based and thus immersive and 3D, leverages requirements in text form via ReqIF, yet supports additional requirements modeling in ArchiMate (which provides broad modeling support), supports cross-diagram traceability, and integrates test dependency and test coverage for enhanced V&V traceability. In utilizing available standardized formats such as ReqIF and ArchiMate, to support a non-proprietary and tool-independent integration platform. As they are non-standardized, any tool-generated code coverage or test report format can be converted into our import format and utilized.

III. Solution Concept

A. Solution Positioning

While the solution concept in this paper is focused on V&V and specifically traceability support, our other solution concepts that address other aspects in the Software Engineering (SE) and Enterprise Architecture (EA) area are shown in Figure 1. VR-V&V utilizes our generalized VR Modeling Framework (VR-MF) (detailed in [11]). VR-MF provides a VR-based domain-independent hypermodeling

framework addressing four aspects requiring special attention when modeling in VR: visualization, navigation, interaction, and data retrieval. Our VR-based solutions specific to SE (VR-SE) include: VR-V&V (the focus of this paper, shown in black), which extends VR-TestCoverage [1], and VR-Git [29]. In the modeling area, VR-UML [9] and VR-SysML [10] and VR-SysML+Traceability [15]. Modeling support extending into the EA area includes VR-EA [11], which visualizes EA ArchiMate models in VR; VR-ProcessMine [30] supports process mining and analysis in VR; and VR-BPMN [31] visualizes Business Process Modeling Notation (BPMN) models in VR. VR-EAT [32] integrates the EA Tool (EAT) Atlas to provide dynamically-generated EA diagrams in VR, while VR-EA+TCK [33] integrates Knowledge Management Systems (KMS) and/or Enterprise Content Management Systems (ECMS), and VR-EvoEA+BP [34].

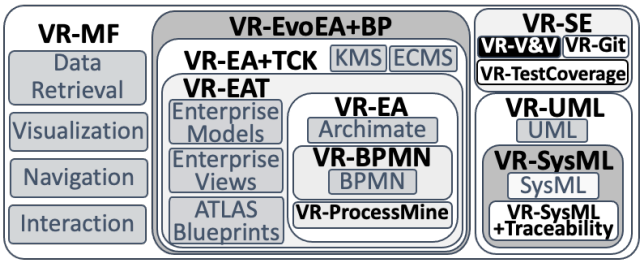

Figure 1. Conceptual map of our various VR solution concepts.

B. V&V Considerations

1) Stakeholders: While V&V typically involves a broad set of artifacts and activities, SW validation inherently involves and references requirements, while SW verification regarding realized SW elements will also typically involve or assess SW testing. Thus, V&V stakeholders are likely to require knowledge of requirements and the ability to assess SW testing coverage, as they are an essential part of V&V assessments. V&V activities may be performed by independent personnel, known as Independent V&V (IV&V), and these stakeholders may not be as familiar with the requirements, various internals of the SW architecture, and associated tests. Thus, an intuitive visualization and accessibility of relevant information and tracing can be supportive for such stakeholders.

2) Testing: Software testing is also a Knowledge Area (KA) within the SWEBOK [35]. Both the SWEBOK and the international software testing standard ISO/IEC/IEEE 29119 [36] include test coverage measures within their test technique descriptions. Test effectiveness is always a challenging factor to measure. While test coverage (a.k.a. code coverage, in this paper we assume statement coverage) as a single factor may not be strongly correlated with test effectiveness [37], it nevertheless is still low to moderately correlated, and this can be helpful and supportive data for the test effort and verification. Considering the adoption rate of test coverage by software developers, for an insight into the industrial popularity of test coverage, of 512 developers randomly surveyed at Google in a 2019 survey [38], 45% indicated they use it (very) often when authoring a changelist and 25% sometimes. When reviewing a changelist, 40% use coverage (very) often and 28% sometimes. Only 10% of respondents never use coverage, which conversely means 90% do. So overall, a substantial number of developers apply code coverage regularly and find value in it. Voluntary adoption at the project level went from 20% in 2015 to over 90% by 2019. As to modeling tests (or test modeling), while a UML Test Profile is available to extend UML, its industrial usage is relatively rare, since the expense of modeling and realizing the solution often exact the project effort and budget, and typically the preference is for utilizing the testing budget for writing and executing tests, rather than expending effort on the modeling of tests, which don't actually expand the testing coverage. The first form of traceability to support verification is to determine which test actually tested which test target. This type of verification is often not performed nor supported by test tooling. Usually, if code coverage is utilized, it usually does not offer a detailed assessment of exactly which test reached which test target line, but rather a summary of which lines or branches were reached via some test suite. Thus, the bidirectional traceability data is typically missing between unit test and test target, and is usually assumed using the test names.

3) Complexity: A V&V visual scalability challenge is that with increasing digitalization, the software scope, capabilities, and features often increase, resulting in increases to requirements, code size, and complexity. Codebases can grow and become very large for software projects, be they open-source, commercial, or other organizations, as exemplified with the over 2 billion Lines of Code (LOC) across 9 million source files in a single monolithic repository accessed by 25k developers at Google [39]. There are estimated to be over 25m professional software developers worldwide [40] who continue to add source code to private and public repositories. One quality aspect to consider is how well this code is tested, and if any codebase changes have been covered by tests. With large code bases, visualization of test coverage can provide helpful insights, especially into what is not covered. As software projects grow in size and complexity, an immersive digital environment can provide an additional visualization capability to comprehend and analyze both the software production code (i.e., test target) and the software test suite and how they relate, as well as determine areas where the code coverage achieved by a test suite is below expectations.

4) Modeling: With regard to the choice of modeling notations, ArchiMate has a much broader modeling scope than UML (and SysML, which extends UML via a profile), overlapping many modeling notations and thus is able to act as a bridge across modeling notations. Besides requirements, ArchiMate also supports modeling externally relevant aspects such as behavior, interfaces, deployment, and infrastructure and how it may interact with other external systems. While UML entails approximately 150 modeling concepts, compared to the approximately 50 in ArchiMate, ArchiMate is relative lightweight, and its simplicity and broad support for enterprise and business modeling suggests it can perhaps more flexibly support the use of requirements with design models. Whereas UML is constrained to fixed

diagram types, ArchiMate permits custom stakeholder-oriented views. UML is object-oriented (OO), whereas ArchiMate is not constrained in this way, and has, e.g., separate service and interface concepts. As to requirements, UML offers primarily use cases. In contrast, The Open Group's Agile Guide for using ArchiMate [41] explicitly mentions modeling user stories, where "epics" (modeled as outcomes), which in turn are realized by "features" (modeled as requirements), which are themselves aggregated from individual "stories" (also modeled as requirements). However, both modeling notations can be used together, as described in by an Open Group whitepaper [42]. Thus, while our solution concept is design model notation agnostic, for demonstration purposes, our prototype realization will focus on ArchiMate.

5) Requirements: Software requirements is a KA within the Software Engineering Body Of Knowledge (SWEBOK) [35]. Both the SWEBOK and the requirements engineering process ISO/IEC/IEEE 29148 [43] mention requirements tracing and traceability, also in conjunction with requirements validation. We selected ArchiMate for requirements traceability modeling, among other reasons for its ability to model actors, system goals, and associated requirements independent of the narrow concept of Use Cases, the only direct form of requirement support that UML offers. Furthermore, ArchiMate offers various motivation elements such as Principles, Constraints, Value, Meaning, Outcome, Driver, Assessment in addition to Goal and Requirement, and these offer broad support for the typical concepts involved during requirements elicitation and related activities. While ArchiMate models support the modeling of such requirements concepts, typically they are nevertheless not the starting point for requirements. Rather, these are often formulated in text form, either more formally in a Software Requirements Specification (SRS) or System Requirements Specification (SyRS) that may be compliant with ISO/IEC/IEEE 29148, or these may come from more agile user stories or use cases. These requirements sources are thus not directly included or mapped in the design model such as ArchiMate. Since the modeling of requirements could incur errors, for V&V we thus consider the requirements source to be of principal character, and wish to have access to these sources in VR. Since ReqIF is a specified exchange format supported by requirements engineering tools, we chose to support importing ReqIF requirements into VR. This ensures that requirement information is complete and nothing is overlooked. This does not preclude the powerful requirements modeling support in ArchiMate, but rather supports V&V of such requirements modeling to the original source while remaining contextually immersed in VR.

6) Traceability: The lack of a traceability standard or exchange format limits automation and tool accessibility. While vendors may have a proprietary solution, typically the inclusion of tracing information is a manual documentation effort utilizing spreadsheets or text documents, as exemplified in Figure 2 as a typical form template, and with a filled-in example in Figure 3.

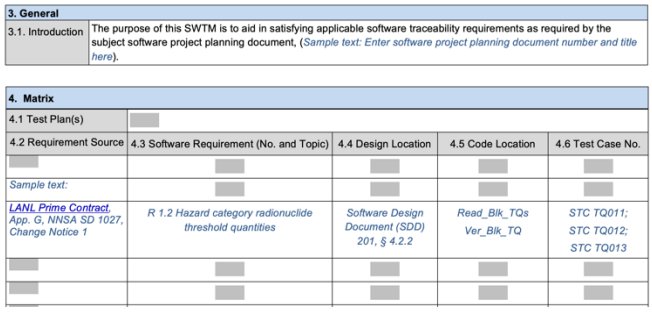

3. General	
3.1. Introduction	The purpose of this SWTM is to aid in satisfying applicable software traceability requirements as required by the subject software project planning document, (*Sample text: Enter software project planning document number and title here*).

4. Matrix				
4.1 Test Plan(s)				
4.2 Requirement Source	4.3 Software Requirement (No. and Topic)	4.4 Design Location	4.5 Code Location	4.6 Test Case No.
Sample text:				
LANL Prime Contract, App. G, NNSA SD 1027, Change Notice 1	*R 1.2 Hazard category radionuclide threshold quantities*	*Software Design Document (SDD) 201, § 4.2.2*	*Read_Blk_TQs Ver_Blk_TQ*	*STC TQ011; STC TQ012; STC TQ013*

Figure 2. Screenshot from a V&V traceability matrix form [5].

Unique Number	Requirement	Design Section	Test Case(s)
SR 3 Remove source from home repository	A capability must be provided for a user to remove a source from its home repository.	4.3	8-24
SR 3.1	The user must enter the bar code of the source and his/her Z number and be an authorized user.	4.3	8
SR 3.2	If the source is currently not located in its home repository, the user may still remove it but a warning message must be displayed instructing them to return it to the home repository when they have finished with it.	4.3	188
SR 3.3	A display must be presented indicating the source description and the transfer details.	4.3	10,18,43

Figure 3. Screenshot of an example filled-in V&V traceability matrix [6].

We thus inserted tracing information manually.

C. Data Retrieval

Our solution concept includes a data hub, which is used to handle the importing, adapting, and storing of data for internal VR access. It supports the import of XML-based ArchiMate Model Exchange File Format [44] and ReqIF files to an internal JSON format stored in a local database accessible to the VR implementation.

D. Visualization in VR

A plane is used to group the production code (test suite target) as well as the test suite. A tree map using a step pyramid paradigm (or mountain range) is used to stack containers (i.e., groups, collections, folders, directories, packages) in the third dimension (height) on the plane.

For modeling test target to test source dependencies, a visualization challenge was that we initially thought we could depict the test target code by simply overlaying a layer on the production code and indicating which test "covered" what production code. However, once we completed the dependency analysis of large projects, we found that while one test may have a test target focus, it nevertheless may indirectly invoke various other dependent portions of the test target, resulting in n-m relations between tests and the test targets. This quickly becomes visually cluttered. Thus, we chose to keep the visual depiction of the test suite separated from the test target (since it can have its own hierarchical organization), yet apply the same visualization paradigm to depict "containers" or collections as packages or folders.

E. Navigation in VR

The space that can be traversed in VR can become quite large, whereas the physical space of the VR user may be constrained, e.g., to a desk. Thus, the left controller is used for controlling flight (moving the VR camera), while the right controller is used for interaction.

F. Interaction in VR

Since interaction in VR is not yet standardized, in our concept, user-element interaction is supported primarily through the VR controllers and our *VR-Tablet*. The VR-Tablet is used to provide context-specific detailed element information, supporting an internet browser for access to any documentation. It provides a *virtual keyboard* for text entry via laser pointer key selection. While it may be potentially cumbersome to enter text via a virtual keyboard in VR compared to a real keyboard, most V&V traceability analysis will likely be focused on confirming or marking or noting issues. A potential workaround would be to record the audio during the immersion and then transcribe the notes outside of VR. Our solution could be readily extended to add annotation capabilities to elements directly.

IV. Realization

To avoid redundancy, only realization aspects not explicitly mentioned in the concept or in the evaluation sections are described in this section.

The logical architecture of our VR implementation is shown in Figure 4. VR was realized with Unity and tested with HTC Vive. Internally, besides any localized intra-model graphs, a MetaGraph script is used to determine and model both inter- and intra-relations (edges) between elements (nodes) to support bidirectional tracing across any elements or models. All exported data is stored in the data hub and accessed via scripts from Unity. The JSONUtility library was used for JSON processing.

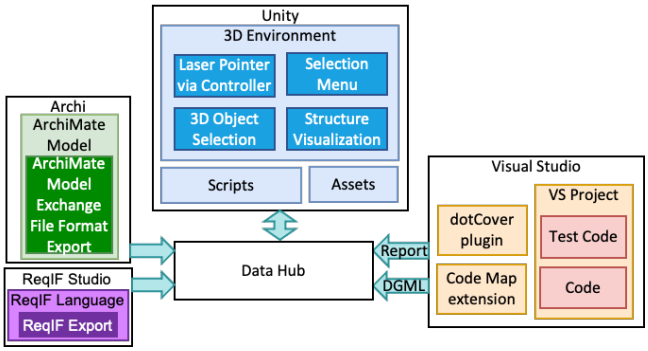

Figure 4. VR-V&V logical architecture.

A. Requirements Traceability with ReqIF and ArchiMate

While our VR-V&V requirements traceability solution concept is generic, for the prototype demonstration we focused on supporting ReqIF and ArchiMate. As shown in Figure 5, the content of an XML-based ReqIF file consists of a ReqIF Header, ReqIF ToolExtensions, and ReqIF CoreContent. CoreContent consists of primitive strongly-typed Datatypes definitions (String, Boolean, Integer, Real, Enumeration, Date, and XHTML that can include an image). SpecTypes are used to define requirement types, such as functional, quality, performance requirements, including their attributes and possible relationship types. A SpecObject is an actual requirement, and acts as container for a requirement and holds user-defined attributes, each of a specific SpecType and/or Datatype. SpecRelations represent relationships between SpecObjects and can have attributes. Specifications are a structured view of SpecObjects using hierarchical trees. A RelationGroup can be used to group relationships. The ReqIFSharp [45] library was used for importing ReqIF files.

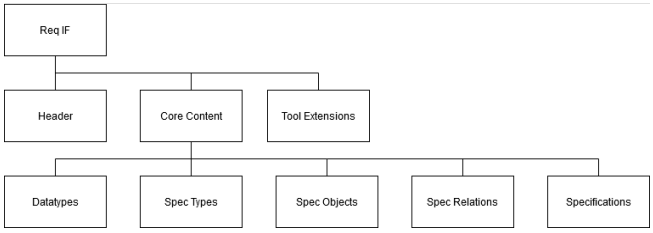

Figure 5. ReqIF structure.

The ArchiMate Exchange File (XF) format consists of three XML Schema Definitions (XSDs) that build on or include the prior: first model, then view, and then diagram exchange. Since ArchiMate is much more involved and is a full enterprise modeling language, the EF is also much more involved and won't be described here, we refer to [44] for more information.

To demonstrate traceability, in ReqIF Studio [46] ArchiMate element ID strings were manually added to ReqIF SpecObjects as External Elements: attribute TraceForeignId (e.g., id-791), TraceTypeHint (e.g., BusinessActor), TraceOriginName (filename), TraceOriginType (e.g., ArchiMate), and Trace Text to optionally name the trace, as shown in Figure 6.

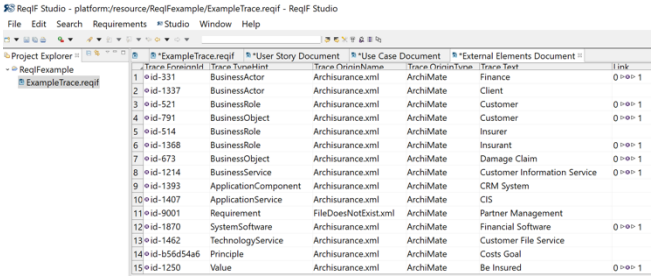

Figure 6. ReqIF Studio External Elements used for ArchiMate tracing.

Figure 7. ReqIF file snippet example of use case.

Alternatively, Requirement IDs could also be added to ArchiMate element properties to refer to the requirement. These ReqIF attributes were utilized by the MetaGraph to determine the traces. An example use case snippet from a ReqIF file is shown in Figure 7. A user story example ReqIF file snippet is shown in Figure 8.

```
<SPEC-OBJECT IDENTIFIER="_8JA3gPUwEeqsfJ3Avr3-mA" LAST-CHANGE="2020-09-12T21:51:31.849+02:00">
  <VALUES>
    <ATTRIBUTE-VALUE-STRING THE-VALUE="req-2">
      <DEFINITION>
        <ATTRIBUTE-DEFINITION-STRING-REF>__vdpIPTVEeq8E_NRH5eshA</ATTRIBUTE-DEFINITION-STRING-REF>
      </DEFINITION>
    </ATTRIBUTE-VALUE-STRING>
    <ATTRIBUTE-VALUE-STRING THE-VALUE="As a Customer, I want to buy Travel Insurance so that I can be insured.">
      <DEFINITION>
        <ATTRIBUTE-DEFINITION-STRING-REF>_1mYgUPTVEeq8E_NRH5eshA</ATTRIBUTE-DEFINITION-STRING-REF>
      </DEFINITION>
    </ATTRIBUTE-VALUE-STRING>
    <ATTRIBUTE-VALUE-STRING THE-VALUE="Buy Travel Insurance">
      <DEFINITION>
        <ATTRIBUTE-DEFINITION-STRING-REF>_xxvLgPX9Eeqx1rmdBdu4Tw</ATTRIBUTE-DEFINITION-STRING-REF>
      </DEFINITION>
    </ATTRIBUTE-VALUE-STRING>
  </VALUES>
  <TYPE>
    <SPEC-OBJECT-TYPE-REF>_FCFrQPTUEeqCtOKNSr8gpQ</SPEC-OBJECT-TYPE-REF>
  </TYPE>
</SPEC-OBJECT>
```

Figure 8. ReqIF file snippet example of user story.

To compare the realization of our VR visualization of an ArchiMate model, we use the ArchiSurance [47] example. The 2D view available in Archi [48] is shown in Figure 9. The equivalent ArchiMate diagram in VR-V&V is shown in Figure 10. Our backplane concept, with randomly colored traces of elements that exist on other diagram planes, is depicted in Figure 11. To reduce visual clutter across the diagrams, these leave from below the element and go to a backplane on which all ArchiMate diagrams are aligned, allowing one to follow a trace between diagram planes. This capability is not available in typical ArchiMate tools that offer 2D views.

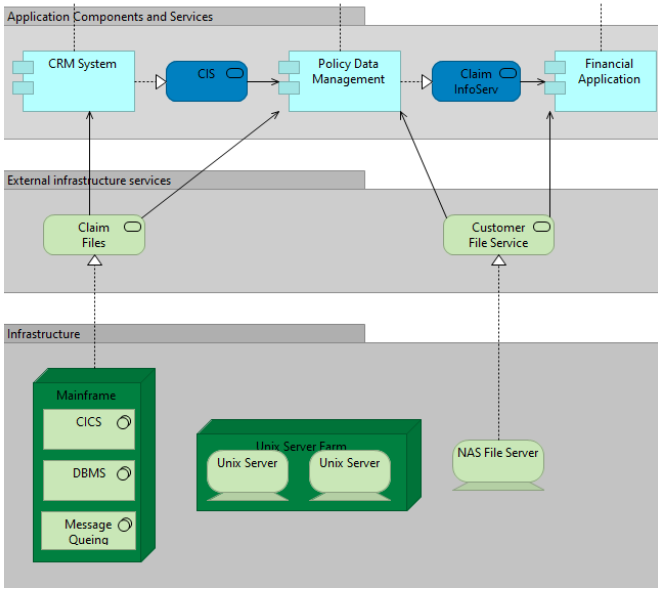

Figure 9. Screenshot of partial model of ArchiMate ArchiSurance example in the desktop Archi tool.

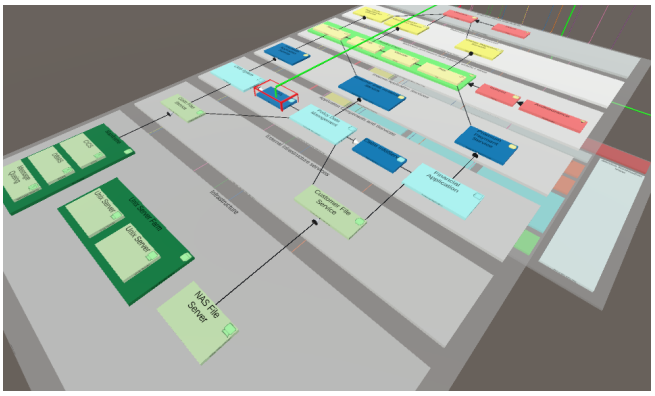

Figure 10. ArchiMate ArchiSurance example model in VR-V&V.

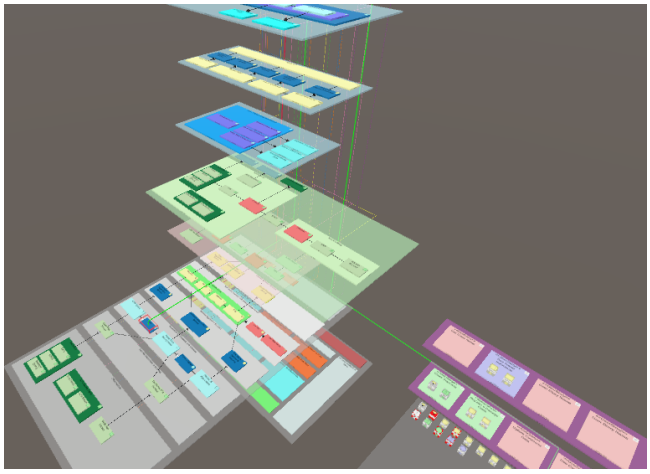

Figure 11. ArchiMate ArchiSurance example model in VR-V&V.

B. *Test Tracing Realization*

While our VR-V&V test coverage solution concept is generic, for the prototype demonstration we focused on the .NET platform. As a test coverage tool, we utilized JetBrains dotCover. This Microsoft Visual Studio plugin is a .NET Unit test runner and code coverage tool that can generate a statement coverage report in JSON, XML, etc. as shown in Figure 12. While it is a static analysis tool, it can also import coverage reports. A challenge we faced is that among the coverage tools we considered, they only report on dependencies between test targets, and do not explicitly indicate or name direct dependencies to the invoking test.

Thus, to determine C# code dependencies, Visual Studio 2022 Enterprise Edition (EE) was used, which provides a Code Map that is stored as a Directed Graph Markup Language (DGML) file. Its XML-like format is converted to JSON as shown in Figure 13. This dependency report is then partitioned into a node report and a link report. Only direct dependencies between test and test target are considered, otherwise the dependency structure could readily become very complex with large sets of intermediate nodes and their interdependencies.

```
{
  "Children" : [
    {
      "DotCoverVersion": "2021.2.2",
      "Kind": "SolutionRoot",
      "CoveredStatements": 688,
      "TotalStatements": 4869,
      "CoveragePercent": 14,
      "Children": [
        {
          "Kind": "SolutionFolder",
          "Name": "APIs",
          "CoveredStatements": 202,
          "TotalStatements": 3728,
          "CoveragePercent": 5,
          "Children": [
            {
              "Kind": "Project",
              "Name": "Geocoding.Google",
              "CoveredStatements": 190,
              "TotalStatements": 794,
              "CoveragePercent": 24,
              "Children": [
                {
                  "Kind": "Assembly",
                  "Name": "(4.0.0.0, .NETStandard,Version=v1.3)",
                  "CoveredStatements": 190,
                  "TotalStatements": 397,
                  "CoveragePercent": 48,
                  "Children": [
```


Figure 12. DotCover coverage report snippet for the Geocoding.net project.


```
{
  "DirectedGraph": {
    "-DataVirtualized": "True",
    "-Layout": "Sugiyama",
    "-ZoomLevel": "-1",
    "-xmlns": "http://schemas.microsoft.com/vs/2009/dgml",
    "Nodes": {
      "Node": [
        {
          "-Id": "(@1 @21 @107 Member=get_ShortName)",
          "-Category": "CodeSchema_Method",
          "-Bounds": "-3238.24687463366,-1648.42218743455,118.52,25.96",
          "-CodeSchemaProperty_IsCompilerGenerated": "True",
          "-CodeSchemaProperty_IsPublic": "True",
          "-DelayedCrossGroupLinksState": "Fetched",
          "-Label": "get_ShortName",
          "-self-closing": "true"
        },
        {
          "-Id": "(@1 @21 @109 @1033)",
          "-Category": "CodeSchema_Field",
          "-Bounds": "-2998.79012658679,-1526.46051751268,115.19,25.96",
          "-CodeSchemaProperty_IsPublic": "True",
          "-CodeSchemaProperty_IsStatic": "True",
          "-DelayedCrossGroupLinksState": "Fetched",
          "-Label": "Neighborhood",
          "-self-closing": "true"
        },
        {
          "-Id": "(@1 @21 @109 @1055)",
          "-Category": "CodeSchema_Field",
          "-Bounds": "-2998.79004032377,-1414.62055169237,96.2833333333333,25.96",
          "-CodeSchemaProperty_IsPublic": "True",
          "-CodeSchemaProperty_IsStatic": "True",
          "-DelayedCrossGroupLinksState": "Fetched",
          "-Label": "PostalCode",
          "-self-closing": "true"
        },
```


Figure 13. Code Map snippet (in JSON) for the Geocoding.net project for determining dependencies.

With regard to VR visualization, to attempt to retain the intuitive paradigm of test "coverage," we elected to place the test suite visualization directly above the test target, rather than on the sides as shown in Figure 14. That way, dependencies can be followed from top to bottom during VR navigation. Since the most concrete tests are typically the smallest (greatest depth being the structural leaves), the test suite uses depth to bring these closer to its target. Dependencies are then shown as lines between the test and test target, analogous to puppet strings. A selected line can be either highlighted or alternatively configured to ghost all others.

Testers focused on test coverage are typically concerned about the overall coverage (e.g., to compare its level against some high-level test goal), while also concerned about assessing details and risks as to which areas were not covered by tests. Thus, in VR our visualization of the System Under Test (SUT) or test target is shown on a plane using stepped pyramids for a 3D effect, with the coverage percentages for a container (folder, directory, package) shown on each side.

The lowest level container is on the bottom and represents the entire project. The test suite is projected above this onto a separate plane and upside-down, also using stepped pyramids for containers.

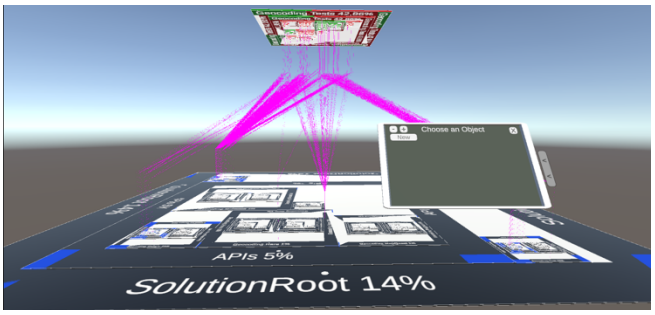

Figure 14. VR-V&V: test suite and test results visible on top, test target and code coverage shown on bottom; the VR-Tablet is visible on the right as are dependencies (magenta lines).

The test coverage of the test targets is indicated via a bar on all four sides so that from any perspective the coverage is visually indicated as seen in Figure 15. A bar graph is used on all sides, with blue visually indicating the percentage of coverage and black used for the rest (the exact coverage percentage is also shown numerically). A stepped pyramid paradigm is used to portray the granularity, with the highest cubes having the finest granularity or depth, and the lowest being the least granular. For instance, a user can quickly hone in on overall areas with little to no blue, meaning that coverage there was scarce, and one can quickly find and focus on details (without losing the overview) by focusing on the higher elevations.

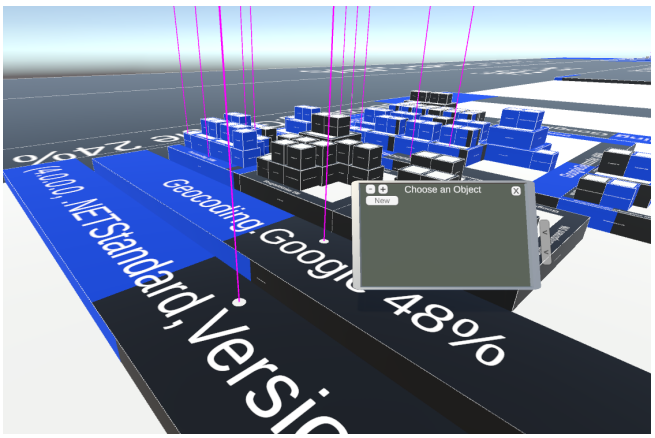

Figure 15. VR-V&V: test coverage showing stepped pyramid with highest points being finest granularity.

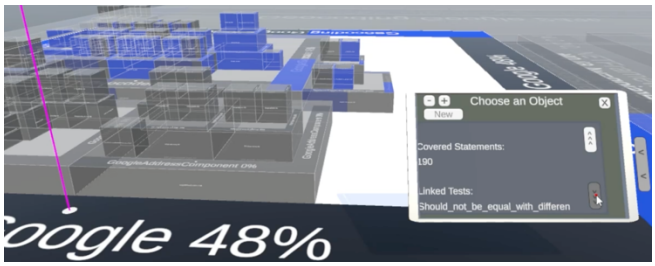

Figure 16. VR-Tablet showing coverage report details for the selected element (non-selected elements become transparent).

Selecting a test target element causes all other target elements and unassociated dependency links to become transparent, while element-relevant details from the coverage report can be inspected in the VR-Tablet as shown in Figure 16.

V. Evaluation

We base the evaluation of our solution concept on design science method and principles [49], in particular, a viable artifact, problem relevance, and design evaluation (utility, quality, efficacy). To evaluate our prototype realization of our solution concept, a case study is used based on two main scenarios supporting V&V: 1) requirements and design model tracing, and 2) test coverage and test source tracing.

A. Requirements Traceability with ArchiMate Scenario

For an example ArchiMate design model we used the ArchiSurance [47] to demonstrate requirements traceability between ReqIF-based requirements and an ArchiMate model in VR. The requirements examples used are shown in ReqIF Studio for use cases in Figure 17 and user stories in Figure 18. User stories and use cases are written as plain text.

For visualization in VR, requirements specified in a ReqIF file are placed on purple planes, with either all on a single plane or split across multiple planes if desired. A requirement can be a use case (denoted with the stereotype <<UseCase>>), a user story (denoted by the stereotype <<UserStory>>), or any other type of requirement. The color of the requirement indicates the number of relations with external elements:

- if none, it is colored red (perceived as peach here, as a warning the requirement has no trace and may be unaddressed);
- if it has at least one relation and all elements are shown, it is green (see Figure 19);
- and if it relates to more elements than can be shown on the plane, it is blue.

This can be seen in Figure 20, where only two elements are seen in the requirement, but once selected, actually four elements are traced to the external elements plane below. A selected element is outlined with red.

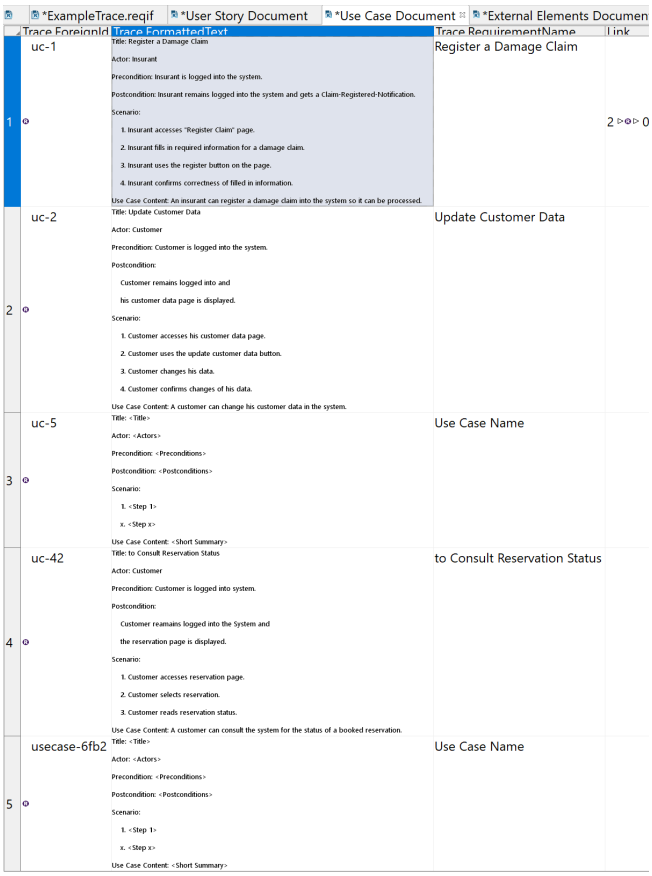

Figure 17. Screenshot of a use case document in ReqIF Studio.

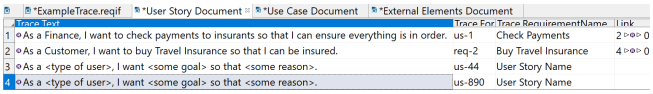

Figure 18. Screenshot of a user story document in ReqIF Studio.

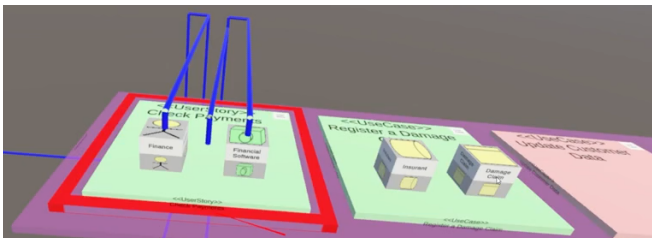

Figure 19. Selected user story (left) with requirements traces (blue) showing referenced ArchiMate elements; further use cases (to its right) depicted on requirements plane.

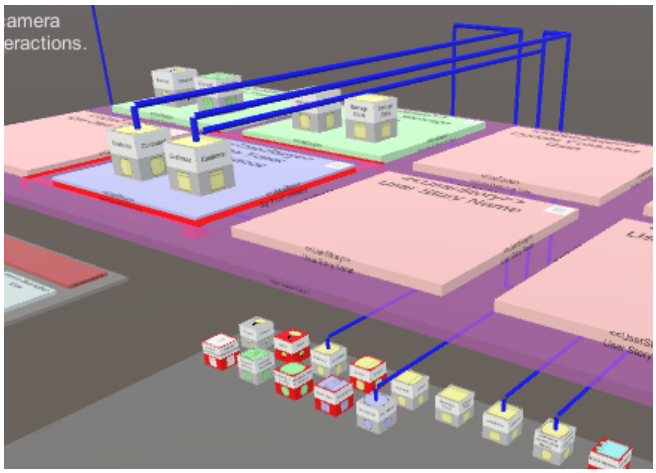

Figure 20. Selecting a blue requirement highlights additional external elements.

As shown in Figure 21, external elements specified in the ReqIF file are placed on a gray external elements plane shown below the requirements plane, and used to relate requirements elements to ArchiMate elements. Any external elements that are missing links or relations to a requirement (SpecObject, e.g., Use Case / User Story) have red colored cubes to draw attention a potential issue, while elements with satisfied associations remain gray cubes to not draw attention. Since an ArchiMate model is present and these elements are linked to it, those icons are used to indicate the type. If an element is non-existent in the ArchiMate model, then a question mark is used as its icon (the VR-tablet will still provide access to its details, the available text as provided in the ReqIF file).

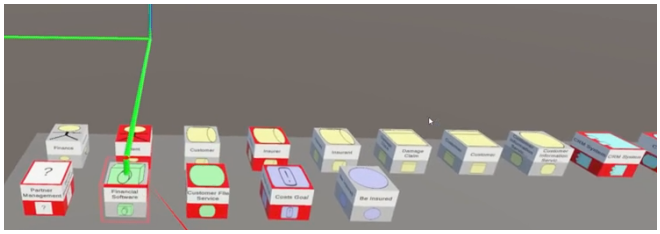

Figure 21. External elements plane: Financial Software element selected (outlined in red), green trace to location on other planes; bottom left shows an unassociated element (red) of unknown type (question mark icon).

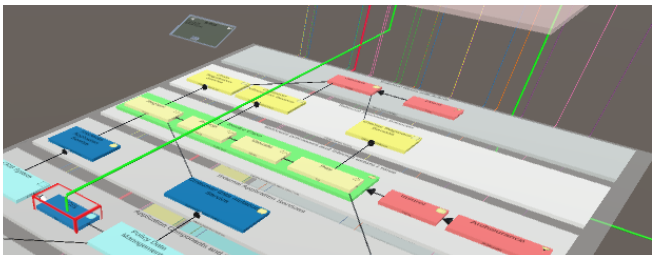

Figure 22. Highlighted ArchiMate element (red box) and green trace above.

On ArchiMate diagrams in VR, any connectors on the ArchiMate diagrams (that lie flat) have the same layout and meaning as in ArchiMate. We introduced backplane traces (see Figure 22 and Figure 23) to link and make apparent identical elements on different diagram planes. These backplane traces are randomly multi-colored and trace to the same identity elements on other diagrams and depart below the element and follow along a backplane to reduce clutter.

Selecting an external item (Figure 21) or an ArchiMate element referenced within a requirement (Figure 23) will highlight the element itself and all other elements representing the underlying artefact in the MetaGraph with an outlined red box (Figure 24). This will also produce a green trace line departing above the element linking these same elements across diagrams. A blue trace line also links the containing requirement to the external element plane.

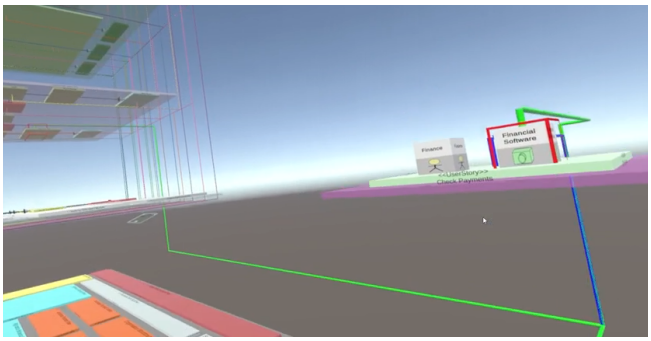

Figure 23. Financial Software element in requirement user story outlined in red with green trace to its location on other planes.

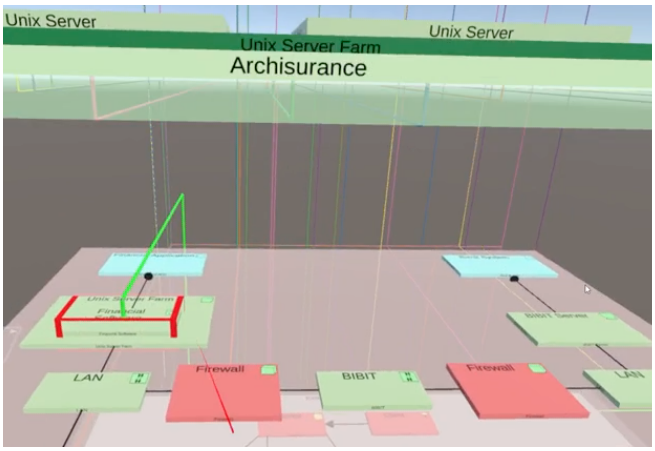

Figure 24. Financial Software element in ArchiMate diagram outlined in red with green trace its location on other planes.

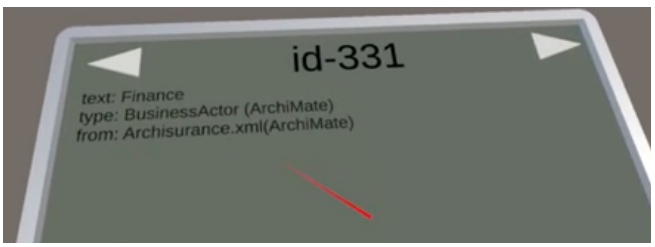

Figure 25. VR-Tablet showing details for a selected external element (not associated here with a diagram).

The VR-Tablet enables access to selected element details while in VR, such as an external element (see Figure 25), a user story (see Figure 26), a use case (see Figure 27), or an Archimate diagram element (see Figure 28).

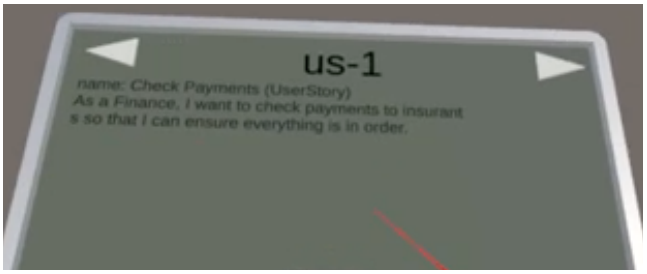

Figure 26. VR-Tablet showing details of a selected user story.

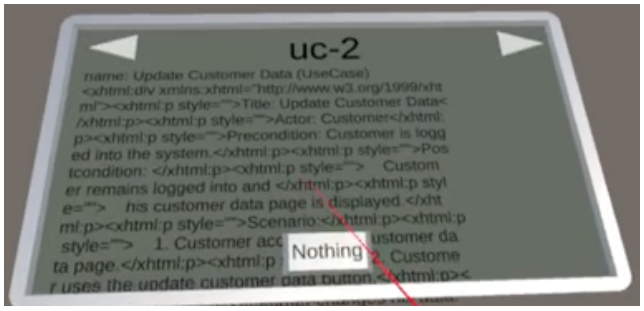

Figure 27. VR-Tablet showing details of a selected use case.

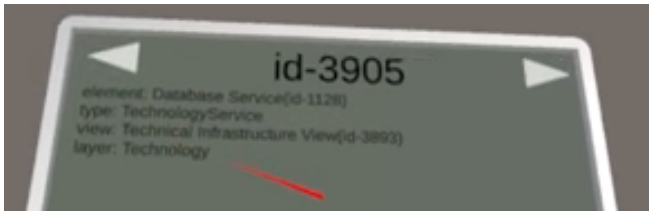

Figure 28. VR-Tablet showing details of an element selected on an ArchiMate diagram.

Thus, VR-V&V helps support trace analysis of requirements and associated elements to design model elements such as those in ArchiMate. It shows the feasibility of supporting V&V in VR, and that analogously other design modeling notations could be similarly supported. Hence, VR-V&V can support software comprehension for V&V traceability tasks by partially addressing invisibility, making links and traces visibile in the digital reality of VR, and addressing complexity limitations via the unlimited space available to present and visualize all design diagrams and requirements comprehensively.

B. Test Tracing Scenario

Our test coverage scenario considers V&V support for analyzing: 1) test results, 2) test coverage, and 3) test dependencies. For demonstration purposes, Geocoding.net [50] was used as an example C# project. However, any C# project could be used by the prototype, and currently any coverage tool could be used by mapping and transforming the report format to the DotCover JSON format.

1) Test Result Visualization

In VR, tests (and their containers) in the test suite (a.k.a. test source) are colored based on the test result status: green for successful, red if any test failed, and yellow for other (such as ignored). To depict test results and overall pass (or success) rate, the test suite is visualized as a tree map of all tests using a step pyramid for the third dimension to indicate granularity via depth. Analogously to how coverage was shown as a colored bar on all four sides of a container, on the test suite green is proportionally shown for success rate and red for failure (yellow for other), with its numerical value also given as shown in Figure 29.

Figure 29. Test suite overview; bar indicates pass percentage for a collection (green for pass, red for failed).

A closeup view showing how test case and unit test information is provided, showing the test cases (lowest and closest to the test target), the test unit (showing name and percentage), and a test container (folder or directory) is provided in Figure 30. The VR-Tablet can be used to inspect the test results for a selected test.

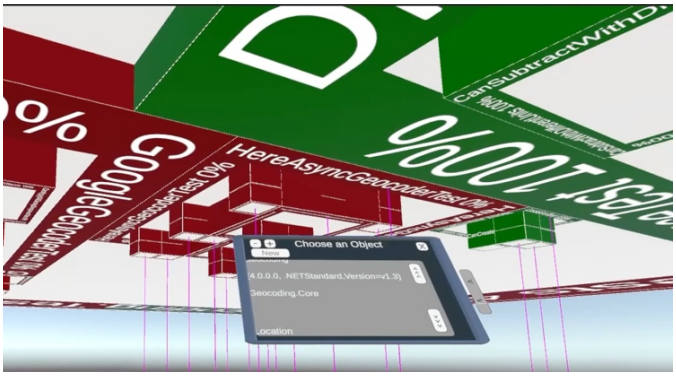

Figure 30. Test suite success shown by test case, test unit, and test container (folder or directory).

2) Test Coverage Visualization

Coverage of the test targets is shown as a bar on all four sides and on the elevation, with the blue area visually indicating the percentage of coverage, and black used for the rest, with the percentage also shown numerically, as shown in Figure 15. Details on a coverage target can also be retrieved via the VR Tablet as shown in Figure 16.

3) Test Dependency Trace Visualization

V&V support for test dependencies is typically not supported by test tools. Thus, VR-V&V supports a test

dependency view, with which stakeholders can view which tests are directly invoking or reaching which target code. Typically, by convention tests are named in such a way to express the test target, yet the actual dependencies could nevertheless differ from expectations. This is especially true if the test suite consists not only of unit tests but also integration or system tests. By eliminating the guess work, dependencies could be used to determine which tests are primarily reaching a target, and then focus on extending that test in order to increase the target coverage. One challenge is that there is not necessarily a 1-1 match of a test to its test target, thus dependency links provide a way to visualize these hitherto hidden dependencies.

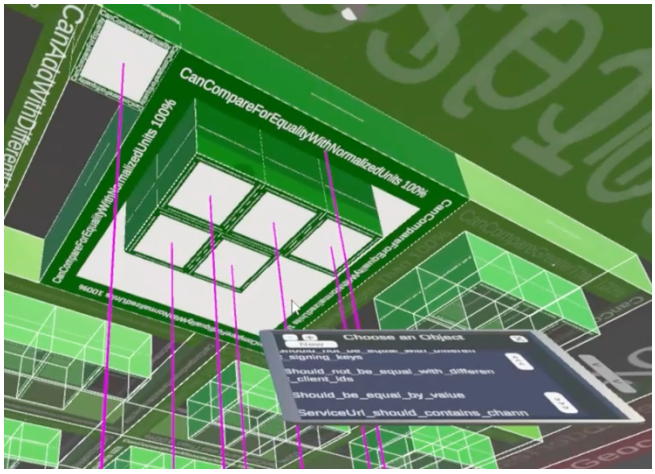

Figure 31. Magenta traces can be followed to dependent test cases.

VR-V&V depicts the test dependencies of a selected target as a magenta-colored trace line. When a selected test target or trace is followed, the associated test cases in the test suite are opaque, perceived as dark green in Figure 31. And tests can be followed to the most granular level of the test case which remain opaque as seen in Figure 32. Unassociated tests are made partially transparent (perceived as bright green, bright red, or grey).

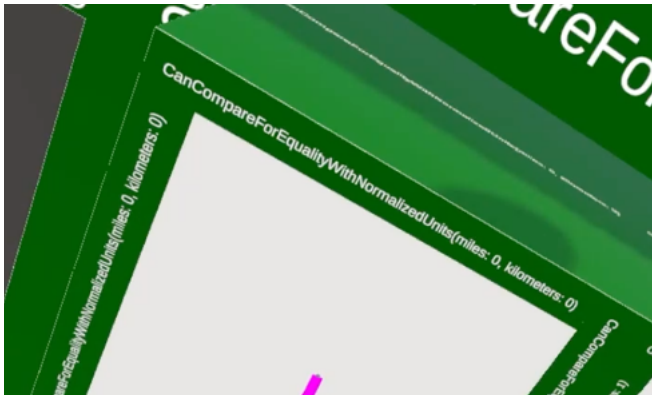

Figure 32. Bottom view showing dependent test cases and pass rate.

The VR-Tablet can be used to inspect test report details about a selected test object, with the test method (CanCompareForEqualityWithNormalizedUnits), test data input values (miles: 1, kilometers: 1.609344), and test status (success) shown in Figure 33.

Figure 33. VR-Tablet showing test case details.

Figure 34. When a test element is selected, non-applicable target areas are greyed out.

These traces can be followed to the test target plane to determine what (sub)target(s) a selected test is actually reaching, as can be seen in Figure 34. The non-relevant test target areas are then partially transparent.

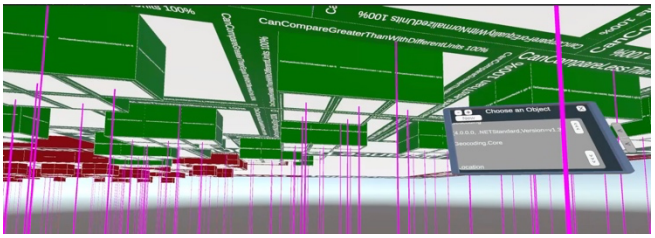

Figure 35. All test dependencies shown (by toggling selection).

By unselecting a test element, all dependency traces are restored and all test elements opaque, as can be seen in Figure 35. Thus, one can trace overall test groups or determine that certain tests are perhaps in preparation, or not (as yet) traceable or related to the test target if trace dependencies are missing. E.g., this might occur if tests were written before the production code has been implemented (e.g., in the case of acceptance test-driven techniques). Alternatively, this could be an indicator of a test suite and test target mismatch, perhaps if the production code was significantly changed without making associated changes to the test suite.

C. Discussion

The test tracing scenario shows the ability of VR-V&V to support test result tracing, test coverage, and test dependency tracing. To reduce test redundancy, measuring test target coverage can help focus test development on those areas that are not yet sufficiently tested or have the most risk. As software projects grow, it can be difficult to visualize both the software product and the software testing area and their dependencies. While direct tracing of requirements to tests was not shown in the evaluation, its feasibility is apparent via inclusion of test associations in ReqIF SpecObject attributes using a test-based TraceOriginType and associated attributes, analogous to the ReqIF scenario.

VI. Conclusion

As software size and its quality expectations grow, its invisibility and complexity affect software comprehension for V&V stakeholders. VR-V&V contributes an immersive solution concept for supporting bidirectional traceability of requirements to design elements and analysis of software testing dependencies and coverage. The prototype realization showed the feasibility of supporting immersive bidirectional traceability as well as immersive software test coverage and analysis. The evaluation results based on a case study demonstrated its capabilities, in particular traceability support involving ReqIF, ArchiMate models, test results, test coverage, and test source to test target dependency tracing. Performing analysis tasks in VR provides a unique immersive experience that can enhance and make visible often "invisible" traces between various digital artifacts, while providing a potential motivational aspect to V&V tasks in general.

Future work includes: integration with VR-SysML, VR-UML, and VR-Git with expanded support for traceability across of all lifecycle artifacts; support for V&V collaboration and annotations; and conducting a comprehensive empirical study. An automated approach for detecting and associating test and code artifacts with requirements is described in our prior work VR-SysML+Traceability. We thus intend to explore automated code-level traceability support and integration of VR-Git to support commit traceability.

Acknowledgment

The author would like to thank Jakob Loskan and Lukas Tobias Westhäußer and for their assistance with the design, implementation, figures, and evaluation.

References

[1] R. Oberhauser, "VR-TestCoverage: Test Coverage Visualization and Immersion in Virtual Reality," The Fourteenth International Conference on Advances in System Testing and Validation Lifecycle (VALID 2022), IARIA, 2022, pp. 1-6.

[2] IEEE, "IEEE Standard for Software Quality Assurance Processes," IEEE Std 730-2014, IEEE, 2014.

[3] IEEE, "Systems and software engineering—Vocabulary," ISO/IEC/IEEE 24765:2010, IEEE, 2010.

[4] IEEE, "IEEE Standard for System, Software, and Hardware Verification and Validation," IEEE Std 1012-2016, IEEE, 2017.

[5] Los Alamos National Laboratory, "Form 3056 - Software Requirements Traceability Matrix (SWTM)," 2018. [Online]. Available from: https://engstandards.lanl.gov/esm/software/Form-3056.docx 2023.11.13

[6] Los Alamos National Laboratory, "Source Tracker Software Requirements Traceability Matrix," 2016. [Online]. Available from: https://engstandards.lanl.gov/esm/software/Form-3056.docx 2023.11.13

[7] F.P. Brooks, Jr., The Mythical Man-Month. Boston, MA: Addison-Wesley Longman Publ. Co., Inc., 1995.

[8] R. Müller, P. Kovacs, J. Schilbach, and D. Zeckzer, "How to master challenges in experimental evaluation of 2D versus 3D software visualizations," In: 2014 IEEE VIS International Workshop on 3Dvis (3Dvis), IEEE, 2014, pp. 33-36.

[9] R. Oberhauser, "VR-UML: The unified modeling language in virtual reality – an immersive modeling experience," International Symposium on Business Modeling and Software Design, Springer, Cham, 2021, pp. 40-58.

[10] R. Oberhauser, "VR-SysML: SysML Model Visualization and Immersion in Virtual Reality," International Conference of Modern Systems Engineering Solutions (MODERN SYSTEMS 2022), IARIA, 2022, pp. 59-64.

[11] OMG, "Unified modeling language version 2.5.1," Object Management Group, 2019

[12] OMG, "OMG Systems Modeling Language Version 1.6," Object Management Group, 2019.

[13] R. Oberhauser and C. Pogolski, "VR-EA: Virtual Reality Visualization of Enterprise Architecture Models with ArchiMate and BPMN," In: Shishkov, B. (ed.) BMSD 2019. LNBIP, vol. 356, Springer, Cham, 2019, pp. 170–187.

[14] Open Group, "ArchiMate 3.2 Specification," The Open Group, 2022.

[15] R. Oberhauser, "VR-SysML+Traceability: Immersive Requirements Traceability and Test Traceability with SysML to Support Verification and Validation in Virtual Reality," International Journal on Advances in Software, Volume 16, Numbers 1 & 2, 2023, pp. 23-35. ISSN: 1942-2679

[16] OMG, "Requirements Interchange Format (ReqIF) Version 1.2", OMG, 2016

[17] Y. Li and W. Maalej, "Which Traceability Visualization Is Suitable in This Context? A Comparative Study," In: Regnell, B., Damian, D. (eds) Requirements Engineering: Foundation for Software Quality (REFSQ 2012), LNCS, vol 7195. Springer, Berlin, Heidelberg, 2012. https://doi.org/10.1007/978-3-642-28714-5_17

[18] Z.S.H. Abad, M. Noaeen, and G. Ruhe, "Requirements Engineering Visualization: A Systematic Literature Review," 2016 IEEE 24th International Requirements Engineering Conference (RE), Beijing, China, 2016, pp. 6-15, doi: 10.1109/RE.2016.61.

[19] A.A. Madaki and W.M.N.W. Zainon, "A Review on Tools and Techniques for Visualizing Software Requirement Traceability," In: Mahyuddin, N.M., Mat Noor, N.R., Mat Sakim, H.A. (eds) Proceedings of the 11th International Conference on Robotics, Vision, Signal Processing and Power Applications, Lecture Notes in Electrical Engineering, vol 829, Springer, Singapore, 2022. https://doi.org/10.1007/978-981-16-8129-5_7.

[20] IBM Engineering Requirements Management DOORS Next. [Online]. Available from: https://www.ibm.com/products/requirements-management-doors-next 2023.11.13

[21] Perforce Helix ALM. [Online]. Available from: https://www.perforce.com/products/helix-alm 2023.11.13

[22] Sparx Systems Enterprise Architect. [Online]. Available from: https://sparxsystems.com/enterprise_architect_user_guide/14.0/model_navigation/elementrelationshipmatrix.html 2023.11.13

[23] J. Vincur, P. Navrat, and I. Polasek, "VR City: Software analysis in virtual reality environment," In 2017 IEEE international conference on software quality, reliability and security companion (QRS-C), IEEE, 2017, pp. 509-516.

[24] K. Dreef, V.K. Palepu, and J.A. Jones, "Global Overviews of Granular Test Coverage with Matrix Visualizations," 2021 Working Conference on Software Visualization (VISSOFT), 2021, pp. 44-54, doi: 10.1109/VISSOFT52517.2021.00014

[25] A. Rahmani, J.L. Min, and A. Maspupah, "An evaluation of code coverage adequacy in automatic testing using control flow graph visualization," In 2020 IEEE 10th Symposium on Computer Applications & Industrial Electronics (ISCAIE), IEEE, 2020, pp. 239-244.

[26] F. Pecorelli, G. Di Lillo, F. Palomba, and A. De Lucia, "VITRuM: A plug-in for the visualization of test-related metrics," Proc. Int'l Conf. on Adv. Visual Interfaces (AVI '20), ACM, 2020, pp. 1-3, doi: 10.1145/3399715.3399954

[27] K. Alemerien and K. Magel, "Examining the effectiveness of testing coverage tools: An empirical study," Int'l J of Software Engineering and its Applications, 8(5), 2014, pp.139-162.

[28] K. Sakamoto, K. Shimojo, R. Takasawa, H. Washizaki, and Y. Fukazawa, "OCCF: A Framework for Developing Test Coverage Measurement Tools Supporting Multiple Programming Languages," 2013 IEEE Sixth International Conference on Software Testing, Verification and Validation, 2013, pp. 422-430, doi: 10.1109/ICST.2013.59

[29] R. Oberhauser, "VR-Git: Git Repository Visualization and Immersion in Virtual Reality," The Seventeenth International Conference on Software Engineering Advances (ICSEA 2022), IARIA, 2022, pp. 9-14.

[30] R. Oberhauser, "VR-ProcessMine: Immersive Process Mining Visualization and Analysis in Virtual Reality," International Conference on Information, Process, and Knowledge Management (eKNOW 2022), IARIA, 2022, pp. 29-36.

[31] R. Oberhauser, C. Pogolski, and A. Matic, "VR-BPMN: Visualizing BPMN models in Virtual Reality," In: Shishkov, B. (ed.) BMSD 2018. LNBIP, vol. 319, Springer, Cham, 2018, pp. 83–97. https://doi.org/10.1007/978-3-319-94214-8_6

[32] R. Oberhauser, P. Sousa, and F. Michel, "VR-EAT: Visualization of Enterprise Architecture Tool Diagrams in Virtual Reality," In: Shishkov B. (eds) Business Modeling and Software Design. BMSD 2020. LNBIP, vol 391, Springer, Cham, 2020, pp. 221-239. doi: 10.1007/978-3-030-52306-0_14

[33] R. Oberhauser, M. Baehre, and P. Sousa, "VR-EA+TCK: Visualizing Enterprise Architecture, Content, and Knowledge in Virtual Reality," In: Shishkov, B. (eds) Business Modeling and Software Design. BMSD 2022. LNBIP, vol 453, pp. 122-140. Springer, Cham. doi:10.1007/978-3-031-11510-3_8

[34] R. Oberhauser, M. Baehre, and P. Sousa, "VR-EvoEA+BP: Using Virtual Reality to Visualize Enterprise Context Dynamics Related to Enterprise Evolution and Business Processes," In: Shishkov, B. (eds) Business Modeling and Software Design. BMSD 2023. LNBIP, vol 483. Springer, Cham, 2023. https://doi.org/10.1007/978-3-031-36757-1_7

[35] ISO/IEC, "Software Engineering — Guide to the software engineering body of knowledge (SWEBOK)," ISO/IEC TR 19759:2015, 2015.

[36] ISO/IEC/IEEE, "International Standard - Software and systems engineering--Software testing--Part 4: Test techniques," ISO/IEC/IEEE 29119-4:2015, 2015, doi: 10.1109/IEEESTD.2015.7346375

[37] L. Inozemtseva and R. Holmes, "Coverage is not strongly correlated with test suite effectiveness," Proc. 36th Int'l Conf. on Software Eng. (ICSE 2014), ACM, 2014, pp. 435-445.

[38] M. Ivanković, G. Petrović, R. Just, and G. Fraser, "Code coverage at Google," Proc. 2019 27th ACM Joint Meeting on European Software Engineering Conf. and Symposium on the Foundations of Software Eng., ACM, 2019, pp. 955-963.

[39] R. Potvin and J. Levenberg, "Why Google stores billions of lines of code in a single repository," Communications of the ACM 59, 7 (July 2016), 2016, pp. 78–87. https://doi.org/10.1145/2854146

[40] Evans Data Corporation. [Online]. Available from: https://evansdata.com/press/viewRelease.php?pressID=293 2023.11.13

[41] The Open Group, "Agile Architecture Modeling Using the ArchiMate Language," Guide (G20E), The Open Group, 2020.

[42] The Open Group, "Using the ArchiMate® Language with UML," White Paper (W134), The Open Group, 2013.

[43] ISO/IEC/IEEE, "ISO/IEC/IEEE International Standard - Systems and software engineering -- Life cycle processes -- Requirements engineering," in ISO/IEC/IEEE 29148:2018(E), 2018, doi: 10.1109/IEEESTD.2018.8559686.

[44] The Open Group, "ArchiMate Model Exchange File Format for the ArchiMate Modeling Language, Version 3.0," U191, 2019.

[45] ReqIFSharp. [Online]. Available from: https://reqifsharp.org 2023.11.13

[46] ReqIF Studio. [Online]. Available from: https://www.reqif.academy/software/reqif-studio/ 2023.11.13

[47] The Open Group: ArchiSurance Case Study, Version 2. The Open Group (2017a).

[48] Archi. [Online]. Available from: https://www.archimatetool.com 2023.11.13

[49] A.R. Hevner, S.T. March, J. Park, and S. Ram, "Design science in information systems research," MIS Quarterly, 28(1), 2004, pp. 75-105

[50] Geocoding.net [Online]. Available from: https://github.com/chadly/Geocoding.net 2023.11.13

Fine-tuning BERT with Bidirectional LSTM for Fine-grained Movie Reviews Sentiment Analysis

Gibson Nkhata, Susan Gauch
Department of Computer Science & Computer Engineering
University of Arkansas
Fayetteville, AR 72701, USA
Email: gnkhata@uark.edu, sgauch@uark.edu

Usman Anjum, Justin Zhan
Department of Computer Science
University of Cincinnati
Cincinnati, OH 45221, USA
Email: anjumun@ucmail.uc.edu, zhanjt@ucmail.uc.edu

***Abstract*—Sentiment Analysis (SA) is instrumental in understanding people's viewpoints, facilitating social media monitoring, recognizing products and brands, and gauging customer satisfaction. Consequently, SA has evolved into an active research domain within Natural Language Processing (NLP). Many approaches outlined in the literature devise intricate frameworks aimed at achieving high accuracy, focusing exclusively on either binary sentiment classification or fine-grained sentiment classification. In this paper, our objective is to fine-tune the pre-trained BERT model with Bidirectional LSTM (BiLSTM) to enhance both binary and fine-grained SA specifically for movie reviews. Our approach involves conducting sentiment classification for each review, followed by computing the overall sentiment polarity across all reviews. We present our findings on binary classification as well as fine-grained classification utilizing benchmark datasets. Additionally, we implement and assess two accuracy improvement techniques, Synthetic Minority Oversampling Technique (SMOTE) and NLP Augmenter (NLPAUG), to bolster the model's generalization in fine-grained sentiment classification. Finally, a heuristic algorithm is employed to calculate the overall polarity of predicted reviews from the BERT+BiLSTM output vector. Our approach performs comparably with state-of-the-art (SOTA) techniques in both classifications. For instance, in binary classification, we achieve 97.67% accuracy, surpassing the leading SOTA model, NB-weighted-BON+dv-cosine, by 0.27% on the renowned IMDb dataset. Conversely, for five-class classification on SST-5, while the top SOTA model, RoBERTa+large+Self-explaining, attains 55.5% accuracy, our model achieves 59.48% accuracy, surpassing the BERT-large baseline by 3.6%.**

***Index Terms*—Sentiment analysis; movie reviews; BERT, bidirectional LSTM; overall sentiment polarity.**

I. Introduction

This paper builds upon our prior research [1] into sentiment analysis (SA) of movie reviews using Bidirectional Encoder Representations from Transformers (BERT) [2] and computing overall polarity within the scope of binary sentiment classification. Still, SA aims to discern the polarity of emotions (e.g., happiness, sorrow, grief, hatred, anger, and affection) and opinions derived from text, reviews, and posts across various media platforms [3]. It plays a crucial role in gauging public sentiment, serving as a potent marketing tool for comprehending customer emotions across diverse marketing campaigns. SA significantly contributes to social media monitoring, brand recognition, customer satisfaction, loyalty, advertising effectiveness, and product acceptance. Consequently, SA stands as one of the most sought-after and impactful tasks within Natural Language Processing (NLP) [4]. It encompasses polarity classification, involving binary categorization, and fine-grained classification, encompassing multi-scale sentiment distribution.

Movie reviews serve as a crucial means to evaluate the performance of a film. While assigning a numerical or star rating offers a quantitative assessment of a movie's success or failure, a collection of movie reviews offers a qualitative exploration of various aspects within the film. Textual movie reviews provide insights into strengths and weaknesses of a movie, allowing for a deeper analysis that gauges the overall satisfaction of the reviewer. This study focuses on SA of movie reviews due to the availability of standardized benchmark datasets and the existence of significant qualitative works within this domain, as highlighted in publications such as [5].

BERT stands as a renowned pre-trained language representation model, demonstrating strong performance across various NLP tasks such as named entity recognition, question answering, and text classification [2]. Its versatility extends to information retrieval, where it has been leveraged to construct efficient ranking models for industry-specific applications [6]. Additionally, its adaptability is evident in applications like extractive summarization of text, as successfully demonstrated in [7], and in question answering tasks, where it yielded satisfactory results as seen in [8]. The model's efficacy was further highlighted in data augmentation strategies, leading to superior outcomes, as exemplified in [9]. While BERT has found primary use in SA [10], its accuracy on certain datasets remains a challenge.

Ambiguity in NLP, particularly SA, arises due to the complexity of language. Words and phrases often carry multiple meanings or interpretations based on context, making it challenging to accurately discern sentiment. This challenge is evident in instances where words might have different connotations depending on their context within a sentence or across diverse texts. BERT addresses this issue by leveraging its bidirectional context understanding [2]. Unlike earlier models that processed language in one direction, BERT comprehends words based on both preceding and succeeding

Extend version of Sentiment Analysis of Movie Reviews Using BERT, presented at The Fifteenth International Conference on Information, Process, and Knowledge Management, eKNOW23, Venice, Italy, 2023.

words, allowing it to capture a more nuanced understanding of context. Therefore, BERT can better grasp the intricate meanings and resolve ambiguities present in natural language, thereby improving SA accuracy.

Bidirectional Long Short-Term Memory (BiLSTM) networks are also very popular for text classification in NLP [11]. BiLSTM is beneficial in SA due to its ability to capture contextual information from both past and future inputs in long sequences [12]. In SA, context is crucial, words derive their meaning not just from preceding words but also from the subsequent ones. BiLSTMs excel in capturing this bidirectional context by processing sequences in two directions simultaneously: forward (from the beginning to the end of a sequence) and backward (from the end to the beginning). This capability enables BiLSTMs to model more nuanced and complex dependencies in text, leading to improved SA performance compared to unidirectional models.

Fine-tuning is a common technique for transfer learning. The target model copies all model designs with their parameters from the source model except the output layer and fine-tunes these parameters based on the target dataset [2]. The main benefit of fine-tuning is no need to train the entire model from scratch, reducing the training time of the target model. Hence, we are fine-tuning BERT by coupling BiLSTM and training the model on movie reviews SA benchmarks. BERT, with its attention mechanisms and bidirectional context understanding, captures rich contextual information [2]. Combining it with a BiLSTM enhances this capability further. The ability of the BiLSTM to retain long-range dependencies complements contextual understanding of BERT, leading to a more nuanced comprehension of sentiment in text. The efficacy of this amalgamation is corroborated by conducting an ablation study in our experiments.

In our approach, we derive an overall polarity from the output vector generated by BERT+BiLSTM, employing a heuristic algorithm adapted from [13]. This algorithm is tailored uniquely in our study, addressing the specifics of the output vectors derived from binary, three-class, four-class, or five-class sentiment classifications. As a result, our work implements four distinct iterations of the algorithm, each corresponding to one of the four different sentiment classification tasks undertaken in this research.

Previous studies have predominantly focused on either binary sentiment classification or fine-grained SA, rarely combining both aspects. This paper addresses this gap by presenting an approach that fine-tunes BERT specifically for SA on movie reviews. Our objective is to conduct a comparative analysis encompassing both binary and fine-grained sentiment classifications. Through the integration of BERT and BiLSTM architecture, our fine-tuning methodology caters to both binary and fine-grained sentiment classification tasks. Notably, our approach surpasses state-of-the-art (SOTA) models in accuracy using our best-performing method. To address the challenge of class imbalance in fine-grained classification, we implement oversampling and data augmentation techniques on the respective datasets before feeding the data into the model classifier.

The main contributions in this work are as follows:

- Fine-tune BERT by coupling it with BiLSTM for both binary and fine-grained sentiment classification on well-known benchmark datasets and achieve accuracy that surpasses SOTA models.
- Refine techniques to enhance the model's accuracy in fine-grained sentiment classification.
- Compute the overall sentiment polarity of predicted reviews based on the output vector from BERT+BiLSTM.
- Compare and evaluate our experimental outcomes against the results obtained from other studies, including those from SOTA models, using benchmark datasets.

This paper is organized as follows: Section II describes the related work, Section III details the methodology, Section IV discusses the experiments and results, and finally, Section V presents the conclusion and discusses future work.

II. Related work

This section covers relevant literature concerning SA, the intersection of deep learning and SA, particularly focusing on movie reviews SA, and the role of BERT in SA.

A. SA

SA within NLP remains an active area of research. [14] introduced a step-by-step lexicon-based SA method using the R open-source software. The study conducted polarity classification on 1,000 movie reviews from the IMDb dataset, achieving an accuracy of 81.30% by evaluating built-in lexicons.

In a contrasting approach, [3] explored traditional machine learning techniques, i.e., Naive Bayes (NB), K-Nearest Neighbours (KNN), and Random Forests, for SA on IMDb movie reviews. Their findings highlighted NB as the top performer, achieving an accuracy of 81.45%.

A different route was taken in [4], deploying an ensemble generative technique across multiple machine learning approaches for movie reviews SA, achieving an accuracy of 90.57%. Conversely, [15] focused on the Cornell movie review dataset, solely utilizing KNN with the information gain technique, yielding an accuracy of 90.8%. These studies underscore the effectiveness of KNN in traditional machine-learning methods for movie reviews SA.

A novel approach by training document embeddings using cosine similarity and feature combination with NB weighted bag of *n*-grams was proposed in [16]. Their comparison between training document embeddings using cosine similarity and dot product favored cosine similarity, achieving an accuracy of 91.42% on the IMDb dataset. In addition, [17] applied mixed objective function for binary classification on SA on IMDb benchmark. Their approach reported an error rate of 9.95%. The aforementioned models targeted polarity or binary sentiment classification only. Nevertheless, both binary classification and fine-grained classifications on SA were implemented in the following two studies. [18] used transfer learning, while [19], utilised entailment and few-shot learning. Both studies used IMDb, SST-2, and MR benchmarks

for binary classification, and Yelp and SST-5 for fine-grained classification. Average accuracy of 87.57% is reported in [18] on binary datasets, while [19] has reported 88.16%. For fine-grained classification, they reported average accuracy of 52.65% and 54.65%, respectively.

In our work, we adopt both polarity and fine-grained classifications from [19] but use deep learning techniques and the BERT pre-trained language model. We also adopt transfer learning from [18].

B. Deep learning

This section explores the realm of deep learning applied to both the general SA task and specifically to movie reviews SA.

1) Deep Learning on SA: Deep learning stands as a SOTA technique for many NLP tasks, including SA. In a study by [20], Character-level Convolutional Neural Networks (CCNNs) were explored for text classification using Yelp and Amazon benchmarks. These CCNNs were compared against bag-of-words, n-grams, their TF-IDF variants, word-based CNNs, and Recurrent Neural Networks (RNNs). Reported error rates were 7.82% and 6.93% on the Yelp and Amazon benchmarks, respectively. Notably, on Yelp, the *n*-grams model outperformed the CCNNs with a 6.36% error rate. The study highlighted several influencing factors on model performance, including dataset size, text curation, and the alphabet used, specifically distinguishing between uppercase and lowercase letters.

In a separate study, [21] introduced a unique approach using CNNs with meta-networks to learn context-sensitive convolutional filters for text processing. Applying this approach on Yelp, they achieved a lower error rate of 4.89% compared to the former CCNNs approach. However, deeper networks pose increased computational complexity, impacting practical applications. Addressing this, [22] proposed shallow word-based Deep Pyramid CNNs (DPCNN) for text categorization. They studied deepening word-level CNNs to capture comprehensive text representations without significantly increasing computational costs. Evaluating on Yelp and Amazon datasets, their method achieved error rates of 7.88% and 7.92%, respectively.

2) Deep Learning on Movie Reviews SA: To commence, [23] explored the performances of RNNs and CNNs architectures for SA of movie reviews. They utilized pre-defined 300-dimensional vectors from word2vec [24] instead of training word vectors along with other parameters using samples. The study indicated that CNNs outperformed RNNs, achieving the best accuracy of 46.4% on the SST dataset. It was concluded that basic RNNs were inefficient in capturing the structural and contextual properties of sentences. Basic RNNs encounter issues such as vanishing or exploding gradients, leading to model underfitting and overfitting when networks become very deep. Addressing this challenge, [25] proposed Coupled Oscillatory RNN (CoRNN), a time-discretization of a system of second-order ordinary differential equations, which mitigated the exploding and vanishing gradient problem. CoRNN achieved 87.4% accuracy on IMDb by precisely bounding the gradients of hidden states.

LSTMs also contribute to mitigating these problems. [26] applied LSTM on movie review SA, exploring different hyperparameters like dropout, number of layers, and activation functions. Their LSTM configuration, including embedding, LSTM layer, dense layer, 0.5 dropout, and 100 LSTM units, achieved an accuracy of 88.46% on IMDb. Although LSTMs handle longer sequences efficiently, whether the incorporated gates in the LSTM architecture offer sufficient generalization or additional data training is required remains unclear [11]. To address this, [17] applied a BiLSTM network using a mixed objective function for text classification, employing both supervised and unsupervised approaches. Their study showcased that a simple BiLSTM model using maximum likelihood training delivered competitive performance in polarity classification, reporting a 6.07% error rate.

Although BiLSTM displayed superior results compared to other deep learning methods, room for performance enhancement remains at a 6.07% error rate. Hence, in our work, BiLSTM is adopted to further improve performance in this task.

C. BERT

This section delves into works that utilize BERT for SA and specifically for analyzing movie reviews.

1) BERT and SA: BERT stands out as a renowned SOTA language model for its exceptional performance across various NLP tasks. For instance, in the realm of SA, [27] delved into attention mechanisms and pre-trained hidden representations of BERT for Aspect-Based SA (ABSA). Their analysis revealed BERT's utilization of minimal self-attention heads to encode contextual words, such as prepositions or pronouns indicating an aspect, and opinion words associated with aspects. Conversely, [28] explored the potential of contextualized embeddings from BERT in an end-to-end ABSA task, focusing on integrating BERT embeddings with various neural models. Their findings showcased the impressive performance of BERT when combined with models like Gated Recurrent Units (GRU).

In a similar vein, [29] leveraged the pre-trained BERT model for target-dependent sentiment classification, examining its context-aware representation for potential improvements in ABSA. Their study revealed that coupling BERT with complex neural networks previously effective with embedding representations did not add substantial value to ABSA.

Other investigations of BERT involve transfer learning approaches. [30] fine-tuned a pre-trained BERT model for ABSA by transforming ABSA into a sentence-pair classification task, achieving an impressive 92.8% accuracy on the SentiHood dataset. Meanwhile, [31] explored BERT for fine-tuning on Review Reading Comprehension (RRC) and ABSA tasks, generating a ReviewRC dataset from a benchmark for ABSA. Their novel post-training fine-tuning approach on BERT achieved an accuracy of 90.47%.

These studies collectively showcase effective fine-tuning techniques with BERT, particularly in ABSA tasks. In our work, inspired by the coupling technique used in [28], we opt to couple BERT with BiLSTM for the movie reviews SA task.

2) BERT and Movie Reviews SA: In the realm of movie reviews, [32] employed BERT to transform words into contextualized word embeddings. They fine-tuned BERT's parameters using the IMDb movie reviews corpus through Inductive Conformal Prediction (ICP), achieving an accuracy of 92.28%. In contrast, [33] pursued a different approach, comparing BERT against SentiWordNet [34], logistic regression, and LSTM for Movie Reviews SA on the IMDb dataset. Their study aimed to ascertain the relative efficacy of the four SA algorithms, highlighting the undeniable superiority of the pre-trained advanced supervised BERT model in text sentiment classification. BERT notably outperformed other models, achieving an accuracy of 92.31%. Notably, both studies focused on binary classification.

Conversely, [10] employed BERT for both binary and fine-grained classifications on SST-2 and SST-5 datasets, respectively. Their model showcased superior performance compared to other deep learning-based models, such as CNN and RNN, achieving an accuracy of 93.7% on SST-2 and 55.5% on SST-5 tasks.

It is evident that deep learning techniques have proven to be the most accurate approaches for SA. Transfer learning, particularly fine-tuning BERT, consistently yields outstanding results. However, despite the reported advancements and the capabilities of BERT, there remains significant potential to further enhance the pre-trained language model's performance in this field. Furthermore, many studies have predominantly focused on either polarity sentiment classification or fine-grained sentiment classification, overlooking an exploration into how the categorical scope of sentiment polarities affects model robustness. Additionally, most researchers have not evaluated their approaches across a wide spectrum of available benchmark datasets for SA. For instance, results are often reported exclusively for IMDb or SST variants.

Therefore, our current work aims to fine-tune BERT by coupling it with BiLSTM for both polarity classification and fine-grained sentiment classification, given that these techniques have demonstrated superior performance in the existing literature. Leveraging transfer learning insights from [18], we extend previous methodologies by computing the overall polarity of sentiments, as demonstrated in [13]. While a prior study computed overall polarity based on a single output vector derived from Twitter replies using LSTM for three-class classification, we intend to compute this using the output vector obtained from BERT coupled with BiLSTM, tailored to each specific classification task. Our experimental evaluations will encompass diverse benchmark datasets as shown in Section IV.

III. Methodology

This section discusses various techniques employed in this study, encompassing SA, BERT, BiLSTM, fine-tuning BERT with BiLSTM, different classification tasks, techniques for performance enhancement, computation of overall polarity, and an overview of the entire study.

A. SA

SA is a sub-domain of opinion mining, focusing on extracting emotions and opinions regarding a specific topic from structured, semi-structured, or unstructured textual data [35]. It can be approached either as a binary or fine-grained sentiment classification task. In binary classification, machine learning models categorize text into positive or negative sentiment categories. In contrast, fine-grained classification involves utilizing more than two sentiment classes, enabling the computation of multi-scale sentiment distribution. In our context, we investigate both classifications. Our aim is to explore the robustness and consistency of the model in generalization across varying categorical scopes of sentiment polarities.

B. Model Architecture

The model architecture consists of BERT, BiLSTM and a fully connected dense layer.

1) BERT: BERT was introduced by researchers from Google [2]. BERT primarily focuses on pre-training deep bidirectional representations from unlabeled text by jointly considering both left and right contexts across all layers of the model. Consequently, BERT can be fine-tuned with a single additional layer for various downstream tasks such as SA, question answering, and more. Pre-training of BERT involved two unsupervised tasks.

a) Masked Language Modeling: For this task, 15% of the tokens within the input sequence undergo random masking. Subsequently, the complete input sequence is processed through a deep bidirectional transformer encoder, and the output softmax layer is designed to predict the masked words [2].

b) Next Sentence Prediction: BERT establishes a relationship between two input sentences, denoted as sentence *A* and sentence *B*, by predicting whether these sentences logically follow each other within a specific monolingual corpus. During training, 50% of the inputs consist of sentence pairs where the second sentence is the immediate subsequent sentence in the source document. Conversely, the remaining 50% involve pairs where a random sentence from the corpus is chosen as the second sentence [10].

BERT processes a sequence of input tokens simultaneously due to its multiple attention heads, and the model is primarily available in two sub-models: $\text{BERT}_{\text{BASE}}$ and $\text{BERT}_{\text{LARGE}}$. In this work, we utilize $\text{BERT}_{\text{BASE}}$, which comprises 12 layers, 768 hidden states, 12 attention heads, and 110M parameters. In contrast, $\text{BERT}_{\text{LARGE}}$ features approximately twice the specifications of $\text{BERT}_{\text{BASE}}$. Specifically, the uncased version of $\text{BERT}_{\text{BASE}}$, referred to as *bert-base-uncased*, which processes input tokens in lowercase, is employed in this study.

In BERT, there is a specific format for input tokens. The initial token of each sequence is labeled as [CLS]. This token corresponds to the final hidden layer, gathering and

aggregating all the information within the input sequence, particularly for classification tasks. To distinguish between sentences within a single input sequence, two methods are employed: the use of a special token, [SEP], for separation and the addition of a learned embedding to each token, thereby identifying the sentence to which it belongs.

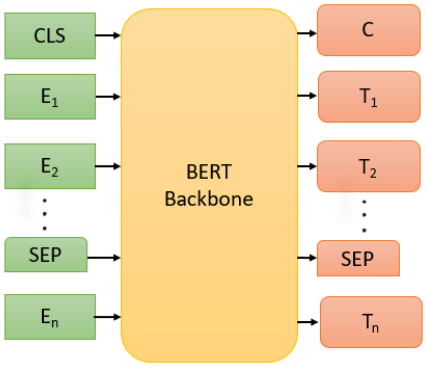

Fig. 1. Simplified diagram of BERT

Figure 1 illustrates a simplified diagram of BERT. E_n denotes the input representation of a single token, generated by summing the respective token, segment, and position embeddings. The *BERT Backbone* symbolizes the primary processing carried out by BERT, while T_n represents the hidden state corresponding to token E_n. Additionally, C represents the hidden state corresponding to the aggregated token [CLS]. Consequently, we utilize C as the input for the fine-tuning components in sentiment classification.

2) BiLSTM: BiLSTM is an LSTM variant that processes input features in both forward and backward directions [12]. This bidirectional characteristic provides BiLSTM an advantage in effectively capturing higher-level sentiment representations from the BERT hidden state *C*. Additionally, BiLSTM inherits the advantageous features of LSTM, including the ability to retain long-distance temporal dependencies and avoiding the issues of vanishing or exploding gradients during backpropagation through time. The enhancement of the performance of the model by supplementing it with the BiLSTM module, as demonstrated in experiments, outperformed the usage of solely BERT with a dense layer.

3) Dense Layer: The hidden state from BiLSTM feeds into a dense layer. This layer, based on the BiLSTM output, generates a higher-level feature set that is readily distinguishable for the targeted number of classes. Finally, a softmax layer is added atop the dense layer to yield the predicted probability distribution for the target classes.

C. Fine-tuning BERT with BiLSTM

Because BERT is pre-trained, there is no necessity to train the entire model from the beginning [2]. Consequently, we simply transfer knowledge from BERT to the added fine-tuning layer and train this layer for SA.

In this study, the fine-tuning process operates as follows. After data pre-processing, three layers are established, one utilizing BERT and the subsequent layers involving BiLSTM and dense networks. The data pre-processing phase generates two input values, known as *attention masks* and *input ids*. These serve as the input embeddings to the model.

The input embeddings are then passed through the BERT module. The dimensionality of these embeddings is contingent on various factors, including the input sequence length, batch-size, and the number of units in BERT's hidden state.

Subsequently, the BiLSTM assimilates information from BERT and forwards it to the dense layer, which predicts the corresponding classes for the input features through the succeeding softmax layer. BERT and BiLSTM share the same hyperparameters, detailed in Section IV under experimental settings.

The fine-tuning process is depicted in Figure 2. Within the figure, *Input features* represent tokens in a review, *Input ids* symbolize an input sequence, and *Attention masks* are binary tensors that highlight the position of the padded indices in a particular sequence to exclude them from attention. These masks use binary values 1 to indicate positions that require attention and 0 for padded values. Padding ensures uniform sequence lengths for input data sentences, a common practice in NLP. Consequently, the padded information is not considered part of the input and has minimal impact on the model's generalization.

The output from BERT matches the dimensionality of the input to BiLSTM, set at 768 and represented by *C*. Only *C* is transmitted to BiLSTM. The BiLSTM layer includes a single hidden component, followed by a dense layer that receives the hidden state *H* from BiLSTM.

D. Classification

In this study, BERT is fine-tuned for both binary (polarity) sentiment classification and fine-grained SA. The fine-grained classification aspect encompasses three distinct tasks: three-class (3-point scale), four-class (4-point scale), and five-class (5-point scale) classifications.

1) Polarity classification: In this context, polarity classification entails classifying a movie review *R* as either conveying a positive or a negative sentiment polarity. This fundamental task is often a cornerstone of SA, as it primarily focuses on discerning between positive and negative sentiments within a text [4].

Additionally, to assess the robustness of the model in handling varying categorical scopes of sentiment polarities, we further perform fine-grained sentiment classification. This involves utilizing different classification scales to gauge how the polarity of an individual review and the overall polarity of a collection of reviews change as the classification becomes more detailed. For instance, if a review is classified as negative in a binary classification dataset, we aim to understand how this polarity aligns when labels are expanded to include highly negative, negative, neutral, positive, and highly positive categories. We extend this analysis to overall sentiment polarity as well. Consequently, we conduct the following fine-grained classification tasks.

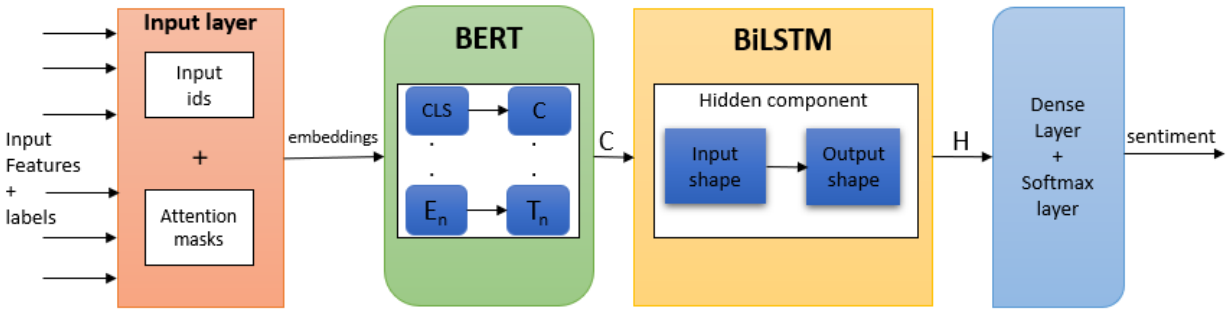

Fig. 2. Fine-tuning part of BERT with BiLSTM

2) Three-class classification: This expands upon binary classification by introducing a neutral class to account for instances where reviewers might not distinctly assign a positive or negative sentiment to a movie due to ambiguous sentiments or a lack of clear preference [13]. Sometimes, the review might contain a balance of positive and negative words, leading to ambiguity in sentiment. Hence, a neutral polarity is introduced to accommodate such cases. In the context of three-class classification, the task is defined as follows: given a movie review *R*, classify it as carrying a negative, neutral, or positive sentiment polarity.

Alternatively, the output vector from binary classification can be directly adapted into three-class classification without altering the label scope in the training data or restarting the training process for the three-class task. By employing a sigmoid activation function or a softmax layer that assigns varying confidence levels to negative and positive classes, a neutral class can be incorporated using a delta value, δ. In this approach, the actual output label can be replaced by a neutral label if the discrepancy between the probabilities of the original two classes is smaller than δ. However, this method necessitates a careful definition of δ to ensure meaningful and accurate outcomes.

3) Four-class classification: This task specifically targets the IMDb dataset. To extend the binary IMDb classification to four classes, we adopt a hierarchical approach using binary tree splitting. This technique, initially introduced in [36], leverages binary segmentation to identify homogeneous nodes within a tree structure. In our scenario, negative reviews are divided into highly negative and negative, while positive reviews are categorized into positive and highly positive, as illustrated in Figure 3. Here, *D* represents the dataset, while *N*, *P*, *HN*, and *HP* symbolize Negative, Positive, Highly Negative, and Highly Positive reviews, respectively. A detailed explanation of the binary tree splitting method's application is provided in Section IV within the IMDb dataset analysis. Consequently, the four-class classification is defined as follows: given a movie review *R*, classify it based on whether it carries a highly negative, negative, positive, or highly positive sentiment polarity.

4) Five-class classification: Five classes are used here as in [10] and [37]. While [37] used the output vector obtained from this classification to estimate the distribution of data examples across the five classes, we use the vector to find the overall sentiment polarity of all the predictions. Five-class task is defined as follows. Given a movie review *R*, classify it as whether carrying a highly negative, negative, neutral, positive, or highly positive sentiment polarity.

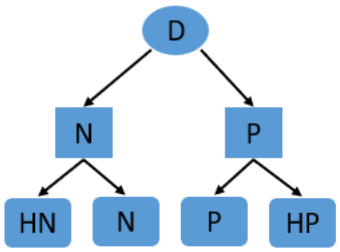

Fig. 3. Binary Tree Splitting

E. Accuracy Improvement Approaches

We utilized distinct data oversampling and augmentation techniques individually to improve the accuracy of the model for fine-grained sentiment classification.

1) Oversampling: The Synthetic Minority Over-sampling TEchnique (SMOTE) was introduced in [38] to address imbalanced datasets problem and enhance model performance. As SMOTE primarily operates with numerical input data, we initially converted reviews from the minority classes into their corresponding numerical features. Subsequently, we used these features as input for SMOTE, which conducted oversampling to balance the dataset.

2) Augmentation: Data augmentation serves to address class imbalance and maximize information extraction from limited resources [39]. We employed NLP Augmenter (NLPAUG), a technique leveraging operations based on abstractive summarization and synonym replacement driven by the proximity of word embedding vectors. Our experiments found this technique successful, and we depict it in Eq. (1):

$$V_{\text{AUG}} = F(V_{\text{IN}}) \tag{1}$$

Here, V_{AUG} represents the output matrix of augmented sentences, where F symbolizes the abstractive summarization augmentation function applied to the input matrix V_{IN} containing raw text data. Both matrices contain n vectors, corresponding to the misrepresented (minority) classes within the dataset. Furthermore, the input vectors comprise randomly sampled data examples from specific misrepresented classes, establishing a one-to-one mapping between input and output vectors.

After applying these techniques, we initially combined the output from SMOTE with the original input data and proceeded to train the model using the SST-5 benchmark dataset. Subsequently, we performed a similar procedure using V_{AUG}.

F. Overall Sentiment Polarity

We define the overall sentiment polarity as follows: Given an output vector *V* from BERT+BiLSTM containing sentiment labels for *N* reviews, we compute the dominant sentiment polarity within the vector. To derive the overall sentiment polarity of the reviews, we input the output vector of BERT+BiLSTM into a heuristic algorithm. In this process, BERT+BiLSTM initially predicts the sentiment category for each review, aggregating the results in an output vector. The occurrences of each class label within the output vector are tallied, and the result is passed to the heuristic algorithm to determine the predominant sentiment polarity for all the reviews collectively.

The algorithm has been modified to compute the overall sentiment polarity from the output vectors of binary, four-class, and five-class classifications. The functionality of the algorithm is dependent on the number of classes in the output vector, necessitating the derivation of three variants of the algorithm for these different classification tasks.

Algorithm 1 outlines the computation of the overall polarity from the output vector of the three-class classification. Initially, if the proportion of neutral reviews exceeds a threshold, set at 85%, the overall polarity is designated as neutral. This threshold acknowledges that a majority of reviews might tend towards a neutral sentiment rather than distinctly positive or negative.

Next, the algorithm considers the distribution of negative and positive sentiments in the output vector. Typically, individual reviews seldom express exclusively positive or negative sentiments. Therefore, if the number of negative reviews exceeds positive reviews by at least 1.5 times, or vice versa, the dominant sentiment determines the overall polarity. This criterion ensures that a sentiment must significantly outweigh the other to influence the overall polarity.

Finally, when the counts of positive and negative reviews are nearly equal, indicating a lack of a clear dominance between positive and negative sentiments, the overall polarity is categorized as neutral once more. This scenario implies a balanced representation of both sentiments across the reviews.

To compute the overall polarity from the binary classification task, Algorithm 2 is derived from Algorithm 1 with modifications to account for the absence of a neutral polarity in binary classification. While Algorithm 1 considers the presence of a neutral sentiment, binary classification does not include this category. Therefore, in Algorithm 2, the logic is adjusted to directly assess the quantities of positive and negative reviews. However, in cases where neither category dominates the sentiment output (i.e., quantities of positive and negative reviews are approximately similar), a neutral sentiment polarity is introduced for the overall polarity computation, representing a tie between positive and negative sentiments.

In our formulations, we employed variable coefficients, namely 1.2 and 1.5, to ascertain the majority gap for decision-making within the algorithms, for comparisons within the algorithms.

Algorithm 2 serves as the foundation for Algorithm 3, enabling the computation of overall polarity from the four-class output vector of BERT+BiLSTM. This algorithm operates hierarchically, taking into account the binary tree splitting illustrated in Figure 3. The hierarchical comparison starts with base classes, progressing to sub-classes within a base class that holds the majority of samples. The process involves aggregating the sample counts of all fine-grained classes under each super class. For instance, the total for the negative super class is derived from the highly negative and negative sub-class totals.

Three distinct scenarios are considered within the algorithm.

Algorithm 1: Overall sentiment polarity computation from three-class classification output vector.

Result: Dominating sentiment polarity for all reviews.

if *#total neutral reviews* $> 85\%$ *of the total reviews* **then**
  overall polarity $\leftarrow$ *neutral*;
else
  if *#total positive reviews >1.5 × # of total negative reviews* **then**
    overall polarity $\leftarrow$ *positive*;
  else if *#total negative reviews >1.5 × # of total positive reviews* **then**
    overall polarity $\leftarrow$ *negative*;
  else
    overall polarity $\leftarrow$ *neutral*;

Algorithm 2: Overall sentiment polarity computation from binary classification output vector.

Result: Dominating sentiment polarity for all reviews.

if *#total positive reviews >1.2 × # of total negative reviews* **then**
  overall polarity $\leftarrow$ *positive*
else if *#total negative reviews >1.2 × # of total positive reviews* **then**
  overall polarity $\leftarrow$ *negative*
else
  overall polarity $\leftarrow$ *neutral*

Algorithm 3: Overall sentiment polarity computation from four-class classification output vector.

```
Result: Dominating sentiment polarity for all reviews.
if # (highly negative reviews + negative reviews) >1.2
  × # of (positive reviews + highly positive reviews)
  then
    if #highly negative reviews >1.5 × # of negative
      reviews then
        overall polarity ← highly negative
    else
        overall polarity ← negative
else if #(positive reviews + highly positive reviews)
  >1.2 × # of (highly negative reviews + negative
  reviews) then
    if #highly positive reviews >1.5 × # of positive
      reviews then
        overall polarity ← highly positive
    else
        overall polarity ← positive
else
    overall polarity ← neutral
```

Algorithm 4: Overall sentiment polarity computation from five-class classification output vector.

```
Result: Dominating sentiment polarity for all reviews.
if #total neutral reviews > 85% of the total reviews
  then
    overall polarity ← neutral
else
    if (#highly negative reviews + #negative reviews)
      >1.2 × # of (positive reviews + highly positive
      reviews) then
        if #highly negative reviews > #1.5 × negative
          reviews then
            overall polarity ← highly negative
        else
            overall polarity ← negative
    else if #(positive reviews + highly positive
      reviews) >1.2 × # of (highly negative reviews +
      negative reviews) then
        if #high positive reviews >1.5 × # of positive
          reviews then
            overall polarity ← highly positive
        else
            overall polarity ← positive
    else
        overall polarity ← neutral
```

In the first case, if the total number of negative reviews across super classes exceeds the total number of positive reviews by at least 1.2 times, and the count of highly negative sub-class reviews is at least 1.5 times that of the negative sub-class, a highly negative overall polarity is assigned. Conversely, if the positive reviews surpass the negative reviews by 1.2 times, and the highly positive sub-class reviews dominate by 1.5 times over the positive sub-class, an overall positive polarity is assigned. Finally, if no significant dominance is observed between the total numbers of negative and positive reviews within the base classes, a neutral overall polarity is assigned.

For base classes, the threshold of 1.2 often works best to determine the dominating class. However, in the more finely-grained sub-classes, such as highly positive and highly negative, a threshold of 1.5 tends to perform better. This distinction is due to the increased granularity of the sub-classes, requiring a higher sample size of the dominating subclass to designate its label as the overall polarity.

For five-class classification, Algorithm 4 extends from Algorithm 3 with an additional initial step. Initially, the overall polarity is evaluated as neutral if the proportion of neutral reviews exceeds a designated threshold, typically set at 85%. Following this initial consideration, the subsequent steps in Algorithm 3 are maintained without alteration.

A simplistic method for determining overall polarity involves tallying the count of labels for each class within the BERT+BiLSTM output vector and assigning overall polarity based on the majority class. However, this basic approach may not adequately represent the dominant sentiment. Consider binary classification, if the output vector consists of 49 positive reviews and 51 negative reviews, the overall polarity will be negative. Yet, a difference of 2 is not conclusive enough to determine the prevailing sentiment across all reviews.

Furthermore, the levels of positivity or negativity vary among reviews in the datasets. To address this, we employ specific formulations in the respective algorithms. These formulations require a significantly higher majority within a class in the output vector to assign its label as the overall sentiment polarity; otherwise, the overall sentiment polarity defaults to neutral.

Additionally, we refined the coefficients to 1.2 and 1.5 in the algorithms based on various observations of the model's behavior across different scenarios. These empirically determined values significantly improved the accuracy of overall polarity computation, closely reflecting the original sentiment polarity of input features.

G. Overview of the Work

Illustrated in Figure 4, the overview of our work encapsulates several key steps. Initially, raw text data undergoes preprocessing to transform it into features compatible with BERT. Subsequently, these features are fed into BERT+BiLSTM through the fine-tuning layer, which configures the necessary hyperparameters for BERT+BiLSTM. Finally, the output vector from BERT+BiLSTM predictions is utilized to compute the overall sentiment polarity.

IV. Experiments

This section provides an insight into the datasets utilized in this study, followed by an in-depth exploration of the data preprocessing techniques. Subsequently, it delves into the experi-

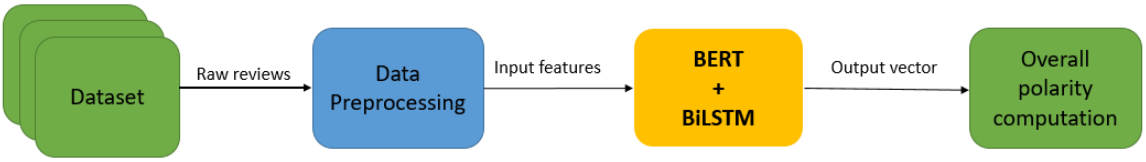

Fig. 4. Overview of our work

mental settings, elucidates the evaluation metrics employed in the experiments, and culminates in a comprehensive discussion of the experimental findings.

A. Datasets

The datasets employed within this study revolve around movie reviews meticulously annotated for SA across a diverse array of scales, specifically, 2-point, 3-point, 4-point, and 5-point gradations. The subsequent elucidation encapsulates the detailed descriptions of these datasets.

1) IMDb movie reviews: The IMDb movie reviews dataset [40], stands as a widely embraced binary SA collection, encompassing a colossal 50,000 reviews sourced from the Internet Movie Database (IMDb). This assortment impeccably balances negativity and positivity, presenting an equal split between negative and positive reviews. Within this study, the dataset assumes a pivotal role in binary classification tasks, further expanding its utility to encompass three-class and four-class classification endeavors. Comprising three fundamental columns (reviews, sentiment score, and label), the dataset's sentiment scores range from integers 1 to 10, excluding the neutral ground of 5 and 6. Reviews carrying scores between 1 to 4 are distinctly labeled as negative, while those within the 7 to 10 spectrum are unequivocally regarded as positive.

In extending the dataset towards a four-class classification paradigm, our approach leveraged the concept of binary-tree splitting, visually represented in Figure 3. Each review within the dataset boasts eight distinct sentiment scores, owing to the absence of scores 5 and 6. Our classification strategy involves categorizing reviews bearing scores 1 and 2 as highly negative, while scores 3 and 4 are tagged as negative. Conversely, scores 7 and 8 merit a positive label, and ratings of 9 and 10 earn the designation of highly positive. For the three-class model, our breakdown was as follows: scores 1, 2, and 3 corresponded to negative sentiment, scores 4 and 7 indicated a neutral stance, and ratings of 8, 9, and 10 were indicative of positive sentiment. We refer to these modified datasets as IMDb-2, IMDb-3, and IMDb-4, representing the binary, three-class, and four-class renditions of the original dataset, respectively.

2) SST: The Stanford Sentiment Treebank (SST) stands as a punctiliously curated corpus adorned with fully labeled parse trees, offering a profound exploration into the intricate nuances of sentiment's compositional impact on language. Originating from the dataset introduced in [41], SST comprises a collection of 11,855 individual sentences meticulously extracted from movie reviews. These sentences underwent parsing via the Stanford parser, resulting in an extensive repository of 215,154 unique phrases diligently annotated by three human judges. Each phrase within this dataset bears a label denoting its sentiment, falling within the spectrum of negative, somewhat negative, neutral, somewhat positive, or positive, equating to the highly negative, negative, neutral, positive, and highly positive labels used within our annotations.

The SST dataset manifests in two distinct versions: SST-5, known as SST fine-grained, employs five labels to characterize sentiment nuances, while SST-2, termed SST binary, simplifies the classification into two primary labels, negative and positive. Within SST-2, negative sentiments encompass judgments labeled as negative or somewhat negative, while positive sentiments entail those marked as somewhat positive or positive. Notably, neutral reviews find no place within SST-2. In our present study, we harness SST-2 for binary classification tasks and SST-5 for more intricate five-class classification endeavors, thus delving deeper into the subtleties of SA within the corpus.

3) MR Movie Reviews: The MR movie reviews dataset encompasses a wealth of movie review documents carefully labeled based on their overarching sentiment polarity, whether they lean positively or negatively, or subjective rating, such as nuanced assessments like two and a half stars. Additionally, it contains sentences categorized according to their subjectivity status, distinguishing between subjective or objective content, and polarity.

Within the scope of this paper, we specifically employ the version introduced in [42], a rigorously curated subset comprising 5,331 positive and 5,331 negative processed reviews. In our experiments, we exclusively harness the MR movie reviews dataset for a singular purpose: the binary classification task. This dataset serves as the cornerstone of our experiments, focusing solely on the polarity aspect of SA.

4) Amazon Product Data dataset: This dataset is an expansive repository housing product reviews and metadata sourced from Amazon, encompassing a staggering 142.8 million reviews dating from May 1996 to July 2014. Its comprehensive scope spans reviews, product metadata, and interlinkages. Initially introduced in [43] as a resource for SA utilizing product review data, it was further utilized in [44] to construct a recommender system operating within a collaborative filtering framework tailored specifically for Amazon products.

Within the context of our study, our focal point centers solely on video reviews within this extensive dataset. Initially, the dataset featured labels graded from scores 1 to 5, signifying a spectrum of polarity strength ranging from highly negative to highly positive sentiments. To streamline our analysis toward

binary classification, we undertook a transformation: scores 1 and 2 were consolidated into a negative label, while scores 4 and 5 were amalgamated into a positive label. Simultaneously, score 3, representing a neutral stance, was omitted, akin to the approach adopted in SST-2 [41].

For the sake of clarity and specificity within our research, we distinguish between Amazon-2 and Amazon-5, representing the binary and five-class versions of the dataset, respectively. Table I provides a comprehensive statistical overview of the datasets employed in our experiments, where categorical labels like H POS (Highly Positive), POS (Positive), NEG (Negative), and H NEG (Highly Negative) elucidate distinct sentiment categories.

B. Data pre-processing

The data pre-processing step was commenced by eliminating empty reviews across all datasets, ensuring a clean and consistent starting point for our analysis. Subsequently, the focus shifted towards implementing recommended data pre-processing measures aimed at translating the raw input data into a format compatible with BERT's comprehension. This undertaking encompassed two pivotal steps integral to the transformation process.

Initially, we generate input examples utilizing the BERT-provided constructor, which operates based on three key parameters: *text_a*, *text_b*, and *label*. Here, *text_a* encapsulates the body of text we aim to classify, specifically, the collection of movie reviews sans their associated labels. The *text_b* parameter, primarily utilized in scenarios involving sentence relationships such as translation or question answering, remains intentionally left blank given its minimal relevance to our current research focus. Meanwhile, *label* serves as the container for the sentiment polarity labels associated with each movie review, representing an essential component of the input features.

For a deeper understanding of this foundational step, additional insights can be gleaned from the original BERT paper [2]. Subsequently, we progress through a series of text pre-processing steps integral to our methodology.

- Lowercase all text, since the lowercase version of $\text{BERT}_{\text{BASE}}$ is being used.
- Tokenize all sentences in the reviews. For example, "this is a very fantastic movie", to 'this', 'is', 'a', 'very', 'fantastic', 'movie'.
- Break words into word pieces. That is 'interesting' to 'interest' and '##ing'.
- Map words to indexes using a vocab file that is provided by BERT.
- Add special tokens: [CLS] and [SEP], which are used for aggregating information of the entire review through the model and separating sentences, respectively.
- Append index and segment tokens to each input to track a sentence that a specific token belongs to.

Following these processes, the tokenizer yields crucial outputs: *input ids* and *attention masks*. These outputs serve as pivotal components, subsequently utilized as inputs alongside the review labels for our model. These elements collectively form the foundational input data fed into our analysis framework.

C. Experimental settings

We conducted fine-tuning on *bert-base-uncased*, a variant of BERT designed to process lowercase tokens. While initializing most of BERT's layers from the model checkpoint, some layers required new initialization. Throughout the training process, we deliberately froze the initial layers containing BERT weights, allowing the primary focus to rest on the latter layers housing the fine-tuning components. These latter layers, holding trainable weights, were continuously updated to minimize loss during the training phase, specifically tailored to the downstream task of SA.

Numerous simulations were executed across the datasets to optimize the hyperparameters of the model. From our exhaustive experiments, the most optimal results emerged with specific hyperparameters. For binary classification, the model exhibited exceptional performance using the Adam optimizer [45], a batch size of 32, a learning rate of 3e-5, an epsilon value of 1e-08, a maximum sequence length of 128, and employing binary cross-entropy loss. Training was conducted over 10 epochs, iterating through each batch.

Conversely, in all fine-grained classifications, a batch size of 64, a learning rate of 1e-4, a maximum sequence length of 256, a decay of 1e-5, alongside the Adam optimizer and sparse categorical cross-entropy loss, facilitated optimal outcomes. This specific version underwent training for 15 epochs, repeating steps for batches. Notably, we observed instances of overfitting when attempting to increase the number of epochs for these respective models.

To facilitate broader adoption and enable replication of our work, the code for this project is readily available [46], ensuring accessibility for interested parties.

D. Evaluation Metrics

In line with the evaluation metrics adopted in [10], our approach also employs accuracy as a performance measure to assess the efficacy of our model in comparison to other models. Accuracy, in its essence, is straightforwardly defined as:

$$accuracy = \frac{number\ of\ correct\ predictions}{total\ number\ of\ predictions} \times 100 \quad (2)$$

E. Results and Discussion

We delineate accuracy comparisons across various datasets and classification tasks in our study. Table II illustrates binary classification results, encompassing a comparison between our model and others. Subsequently, in Table III, we present outcomes for three-class and four-class classifications, exclusively on the IMDb dataset. Last, Table IV delves into five-class classification on SST-5 and Amazon-5 datasets. Across these tables, our model consistently surpasses all others in performance across diverse classification tasks on every

TABLE I
STATISTICS OF THE DATASETS DIVIDED INTO TRAINING AND TEST SETS

Dataset	Train samples					Test samples				
	H POS	POS	NEUTRAL	NEG	H NEG	H POS	POS	NEUTRAL	NEG	H NEG
IMDb-2	-	12500	-	12500	-	-	12500	-	12500	-
MR	-	4264	-	4265	-	-	1067	-	1066	-
SST-2	-	4300	-	4244	-	-	886	-	1116	-
Amazon-2	-	239660	-	37056	-	-	59949	-	9231	-
IMDb-3	-	18227	4816	14958	-	-	4556	1204	3739	-
IMDb-4	11471	8530	-	8234	11767	2867	2132	-	2058	2941
SST-5	1482	2489	1794	2512	1208	370	622	448	628	302
Amazon-5	182000	57688	27767	15168	21863	45500	14421	6941	3791	5465

dataset, solidifying its position as the new benchmark with SOTA accuracy levels.

The analysis of our results reveals a distinct trend: our model excels notably in binary classification tasks. However, a discernible pattern emerges as we move towards finer classification scales, evident across the IMDb, SST, and Amazon datasets showcased in Table II, Table III, and Table IV. As the classification granularity increases, the accuracy of our model experiences a consistent decline.

This decline in accuracy can be attributed to several factors. The primary reason lies in the heightened complexity that arises with an augmented number of classes within a dataset. As the distinctions between classes become more intricate, the task of accurate classification becomes increasingly challenging for the model.

Another contributing factor is the distribution of samples across these classes. Despite the proliferation of classes, the number of samples per class remains constrained by the original dataset size. Consequently, with the expansion of classes, each sentiment category possesses a reduced number of examples available for effective model learning. This scarcity of samples within each sentiment category hampers the ability of the model to learn distinct patterns for accurate predictions, particularly as the categorical spectrum of sentiment polarities widens within a dataset.

Through our experimental observations, a striking finding emerges: the model exhibits robustness and consistency, showcasing resilience even amidst alterations in the categorical scope of sentiment polarities within a specific dataset. To illustrate, we delve into a review snippet sourced from the IMDb benchmark. *"This show is great. Not only is 'Haruhai Suzumiya' a very well written anime show, it also reflects things like Philosophy, Science Fiction and a little religion. Itś hilarious at some points and 'cute' (for lack of a better term) at others. Actually this may be effect to my lack of experience with Japanese anime shows, but it is one of the best of its genre I have seen. I mainly have to give credit to the writers. I havenť seen such brilliant scopes of imagination in a television show since the original Star Trek. I hope the writers continue to add strange new characters and give more insight on the already great characters that have been added"*. In the context of binary classification within IMDb-2, the model confidently designates the text as *Positive*. Similarly, in the three-class classification of IMDb-3, it maintains this classification. However, when exploring the four-class classification in IMDb-4, the model assigns a *Highly Positive* label. This classification aligns impeccably with the sentiment score embedded within the review text, a rating of 9 on a scale of 1 to 10 for goodness.

This astute adaptability demonstrates the proficiency of the model in discerning and leveraging nuanced semantic cues embedded within a dataset. It dynamically adjusts its classification strategy based on the chosen categorical scope, effectively capturing and reflecting the varying degrees of sentiment granularity present within the dataset.

Our experimental findings, showcased in Table V using the SST-5 dataset, include results concerning oversampling with SMOTE and augmentation using NPLPAUG. Two distinct approaches are highlighted: BERT+BiLSTM+SMOTE, utilizing SMOTE in conjunction with BERT and BiLSTM for SA, and BERT+BiLSTM+NLPAUG, employing NLPAUG for augmentation.

Surprisingly, the inclusion of SMOTE in our model exhibits no discernible impact on accuracy. Remarkably, the accuracy of a simpler model, BERT+BiLSTM, employing solely BERT and BiLSTM without any accuracy enhancement techniques, surpasses that of BERT+BiLSTM+SMOTE. This implies that the oversampling technique fails to impart semantic understanding to the model from the augmented data it produces.

Conversely, BERT+BiLSTM+NLPAUG showcases a performance boost, elevating the accuracy of the model from 58.44% to 60.48%. The rationale behind these observations lies in the input transformation process. SMOTE operates on text inputs that have been transformed into BERT features. This transformation introduces noise and disrupts the efficacy of SMOTE, as some semantic nuances are lost during this process. In contrast, NLPAUG operates directly on raw text data, facilitating an easier extraction of semantic information during the learning process. This direct access to raw text enables NLPAUG to enhance the performance of the model by leveraging the inherent semantics present in the data.

To encapsulate the discussion of results, we focus on the comprehensive computation of overall sentiment polarity across all datasets facilitated by our model, as detailed in Table VI. Here, *OP* signifies Overall Polarity. We distinguish between *Original OP*, known prior to input embeddings entering BERT+BiLSTM, and *Computed OP*, derived after the model

TABLE II
ACCURACY (%) COMPARISONS OF MODELS ON BENCHMARK DATASETS FOR BINARY CLASSIFICATION

Model name	Dataset			
	IMDb-2	*MR*	*SST-2*	*Amazon-2*
RNN-Capsule [47]	84.12	83.80	82.77	82.68
coRNN [18]	87.4	87.11	88.97	89.32
TL-CNN [18]	87.70	81.5	87.70	88.12
Modified LMU [48]	93.20	93.15	93.10	93.67
DualCL [49]	-	94.31	94.91	94.98
L Mixed [50]	95.68	95.72	-	95.81
EFL [19]	96.10	96.90	96.90	96.91
NB-weighted-BON+dv-cosine [16]	97.40	-	96.55	97.55
SMART-RoBERTa Large [51]	96.34	97.5	96.61	-
Ours	**97.67**	**97.88**	**97.62**	**98.76**

TABLE III
ACCURACY (%) COMPARISONS FOR THREE AND FOUR CLASS CLASSIFICATION ON IMDD

Model name	Dataset	
	IMDb-3	*IMDb-4*
CNN-RNF-LSTM [52]	73.71	63.78
DPCNN [22]	76.24	66.17
BERT-large [10]	77.21	66.87
Ours	**81.87**	**70.75**

TABLE IV
ACCURACY (%) COMPORISONS OF MODELS ON BENCHMARK DATASETS FOR FIVE CLASS CLASSIFICATION

Model name	Dataset	
	SST-5	*Amazon-5*
CNN+word2vec [23]	46.4	48.85
TL-CNN [18]	47.2	58.1
DRNN [53]	-	64.43
BERT-large [10]	55.5	65.83
BCN+Suffix+BiLSTM-Tied+Cove [54]	56.2	65.92
RoBERTa+large+Self-explaining [55]	59.10	-
Ours	**60.48**	**69.68**

TABLE V
ACCURACY (%) OF OUR MODEL WITH ACCURACY IMPROVEMENT TECHNIQUES ON SST-5

Classification task	Accuracy
BERT+BiLSTM	58.44
BERT+BiLSTM+SMOTE	58.36
BERT+BiLSTM+NLPAUG	**60.48**

predicts sentiments for reviews.

Remarkably, the table demonstrates an intriguing consistency: *Computed OP* aligns precisely with *Original OP* across all datasets. *Original OP* was initially computed by tallying the sample counts for each label within the input features and then applying a specific heuristic algorithm tailored to the classification task. This initial computation was utilized as a benchmark to verify the accuracy of *Computed OP*.

Furthermore, the table also highlights a consistent *Computed OP* across different versions of the same dataset. This uniformity across dataset variations reinforces our confidence in the

TABLE VI
OVERALL POLARITY COMPUTATION ON ALL THE DATASETS

Dataset	Original OP	Computed OP[b]
IMDb-2	Neutral	Neutral
IMDb-3	Neutral	Neutral
IMDb-4	Neutral	Neutral
MR reviews	Neutral	Neutral
SST-2	Neutral	Neutral
SST-5	Neutral	Neutral
Amazon-2	Positive	Positive
Amazon-5	Positive	Positive

ability of the heuristic algorithm to accurately compute the expected overall polarity from the BERT+BiLSTM output vector. This confidence persists despite variations in the categorical scope of sentiment polarities within the movie reviews across different dataset iterations. This robustness ensures that the heuristic algorithm consistently delivers expected and accurate overall polarity computations, emphasizing its reliability and generalizability across diverse datasets.

V. CONCLUSION

In this section, we consolidate our efforts by offering a succinct summary of our work, highlighting the contributions we have made to the domain's knowledge, and outlining prospective avenues for future exploration based on the insights gleaned from our observations.

A. Conclusion

In this endeavor, we have expanded the existing domain knowledge of SA through our primary contributions, showcasing significant advancements:

First, we have adeptly fine-tuned BERT, a pivotal aspect enhancing accuracy within movie reviews SA. Leveraging transfer learning, we coupled BERT with BiLSTM, utilizing BERT-generated word embeddings as inputs for BiLSTM. This amalgamation was instrumental for polarity and fine-grained classification tasks, spanning three-class, four-class, and five-class categorizations across various datasets, i.e., IMDb, MR, SST, and Amazon. Notably, our model consistently outperformed prior works across all classification tasks and datasets.

Moreover, to augment the accuracy of our model for five-class classification, we delved into the impact of employing SMOTE and NLPAUG on SST-5, a notably challenging fine-grained classification benchmark. Intriguingly, SMOTE led to a decrease in accuracy from 58.44% to 58.36%, while NLPAUG remarkably boosted accuracy to 60.48%.

Second, we introduced a heuristic algorithm tailored to the BERT-BiLSTM output vector, dynamically adapting to the specific classification task at hand. Demonstrating its reliability, we confirmed that the original overall polarity aligned perfectly with the computed overall polarity across all datasets. Furthermore, variations within dataset versions exhibited consistent computed overall polarity.

This work marks a pioneering effort, coupling BERT with BiLSTM and applying the resulting model across diverse sentiment classification tasks and benchmark datasets. Notably, it is the first to utilize the output vector of a model for computing overall sentiment polarity. Our exploration not only enhances understanding regarding review polarity but also sheds light on the nuanced shifts in review and overall polarities as classification granularity intensifies. These combined contributions significantly advance the understanding and application of SA within diverse contexts.

B. Future Work

Moving forward, our proposed future endeavors revolve around addressing key challenges in the realm of SA, aiming to enhance model performance and extract deeper insights. One significant area of focus involves exploring strategies to effectively apply accuracy improvement techniques to transformed BERT features, despite the inherent loss of semantic information during their transformation. This endeavor seeks to overcome the limitations posed by the semantic information loss, potentially revolutionizing the effectiveness of these techniques.

Additionally, our exploration will delve into the nuanced contributions of different sentence components to sentiment prediction. This unexplored facet holds immense potential, as the intricate interplay between sentence elements often remains untapped by current methodologies. By dissecting these contributions, we aim to unravel hidden layers of information critical to sentiment prediction, thereby enriching the understanding of sentence structures and their impact on SA.

Furthermore, our future roadmap includes an extensive exploration of alternative pre-trained language models beyond BERT, such as RoBERTa and GPT. This exploration aims to broaden the horizons of our analysis, leveraging the unique capabilities and architectures of these models to potentially enhance SA outcomes. Diversifying our approach by incorporating these SOTA models could unlock new dimensions and avenues for deeper exploration within the field of SA.

ACKNOWLEDGMENT

We would like to express our gratitude to anonymous reviewers for their valuable insights and comments. We also acknowledge the Data Analytics that are Robust and Trusted (DART) project under the National Science Foundation (NSF) for financially supporting this work. We also extend our gratitude to all individuals who contributed to this work.

REFERENCES

[1] G. Nkhata, U. Anjun, and J. Zhan, "Sentiment analysis of movie reviews using bert." The Fifteenth International Conference on Information, Process, and Knowledge Management, eKNOW23, 2023.

[2] J. Devlin, M.-W. Chang, K. Lee, and K. Toutanova, "Bert: Pre-training of deep bidirectional transformers for language understanding," *arXiv preprint arXiv:1810.04805*, 2018.

[3] P. Baid, A. Gupta, and N. Chaplot, "Sentiment analysis of movie reviews using machine learning techniques," *International Journal of Computer Applications*, vol. 179, no. 7, pp. 45–49, 2017.

[4] G. Mesnil, T. Mikolov, M. Ranzato, and Y. Bengio, "Ensemble of generative and discriminative techniques for sentiment analysis of movie reviews," *arXiv preprint arXiv:1412.5335*, 2014.

[5] Z. Bingyu and N. Arefyev, "The document vectors using cosine similarity revisited," *arXiv preprint arXiv:2205.13357*, 2022.

[6] W. Guo, X. Liu, S. Wang, H. Gao, A. Sankar, Z. Yang, Q. Guo, L. Zhang, B. Long, B.-C. Chen *et al.*, "Detext: A deep text ranking framework with bert," in *Proceedings of the 29th ACM International Conference on Information & Knowledge Management*, 2020, pp. 2509–2516.

[7] Y. Liu, "Fine-tune bert for extractive summarization," *arXiv preprint arXiv:1903.10318*, 2019.

[8] Y. He, Z. Zhu, Y. Zhang, Q. Chen, and J. Caverlee, "Infusing disease knowledge into bert for health question answering, medical inference and disease name recognition," *arXiv preprint arXiv:2010.03746*, 2020.

[9] W. Yang, Y. Xie, L. Tan, K. Xiong, M. Li, and J. Lin, "Data augmentation for bert fine-tuning in open-domain question answering," *arXiv preprint arXiv:1904.06652*, 2019.

[10] M. Munikar, S. Shakya, and A. Shrestha, "Fine-grained sentiment classification using bert," in *2019 Artificial Intelligence for Transforming Business and Society (AITB)*, vol. 1. IEEE, 2019, pp. 1–5.

[11] S. Siami-Namini, N. Tavakoli, and A. S. Namin, "The performance of lstm and bilstm in forecasting time series," in *2019 IEEE International Conference on Big Data (Big Data)*. IEEE, 2019, pp. 3285–3292.

[12] A. Graves and J. Schmidhuber, "Framewise phoneme classification with bidirectional lstm and other neural network architectures," *Neural networks*, vol. 18, no. 5-6, pp. 602–610, 2005.

[13] S. T. Arasteh, M. Monajem, V. Christlein, P. Heinrich, A. Nicolaou, H. N. Boldaji, M. Lotfinia, and S. Evert, "How will your tweet be received? predicting the sentiment polarity of tweet replies," in *2021 IEEE 15th International Conference on Semantic Computing (ICSC)*. IEEE, 2021, pp. 370–373.

[14] M. Anandarajan, C. Hill, and T. Nolan, "Sentiment analysis of movie reviews using r," in *Practical Text Analytics*. Springer, 2019, pp. 193–220.

[15] N. O. F. Daeli and A. Adiwijaya, "Sentiment analysis on movie reviews using information gain and k-nearest neighbor," *Journal of Data Science and Its Applications*, vol. 3, no. 1, pp. 1–7, 2020.

[16] T. Thongtan and T. Phienthrakul, "Sentiment classification using document embeddings trained with cosine similarity," in *Proceedings of the 57th Annual Meeting of the Association for Computational Linguistics: Student Research Workshop*, 2019, pp. 407–414.

[17] D. Singh Sachan, M. Zaheer, and R. Salakhutdinov, "Revisiting lstm networks for semi-supervised text classification via mixed objective function," *arXiv e-prints*, pp. arXiv–2009, 2020.

[18] T. Semwal, P. Yenigalla, G. Mathur, and S. B. Nair, "A practitioners' guide to transfer learning for text classification using convolutional neural networks," in *Proceedings of the 2018 SIAM international conference on data mining*. SIAM, 2018, pp. 513–521.

[19] S. Wang, H. Fang, M. Khabsa, H. Mao, and H. Ma, "Entailment as few-shot learner," *arXiv preprint arXiv:2104.14690*, 2021.

[20] X. Zhang, J. Zhao, and Y. LeCun, "Character-level convolutional networks for text classification," *Advances in neural information processing systems*, vol. 28, 2015.

[21] D. Shen, M. R. Min, Y. Li, and L. Carin, "Learning context-sensitive convolutional filters for text processing," *arXiv preprint arXiv:1709.08294*, 2017.

[22] R. Johnson and T. Zhang, "Deep pyramid convolutional neural networks for text categorization," in *Proceedings of the 55th Annual Meeting of the Association for Computational Linguistics (Volume 1: Long Papers)*, 2017, pp. 562–570.

[23] H. Shirani-Mehr, "Applications of deep learning to sentiment analysis of movie reviews," in *Technical report*. Stanford University, 2014.

[24] T. Mikolov, K. Chen, G. Corrado, and J. Dean, "Efficient estimation of word representations in vector space," *arXiv preprint arXiv:1301.3781*, 2013.

[25] T. K. Rusch and S. Mishra, "Coupled oscillatory recurrent neural network (cornn): An accurate and (gradient) stable architecture for learning long time dependencies," *arXiv preprint arXiv:2010.00951*, 2020.

[26] J. D. Bodapati, N. Veeranjaneyulu, and S. Shaik, "Sentiment analysis from movie reviews using lstms." *Ingenierie des Systemes d'Information*, vol. 24, no. 1, 2019.

[27] H. Xu, L. Shu, P. S. Yu, and B. Liu, "Understanding pre-trained bert for aspect-based sentiment analysis," *arXiv preprint arXiv:2011.00169*, 2020.

[28] X. Li, L. Bing, W. Zhang, and W. Lam, "Exploiting bert for end-to-end aspect-based sentiment analysis," *arXiv preprint arXiv:1910.00883*, 2019.

[29] Z. Gao, A. Feng, X. Song, and X. Wu, "Target-dependent sentiment classification with bert," *Ieee Access*, vol. 7, pp. 154 290–154 299, 2019.

[30] C. Sun, L. Huang, and X. Qiu, "Utilizing bert for aspect-based sentiment analysis via constructing auxiliary sentence," *arXiv preprint arXiv:1903.09588*, 2019.

[31] H. Xu, B. Liu, L. Shu, and P. S. Yu, "Bert post-training for review reading comprehension and aspect-based sentiment analysis," *arXiv preprint arXiv:1904.02232*, 2019.

[32] L. Maltoudoglou, A. Paisios, and H. Papadopoulos, "Bert-based conformal predictor for sentiment analysis," in *Conformal and Probabilistic Prediction and Applications*. PMLR, 2020, pp. 269–284.

[33] S. Alaparthi and M. Mishra, "Bert: A sentiment analysis odyssey," *Journal of Marketing Analytics*, vol. 9, no. 2, pp. 118–126, 2021.

[34] S. Baccianella, A. Esuli, F. Sebastiani *et al.*, "Sentiwordnet 3.0: an enhanced lexical resource for sentiment analysis and opinion mining." in *Lrec*, vol. 10, no. 2010, 2010, pp. 2200–2204.

[35] T. Gadekallu, A. Soni, D. Sarkar, and L. Kuruva, "Application of sentiment analysis in movie reviews," in *Sentiment Analysis and Knowledge Discovery in Contemporary Business*. IGI global, 2019, pp. 77–90.

[36] F. Mola and R. Siciliano, "A two-stage predictive splitting algorithm in binary segmentation," in *Computational statistics*. Springer, 1992, pp. 179–184.

[37] S. Rosenthal, N. Farra, and P. Nakov, "Semeval-2017 task 4: Sentiment analysis in twitter," in *Proceedings of the 11th international workshop on semantic evaluation (SemEval-2017)*, 2017, pp. 502–518.

[38] N. V. Chawla, K. W. Bowyer, L. O. Hall, and W. P. Kegelmeyer, "Smote: synthetic minority over-sampling technique," *Journal of artificial intelligence research*, vol. 16, pp. 321–357, 2002.

[39] G. Rizos, K. Hemker, and B. Schuller, "Augment to prevent: short-text data augmentation in deep learning for hate-speech classification," in *Proceedings of the 28th ACM International Conference on Information and Knowledge Management*, 2019, pp. 991–1000.

[40] A. Maas, R. E. Daly, P. T. Pham, D. Huang, A. Y. Ng, and C. Potts, "Learning word vectors for sentiment analysis," in *Proceedings of the 49th annual meeting of the association for computational linguistics: Human language technologies*, 2011, pp. 142–150.

[41] R. Socher, A. Perelygin, J. Wu, J. Chuang, C. D. Manning, A. Y. Ng, and C. Potts, "Recursive deep models for semantic compositionality over a sentiment treebank," in *Proceedings of the 2013 conference on empirical methods in natural language processing*, 2013, pp. 1631–1642.

[42] B. Pang and L. Lee, "Seeing stars: Exploiting class relationships for sentiment categorization with respect to rating scales," *arXiv preprint cs/0506075*, 2005.

[43] X. Fang and J. Zhan, "Sentiment analysis using product review data," *Journal of Big Data*, vol. 2, no. 1, pp. 1–14, 2015.

[44] R. He and J. McAuley, "Ups and downs: Modeling the visual evolution of fashion trends with one-class collaborative filtering," in *proceedings of the 25th international conference on world wide web*, 2016, pp. 507–517.

[45] D. P. Kingma and J. Ba, "Adam: A method for stochastic optimization," *arXiv preprint arXiv:1412.6980*, 2014.

[46] https://github.com/gnkhata1/Finetuning-BERT-on-Movie-Reviews-Sentiment-Analysis, 2022, [Online; accessed June-15-2023].

[47] Y. Wang, A. Sun, J. Han, Y. Liu, and X. Zhu, "Sentiment analysis by capsules," in *Proceedings of the 2018 world wide web conference*, 2018, pp. 1165–1174.

[48] N. R. Chilkuri and C. Eliasmith, "Parallelizing legendre memory unit training," in *International Conference on Machine Learning*. PMLR, 2021, pp. 1898–1907.

[49] Q. Chen, R. Zhang, Y. Zheng, and Y. Mao, "Dual contrastive learning: Text classification via label-aware data augmentation," *arXiv preprint arXiv:2201.08702*, 2022.

[50] D. S. Sachan, M. Zaheer, and R. Salakhutdinov, "Revisiting lstm networks for semi-supervised text classification via mixed objective function," in *Proceedings of the AAAI Conference on Artificial Intelligence*, vol. 33, no. 01, 2019, pp. 6940–6948.

[51] H. Jiang, P. He, W. Chen, X. Liu, J. Gao, and T. Zhao, "Smart: Robust and efficient fine-tuning for pre-trained natural language models through principled regularized optimization," *arXiv preprint arXiv:1911.03437*, 2019.

[52] Y. Yang, "Convolutional neural networks with recurrent neural filters," in *Proceedings of Empirical Methods in Natural Language Processing*, 2018.

[53] B. Wang, "Disconnected recurrent neural networks for text categorization," in *Proceedings of the 56th Annual Meeting of the Association for Computational Linguistics (Volume 1: Long Papers)*, 2018, pp. 2311–2320.

[54] S. Brahma, "Improved sentence modeling using suffix bidirectional lstm," *arXiv preprint arXiv:1805.07340*, 2018.

[55] Z. Sun, C. Fan, Q. Han, X. Sun, Y. Meng, F. Wu, and J. Li, "Self-explaining structures improve nlp models," *arXiv preprint arXiv:2012.01786*, 2020.

An Extended Study on the Usage of Audit Data Analytics within the Accountancy Sector

Lotte Verhoeven and Eric Mantelaers
Research Centre – Future-proof Auditor
Zuyd University of Applied Sciences & RSM Netherlands Accountants N.V.
Sittard/Heerlen, the Netherlands
lotte.verhoeven@zuyd.nl
eric.mantelaers@zuyd.nl

Martijn Zoet
Research Centre – Future-proof Financial
Zuyd University of Applied Sciences
Sittard, the Netherlands
martijn.zoet@zuyd.nl

***Abstract*— Evidence from the various reports and articles as well as the importance of the audit process shows that adjustment and/or improvement of the current audit approach within the accountancy sector is necessary. Research demonstrates that technology can contribute to an improvement of audit quality, by enhancing audit effectiveness and efficiency. Additionally, previous research increasingly recognizes that audit data analytics is likely to transform the conduct of the audit significantly. The goal of this research is to study how Audit Data Analytics is currently used within the audit. In order to answer this question, a survey was distributed via the Dutch National Accountants Association, focusing on how Audit Data Analytics is used in the accountancy sector. This paper extends the previous research** [1]**, including a more detailed literature review, data collection, analysis and results. The results and the non-chronological order of the data analysis types indicate a misinterpretation or lack of understanding of the data analysis types (implemented in the survey) and their chronological order.**

Keywords-audit data analytics; audit quality; process mining; process mining algorithms.

I. INTRODUCTION

Audit quality consistently received substantial attention from regulators and academics over the past years due to numerous audit scandals. Caused by a lack of independent oversight and enforcement, various accounting and audit scandals took place in the beginning of the 21st century. Recent reports from the Dutch Authority for the Financial Markets (AFM), and recent published reports from, among others, the Future Accountancy Sector Committee (CTA) and the Accountancy Monitoring Committee (MCA), show that the quality of annual audits is inadequate [2]–[5]. Internationally the lack of audit quality is also visible. In the Brydon report, Brydon states that the audit quality is insufficient and improvements including new reporting duty with respect to fraud and more auditor transparency are recommended [6]. Evidence from the various reports and articles as well as the importance of the audit process shows that adjustment and/or improvement of the current audit approach within the accountancy sector is necessary [7]. Research demonstrates that technology can contribute to an improvement of audit quality [8].

This research, therefore, focuses on the current usage of Audit Data Analytics (ADA) within the audit. The goal of this research is to achieve a view of the application of ADA within the financial audit. To achieve this, this paper answers the following main question: *How and to what extent is Audit Data Analytics currently used by auditors/accountants?*

The remainder of the paper is organized as follows: Section II describes the relevant literature regarding audit quality and ADA. In Section III, the research method is described, followed by the data collection and analysis in Section IV. Finally, the results, conclusion and future work are presented in Sections V and VI, respectively.

II. LITERATURE REVIEW

Audit quality is a very broad concept and can be defined in various ways. DeAngelo describes audit quality as "the market assessed joint probability that a given auditor will both discover a breach in the client's accounting system and reports the breach" [9]. Whereas the Government Accountability Office uses a more extensive approach and states that high audit quality is achieved when performed according to the corresponding standards and no material misstatements due to error or fraud are present [10]. The legal definition of audit quality is on the other hand very concise, as it states audit quality as either "audit failure" or "no audit failure" [11]. In conclusion, audit quality is a broad concept and difficult to summarize in a single definition. Next to that, these different definitions show that audit quality is not yet recognized universally across the world. As mentioned before, evidence from the various reports and articles as well as the importance of the audit process shows that adjustment and / or improvement of the current approach within the accountancy sector is necessary [1]–[4][7].

Previous research shows that technology/ADA can contribute to an improvement of audit quality [8]. By automating certain audit analyses, more time and resources can be allocated to the interpretation of these analyses. This maximizes the dual aspects of audit quality: independence and expertise [8][9]. Additionally, previous research increasingly recognizes that ADA is likely to transform the conduct of the audit significantly [12]–[14]. As Barr-

Pulliam et al. state: "The use of advanced testing methods such as ADAs can occur at any stage of the audit and can significantly transform the process of auditing financial statements, resulting in enhanced audit effectiveness and audit efficiency – both elements and signals of audit quality" [12]. To support the individual and personal judgement of the auditor, ADA could provide a solution. ADA is a method of using data analysis techniques to evaluate financial information and assess the accuracy and reliability of an organization's financial statements. This involves collecting and examining large amounts of data, and using statistical and computational tools to identify patterns, trends, and anomalies that may indicate potential problems or issues. Data-driven audits are becoming increasingly familiar within the accountancy sector, due to innovation, increase in technology/data and the pursuit of continuous assurance [15]. Data-driven 'control' is also used by the AFM (regulator), as they want to implement data-driven supervision to enhance the efficiency and effectivity of the supervision of audit firms. To achieve this, the AFM will structurally request data from the audit firms to gain insight into the current quality control and risk characteristics [16].

Despite the fact that the use of ADA within the audit practice is relatively new, various previous research has been performed. The Financial Reporting Council (FRC), regulator to auditors, accountants and actuaries and setter of UK's Corporate Governance and Stewardship Codes, conducted a review of the use of technology in the audit of financial statements. Within this review, the FRC found that ADA was currently used mostly for risk assessment and the audit of revenue, and that advanced ADA was only used sporadic [17]. This was also highlighted by Eilifsen et al. who explored the use of ADA in current audit practice in Norway. Eilifsen et al. found that despite the positive attitude with regards to the usefulness of ADA, the use of 'advanced' ADA is rare [18]. Eilifsen et al. also found that this is caused by its complexity and lack of implementation guidelines and confidence in the ability of ADA to provide sufficient and appropriate audit evidence. It is suggested that this is likely to persist until ADA will be incorporated in the audit methodologies and ADA is explicitly supported and accepted by supervisory bodies and standard-setters [18]. However, this research focuses not only on the use of ADA, but also on the sequentially of its use.

To analyze the sequential use of ADA, process mining will be used [19] [20]. Process mining is a technique used to analyze and visualize end-to-end processes, by ordering the events based on the timestamps/event logs. Ordering these events is a crucial step for understanding the sequence of activities within a process and to detect possible deviations from the expected process [19] [20]. As van der Aalst (2011) stated: "Process mining aims to discover, monitor and improve real processes by extracting knowledge from event logs" [20]. The initial stage in process mining involves the utilization of event logs, which document individual activities or events associated with specific cases. These events, arranged in chronological order, collectively represent a single "execution" of the process [21].

For the use of this research process mining algorithms from the Python package 'Pm4py', a Process Mining package for Python, were used [22]. In specific, the heuristic miner will be used. A heuristic analysis simplifies the information by removing redundant details and exceptions, concentrating on the primary behaviors [23].

III. RESEARCH METHOD

The goal of this research is to study how ADA is currently used within the audit. In order to answer this question, a survey was distributed focusing on how ADA is used in the accountancy sector. The survey is distributed via the Dutch National Accountants Association (NBA) across members of the Accounttech working group, a total of 7,008. The members of the NBA are spread over several accountancy firms in the Netherlands and consists out of accounting consultants/auditors (AA in Dutch), chartered auditors (RA in Dutch) and people working in the accountancy sector.

The survey consists of 20 questions which are divided into seven subsections. These subsections relate to 1) composition/descriptive (general), 2) the scope of ADA, 3) assessing the possibility to detect misstatements, 4) sequence, 5) possibility to assist decisions, 6) materiality and 7) phase of the audit in which ADA is used. The questions are answered on a Likert-scale basis [24], in which answers range from '1 – I never use it', to '7 – I always use it'. Likert scales are considered a good fit for analytical purposes, due to their relatively large number of categories [25]. In addition, the respondents were able to answer: 'I don't know' or 'Not relevant'. For the purpose of this research the latter two are classified as '1 – I never use it'.

By formulating the survey questions, the Value Through Analytics (VTA) model from Zoet is used [26]. This model concretizes data analytics into subtypes. The VTA model incorporates the six different types of analyses from Leek and Peng (2015), namely: The 1) descriptive, 2) explanatory, 3) inferential, 4) predictive, 5) causal, and 6) mechanistic [27]. The VTA model also includes the three types of process mining as described by Van der Aalst (2011): discovery, conformance and improvement [28]. The VTA model is a tool to classify data analytics into different categories [29] and is shown in Figure 1. The VTA model distinguishes 54 different types of data analysis which can be derived by walking through the three circles within the model. The inner circle starts with the question: "What do I want to analyze?" In which a 1) process, 2) decision or 3) object can be chosen. The second circle questions "Why do I want to analyze?" Which can be answered by 1) discovery, 2) conformance, and 3) improvement. Finally, the outer circle asks the question "To what extent do I want to analyze it?" The last question indicates the choice to the following types of data analytics: 1) descriptive, 2) explanatory, 3) inferential, 4) predictive, 5) causal, and 6) mechanistic.

Additionally, the types of analysis within the VTA model are layered in sequence, which indicates that if an inferential analysis can be carried out, one should also be able to carry out a descriptive and explanatory analysis.

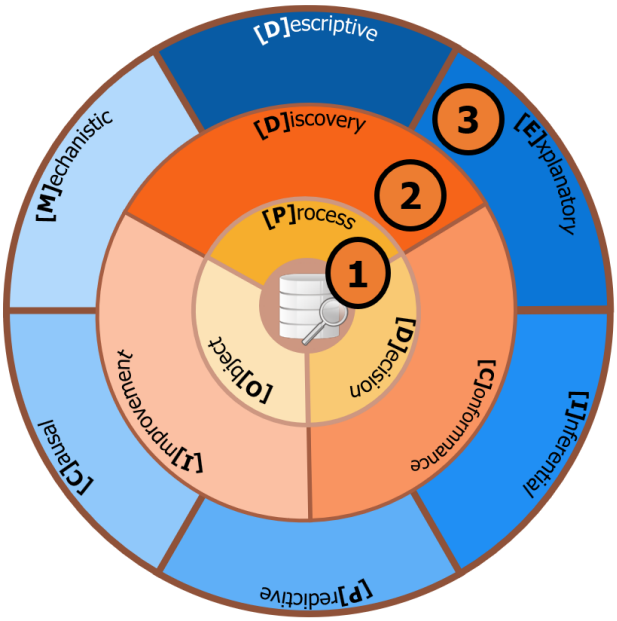

Figure 1. Value Through Analytics model [26]

To assess which competences can be utilized with the help of ADA, a so-called analysis quotient can be computed, which visualizes the type of questions that can be answered [29]. An example of this is shown in Figure 2, in which the questions are set against audit organizations. indicates that an audit organization cannot perform the analysis, green indicates that the type of analysis is standard procedure within each audit. Blue indicates that the analysis is used within every audit, but expertise is needed. Purple indicates that the analysis is executed by only one employee for their own use, but the results are not communicated throughout the team. Finally, yellow indicates that it is not executed for every audit [29].

The survey questions were set up by dr. Mantelaers (chartered auditor) and dr. Zoet, founder of the VTA model [26], based on the analysis quotient. In order to validate and refine the survey questions and to ensure the correct questioning a pilot test was conducted by five master students (Accounting and Control – Maastricht University). Moreover, the pilot test was executed by two members of the Accounttech group, of which one is related to the Post-Master IT-Auditing &Advisory (Erasmus University Rotterdam).

Figure 2. Periodic system types of analyses [29]

Within the survey questions, a particular sequence is followed related to several 'levels' of ADA usage in practice, which can be linked to the data analysis types/levels in the VTA model. In Table I the survey questions are linked to the type of data analyses derived from Figure 2. Each question focuses on the frequency of use of the ADA types as mentioned in Table I. As the questions and data analysis types, are listed in a chronological order, this implies that if an auditor uses ADA type five, the auditor will also be expected to be able to perform ADA type two and four.

TABLE I. SURVEY DESIGN

Survey question	ADA type	ADA description
7.1	2	Object – Discover – Explanatory
7.2	4	Object – Discover – Predictive
7.3	5	Object – Discover – Causal
7.4	7	Object – Discover – Descriptive
7.5	8	Object – Discover – Explanatory
8.1	19	Process – Discover - Descriptive
8.2	20	Process – Discover – Explanatory
8.3	25	Process – Conformance – Descriptive
8.4	26	Process – Conformance – Explanatory
8.5	37	Decision – Discover – Descriptive
8.6	43	Decision – Conformance - Descriptive

The questions were arranged in chronological order, following the sequence and complexity of ADA types. This means that the data analysis types embedded in these questions are used systematically in the expected chronological sequence. This approach of progressing step by step improves the clarity and relevance of the data analysis, making it a more methodical and understandable exploration of the subject matter. With this set up, we expect that ADA types with lower complexity, such as 2, will be utilized more frequently than the more intricate ADA types like 37 or 43. Furthermore, considering the hierarchy of complexity in ADA types, proficiency in

ADA type 5 should imply competence in performing ADA type 7 as well.

The sequence of the data from the survey will be analyzed with the help of process mining algorithms. For the use of this research, a heuristic analysis will be performed due to the scope of possible responses and outcomes. A heuristic analysis eliminates any redundant details and exceptions and focuses on the main behavior [23].

IV. DATA COLLECTION AND ANALYSIS

The survey was distributed to a population of 7,008 respondents in total, of which initially 203 responded, a response rate of 2.90%. The respondents consist out of 167 males and 36 females, of which 72 are a chartered auditor (RA in Dutch) and 39 accounting consultants (AA in Dutch). Around 25% of the respondents works for one of the Big 4 auditing firms (EY, PWC, Deloitte and KPMG). Based on the initial results some first analysis was carried out, this paper includes the total dataset and expands the earlier analysis/research. The final dataset consists out of 609 respondents, a response rate of 8.69%. *The respondents consist out of 488 males, 119 females and 2 (none of) both. Within the respondents there are 198 chartered auditors and 133 accounting consultants. Around 20% works for one of the Big 4 auditing firms.* The most common jobs within the respondents are external auditor (chartered auditor and accounting consultants), accountant in business or public/internal auditor. However, the work experience varies across the respondents as is shown in Table II.

The overall response rate is relatively low, possibly caused by the non-committal nature and scope of the survey. Moreover, surveys are frequently distributed within the Accounttech working group and NBA, which also causes the low response rate. From an NBA perspective this can be considered a representative response rate. The survey was distributed in the first half of 2021.

TABLE II. WORK EXPERIENCE RESPONDENTS

Work experience (in years)	Initial dataset - Number of respondents	Final dataset – Number of respondents
< 5	3	8
5 - 10	22	64
10 – 20	72	201
20 – 30	58	194
> 30	48	142
Total	**203**	**609**

To analyze the outcomes of the survey a heuristic process mining algorithm is applied by using three input variables. These input variables consist out of 1) case concept name, represented by the respondents ID, 2) concept name, represented by the question number and 3) the timestamp, represented by the answer based on the Likert scale. To ensure the chronological order a timestamp is added to the data by converting the Likert scale. In which '7 – I always use it' is matched to the earliest timestamp, as it is always used (used now). '1 – I never use it' is matched to the latest timestamp, since its use will be furthest in the future. The options in between (two to six) are matched accordingly.

V. RESULTS

A. Initial Results

The initial analysis distinguishes 132 types of unique variants within a total of 203 respondents (65.0%). A total overview of the data analysis types in order of usage is shown in Figure 3. The numbers 7.1 until 8.6 refer to the questions of the survey, the link to the data analysis types is shown in Table II. As the Likert scale was converted to a timestamp in order to perform these analyses, the order of the questions depends on the usage of the specific ADA. For example, question 7.1 relates to the use of data analysis: Object – Discover – Explanatory. 60.6% of the respondents (n=123) indicated that this analysis is always used (Likert scale – 7). Due to the rating of '7 – I always use it', this data analysis type is matched to the earliest timestamp and therefore shown at the start of the path in Figure 3.

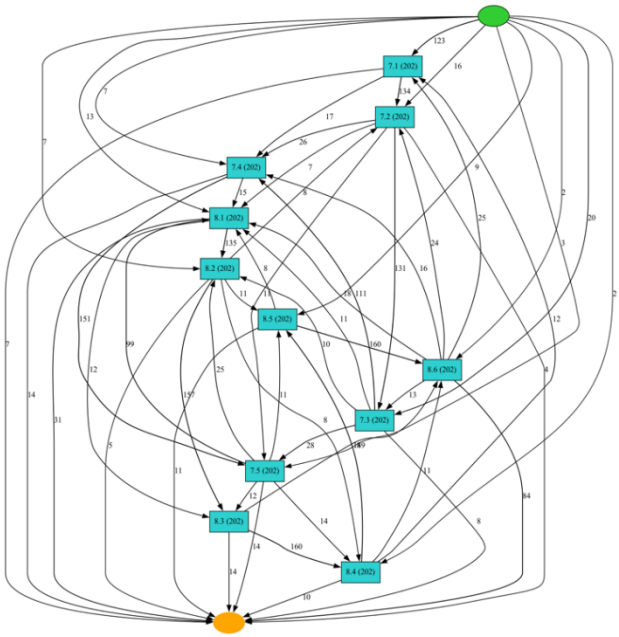

Figure 3. Result heuristic miner.

Due to the high number of unique variants (65.0%), an overview of the top ten variants is shown in Table III. For clarity purposes, the number of occurrences per unique variant is added.

TABLE III. TOP 10 VARIANTS

												Number of occurences
Variant 1	7.1	7.2	7.3	7.4	7.5	8.1	8.2	8.3	8.4	8.5	8.6	58
Variant 2	7.1	7.2	7.3	7.4	7.5	8.2	8.3	8.4	8.5	8.6	8.1	4
Variant 3	7.1	7.2	7.3	8.1	8.2	8.3	8.4	8.5	8.6	7.4	7.5	3
Variant 4	8.1	8.2	8.3	8.4	8.5	8.6	7.1	7.2	7.3	7.4	7.5	2
Variant 5	7.2	7.3	7.4	7.5	8.1	8.2	8.3	8.4	8.5	8.6	7.1	2
Variant 6	7.1	7.3	8.1	8.2	8.3	8.4	8.5	8.6	7.2	7.4	7.5	2
Variant 7	7.1	7.3	7.4	7.5	8.1	8.2	8.3	8.4	8.5	8.6	7.2	2
Variant 8	7.1	7.2	7.5	8.1	8.2	8.3	8.4	8.5	8.6	7.3	7.4	2
Variant 9	7.1	7.2	7.3	7.5	8.1	8.2	8.3	8.4	8.5	8.6	7.4	2
Variant 10	7.1	7.2	7.3	7.4	7.5	8.5	8.6	8.1	8.2	8.3	8.4	2

The most common variant (variant 1) occurs 58 times. This variant is, also chronologically seen, the most logical variant, as the occurrence of the questions are in a chronological order (7.1 to 8.6). This means that the data analysis types, intertwined in the questions, are used in the (expected) chronological order. However, this is only applicable to 28.6% of the respondents (n=58). The number of occurrences for the other variances is widely spread as can be seen for variant two to ten (max. four occurrences per variant). The results from variant two show that question 8.1 (related to data analysis type Process – Discover – Descriptive) is used less compared to question 8.2 to 8.6 (related to the more advanced data analysis types). In variant three to ten a non-chronological order is also apparent, indicating that the more 'basis' analysis types are carried out less frequently than the more 'advanced' types. However, variant four indicates that analyses with regards to a process and/or decision (questions 8.1-8.6) are frequently used, and analysis regarding an object (questions 7.1-7.5) less frequently, despite the fact that most of the analyses regarding 'Objects' are expected to be used standard in every audit, as can be derived from Figure 2.

As the results vary widely, an additional analysis solely on the external auditors (chartered auditor and accounting consultants) as they are expected to have the most experience with regards to audits. Within the total sample, 111 external auditors and 79 unique variants are identified (variance of 71.2%). Compared to the total sample, an even higher variance can be recorded. The results are shown in Figure 4.

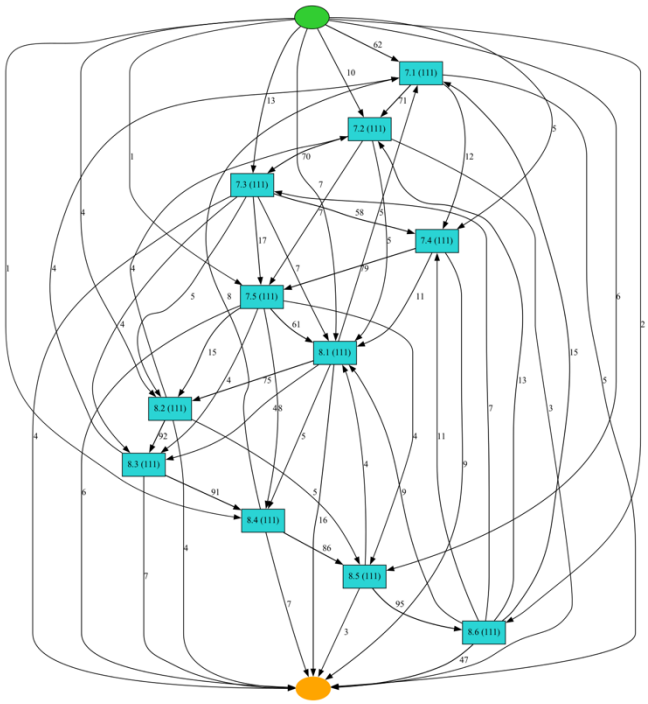

Figure 4. Result heuristic miner external auditors.

Due to the high number of unique variants (65.0%), an overview of the top ten variants is shown in Table IV. For clarity purposes, the number of occurrences per unique variant is added.

TABLE IV. TOP 10 VARIANTS EXTERNAL AUDITORS

												Number of occurences
Variant 1	7.1	7.2	7.3	7.4	7.5	8.1	8.2	8.3	8.4	8.5	8.6	31
Variant 2	7.1	7.3	7.4	7.5	8.1	8.2	8.3	8.4	8.5	8.6	7.2	2
Variant 3	7.1	7.2	7.3	7.4	7.5	8.2	8.3	8.4	8.5	8.6	8.1	2
Variant 4	8.6	8.5	7.2	7.1	7.3	7.4	7.5	8.2	8.3	8.4	8.1	1
Variant 5	8.6	7.2	7.3	7.1	7.4	7.5	8.1	8.2	8.3	8.4	8.5	1
Variant 6	8.5	8.6	8.2	8.3	8.4	7.2	7.5	7.3	7.4	8.1	7.1	1
Variant 7	8.5	8.6	8.1	8.2	8.3	8.4	7.1	7.2	7.5	7.4	7.3	1
Variant 8	8.5	8.6	7.3	7.5	8.1	8.2	8.4	7.1	7.4	7.2	8.3	1
Variant 9	8.5	8.6	7.1	7.2	7.3	7.5	8.2	8.3	8.4	8.1	7.4	1
Variant 10	8.5	8.6	7.1	7.2	7.3	7.4	7.5	8.1	8.2	8.3	8.4	1

The most common variant (variant 1) occurs 31 times. This variant is, also chronologically seen, the most logical variant, as the occurrence of the questions are in a chronological order (7.1 to 8.6). However, this is only applicable to 27.9% of the respondents (n=31). The number of occurrences for the other variances is widely spread as can be seen for variant two to ten (max. two occurrences per variant).

B. Subsequent analysis

In addition to the initial analysis, the analyses were repeated based on the expanded survey (n=609). The analysis based on the expanded survey distinguishes 357 unique variants within a total of 609 respondents (58.6%).

A total overview of the data analysis types in order of usage is shown in Figure 5.

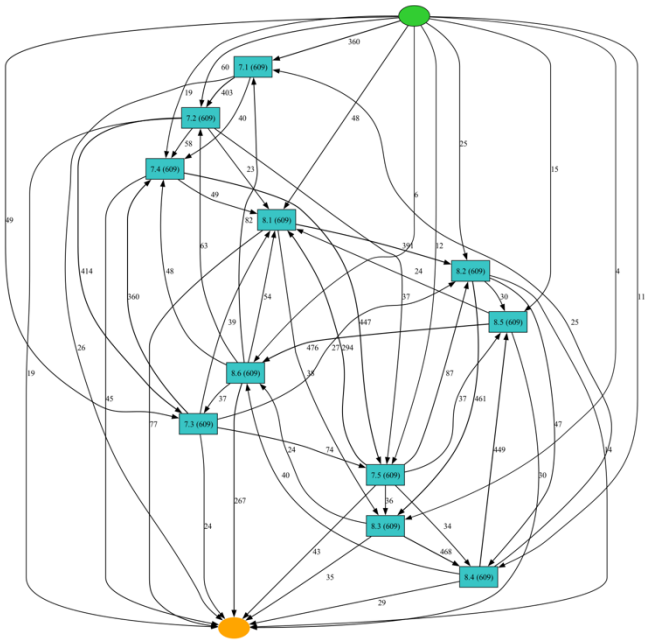

Figure 5. Results heuristic miner – subsequent analysis

Due to the high number of unique variants (58.6%), an overview of the top ten variants is shown in Table V. For clarity purposes, the number of occurrences per unique variant is added.

TABLE V. TOP 10 VARIANTS – SUBSEQUENT ANALYSIS

												Number of occurences
Variant 1	7.1	7.2	7.3	7.4	7.5	8.1	8.2	8.3	8.4	8.5	8.6	179
Variant 2	7.1	7.2	7.3	7.4	7.5	8.2	8.3	8.4	8.5	8.6	8.1	12
Variant 3	8.1	8.2	8.3	8.4	8.5	8.6	7.1	7.2	7.3	7.4	7.5	11
Variant 4	7.1	7.2	7.3	7.5	8.1	8.2	8.3	8.4	8.5	8.6	7.4	8
Variant 5	7.1	7.3	7.4	7.5	8.1	8.2	8.3	8.4	8.5	8.6	7.2	6
Variant 6	7.2	7.3	7.4	7.5	8.1	8.2	8.3	8.4	8.5	8.6	7.1	5
Variant 7	8.1	7.1	7.2	7.3	7.4	7.5	8.2	8.3	8.4	8.5	8.6	4
Variant 8	7.1	7.2	7.4	7.5	8.1	8.2	8.3	8.4	8.5	8.6	7.3	4
Variant 9	7.1	7.2	7.3	8.1	8.2	8.3	8.4	8.5	8.6	7.4	7.5	4
Variant 10	7.1	7.2	7.3	7.4	7.5	8.5	8.6	8.1	8.2	8.3	8.4	4

The most frequent variant, referred to as variant 1, appears 179 times. Chronologically, this variant aligns logically with the sequential order of questions (7.1 to 8.6). Consequently, the data analysis types embedded in these questions are employed in the expected chronological sequence. However, this pattern is applicable to only 29.4% of the respondents (n=179). The occurrences for other variants are widely dispersed, ranging from twelve to four instances for variants two through ten.

Due to the significant variation in results, a supplementary analysis will be carried out focusing solely on the external auditors (who are anticipated to possess the most extensive audit experience. The expanded sample consists of 332 external auditors. Based on the external auditor sample, 195 unique variants were identified (58.7%). This closely reflects the variance observed in the total population. Nevertheless, the anticipated chronological order is acknowledged by only 105 respondents (31.6%). This percentage is marginally higher among external auditors when compared to the total sample. A total overview of the data analysis types in order of usage for the external auditors is shown in Figure 6.

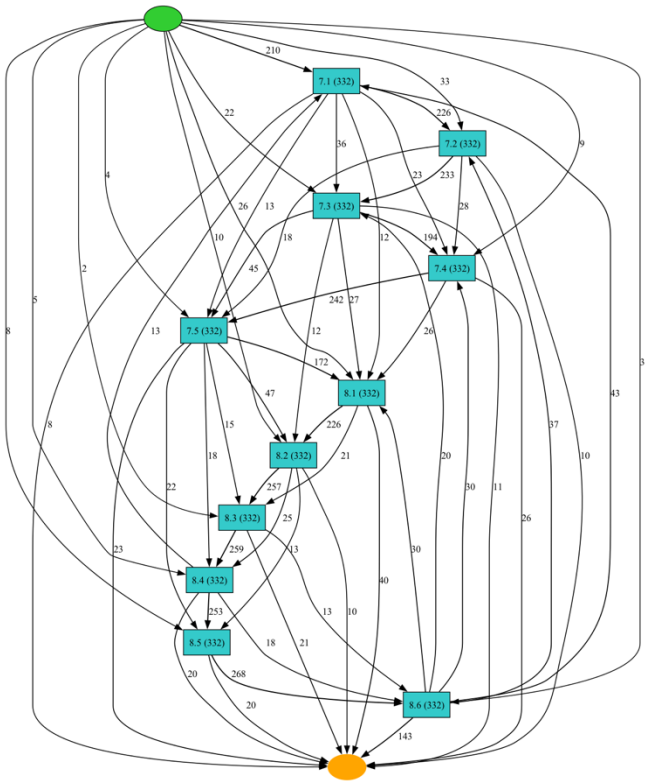

Figure 6. Results heuristic miner external auditors– subsequent analysis

Due to the high number of unique variants (58.7%), an overview of the top ten variants is shown in Table VI. For clarity purposes, the number of occurrences per unique variant is added.

TABLE VI. TOP 10 VARIANTS EXTERNAL AUDITORS – SUBSEQUENT ANALYSIS

												Number of occurences
Variant 1	7.1	7.2	7.3	7.4	7.5	8.1	8.2	8.3	8.4	8.5	8.6	105
Variant 2	8.1	8.2	8.3	8.4	8.5	8.6	7.1	7.2	7.3	7.4	7.5	6
Variant 3	7.1	7.2	7.3	7.5	8.1	8.2	8.3	8.4	8.5	8.6	7.4	6
Variant 4	7.1	7.2	7.3	7.4	7.5	8.2	8.3	8.4	8.5	8.6	8.1	6
Variant 5	7.1	7.3	7.4	7.5	8.1	8.2	8.3	8.4	8.5	8.6	7.2	5
Variant 6	8.1	7.4	7.1	7.2	7.3	7.5	8.2	8.3	8.4	8.5	8.6	3
Variant 7	7.1	7.2	7.4	7.5	8.1	8.2	8.3	8.4	8.5	8.6	7.3	3
Variant 8	7.1	7.2	7.3	7.4	7.5	8.5	8.6	8.1	8.2	8.3	8.4	3
Variant 9	7.2	7.3	7.5	8.1	8.2	8.3	8.4	8.5	8.6	7.1	7.4	2
Variant 10	7.2	7.3	7.4	7.5	8.1	8.2	8.3	8.4	8.5	8.6	7.1	2

The most common variant, variant one, is observed 105 times. It follows a chronological alignment with questions ranging from 7.1 to 8.6, wherein the embedded data analysis types are logically applied in the expected sequence. Notably, this pattern is found in only 31.6% of the respondents (n=105). Occurrences for other variants are widely scattered, with instances ranging from six to two for variants two through ten.

C. Final analysis

Initially, both responses 'I don't know' and 'Not relevant' were categorized under '1- I never use it.' However, in our effort to refine and clarify the dataset, we are revisiting this classification.

To establish a more distinct differentiation, the decision has been made to equate 'Not relevant' with '1 – I never use it.' This choice is grounded in the understanding that 'Not relevant' implies a lack of usage for the particular item. Conversely, 'I don't know' will undergo a dedicated analysis. We recognize that this response cannot be seamlessly linked to the Likert scale without potentially introducing distortions to the overall data overview. This approach allows for a nuanced separation between explicit non-usage, represented by 'Not relevant,' and uncertainty, as indicated by 'I don't know.' By doing so, we aim to preserve an accurate understanding of the dataset, while acknowledging the intricacies associated with the 'I don't know' response. This reconsideration is intended to enhance the overall reliability and interpretability of the data.

First, a descriptive analysis will be performed on the usage of 'I don't know.' On average, each respondent answered 'I don't know' to 0.90 questions. In addition, 17 respondents (out of the 609 total respondents) answered 'I don't know' to all 11 questions. The frequency of 'I don't know' responses for each question is presented in Table VII.

TABLE VII. ANALYSIS RESPONSE 'I DON'T KNOW'

Question	Occurences of 'I don't know'	ADA description	ADA type
7.1	57	Object – Discover – Explanatory	2
7.2	48	Object – Discover – Predictive	4
7.3	56	Object – Discover – Causal	5
7.4	37	Object – Discover – Descriptive	7
7.5	43	Object – Discover – Explanatory	8
8.1	41	Process – Discover - Descriptive	19
8.2	48	Process – Discover – Explanatory	20
8.3	41	Process – Conformance – Descriptive	25
8.4	55	Process – Conformance – Explanatory	26
8.5	61	Decision – Discover – Descriptive	37
8.6	63	Decision – Conformance - Descriptive	43

To enhance clarity, the results are visualized in Figure 7. This shows that for the first questions, relatively more 'I don't know' responses were registered. From question 7.4 onwards, a drop is visible, indicating a decreasing frequency of 'I don't know' responses. However, a notable trend emerges beyond this point, revealing an increasing amount of 'I don't know' responses as the complexity of the data analysis types rises.

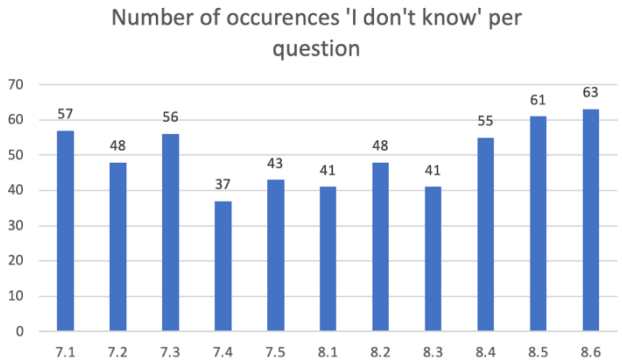

Figure 7. Number of occurences response 'I don't know' per question.

These results indicate that respondents initially grapple with uncertainty in the early questions, possibly due to the novelty of the survey or the initial learning curve. The observed drop in 'I don't know' responses from question 7.4 may suggest a level of familiarity or increased confidence among respondents in handling less complex data analysis types. However, the subsequent rise in 'I don't know' responses from question 7.4 onwards suggests a growing challenge for respondents as the survey progresses into more intricate aspects of data analysis. This pattern underscores the need for targeted support or training in the latter stages of the survey, where the complexity of questions seems to pose a greater difficulty for participants.

Based on the refined dataset, the heuristic process mining algorithm will be reapplied to analyze the results. The refined dataset is identical to the dataset used in the subsequent analysis (V. Results – B), excluding responses labeled 'I don't know' to eliminate noise. This analysis will be conducted on both the entire sample and the subset of external auditors. The entire sample comprises the 609 respondents, excluding the 17 who answered all questions with 'I don't know' (n=592). The analysis based on the expanded survey distinguishes 374 unique variants within a total of 592 respondents (63.2%). A total overview of the data analysis types in order of usage is shown in Figure 8.

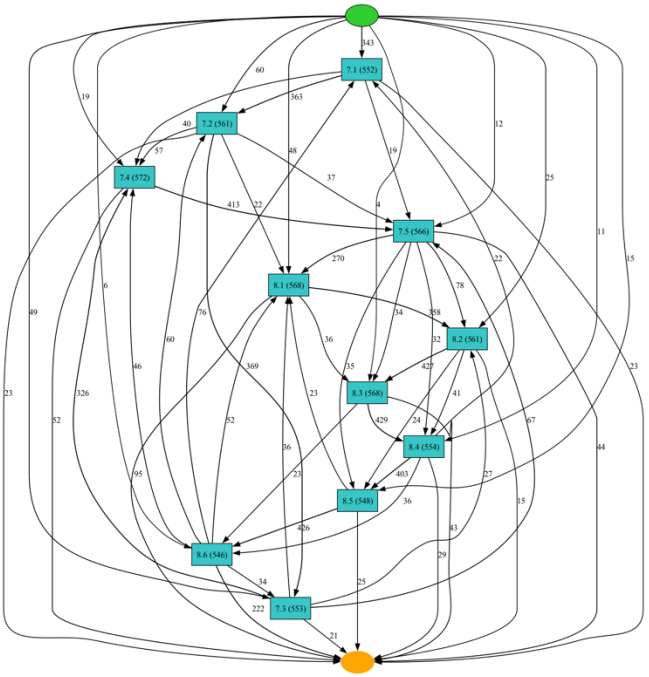

Figure 8. Results heuristic miner – final analysis

Due to the high number of unique variants (63.2%), an overview of the top ten variants is shown in Table VIII. For clarity purposes, the number of occurrences per unique variant is added.

TABLE VIII. TOP 10 VARIANTS – FINAL ANALYSIS

												Number of occurences
Variant 1	7.1	7.2	7.3	7.4	7.5	8.1	8.2	8.3	8.4	8.5	8.6	158
Variant 2	7.1	7.2	7.3	7.4	7.5	8.2	8.3	8.4	8.5	8.6	8.1	12
Variant 3	8.1	8.2	8.3	8.4	8.5	8.6	7.1	7.2	7.3	7.4	7.5	9
Variant 4	7.1	7.2	7.3	7.5	8.1	8.2	8.3	8.4	8.5	8.6	7.4	7
Variant 5	7.1	7.3	7.4	7.5	8.1	8.2	8.3	8.4	8.5	8.6	7.2	6
Variant 6	7.2	7.3	7.4	7.5	8.1	8.2	8.3	8.4	8.5	8.6	7.1	4
Variant 7	7.1	7.2	7.3	8.1	8.2	8.3	8.4	8.5	8.6	7.4	7.5	4
Variant 8	7.1	7.2	7.3	7.4	7.5	8.5	8.6	8.1	8.2	8.3	8.4	4
Variant 9	7.3	7.4	7.5	7.1	7.2	8.1	8.2	8.3	8.4	8.5	8.6	3
Variant 10	7.1	7.5	8.1	8.2	8.3	8.4	8.5	8.6	7.2	7.3	7.4	3

Appearing 158 times, variant 1 stands out as the most frequent. It conforms chronologically to the order of questions (7.1 to 8.6), where the associated data analysis types are logically employed in the anticipated sequence. However, this specific pattern is evident in just 26.7% of the respondents (n=158). The occurrences of other variants are widely distributed, with instances varying from two to four for variants two through ten.

The analysis based on the expanded survey, solely focused on the external auditors, distinguishes 200 unique variants within a total of 323 respondents (61.9%). A total overview of the data analysis types in order of usage is shown in Figure 9.

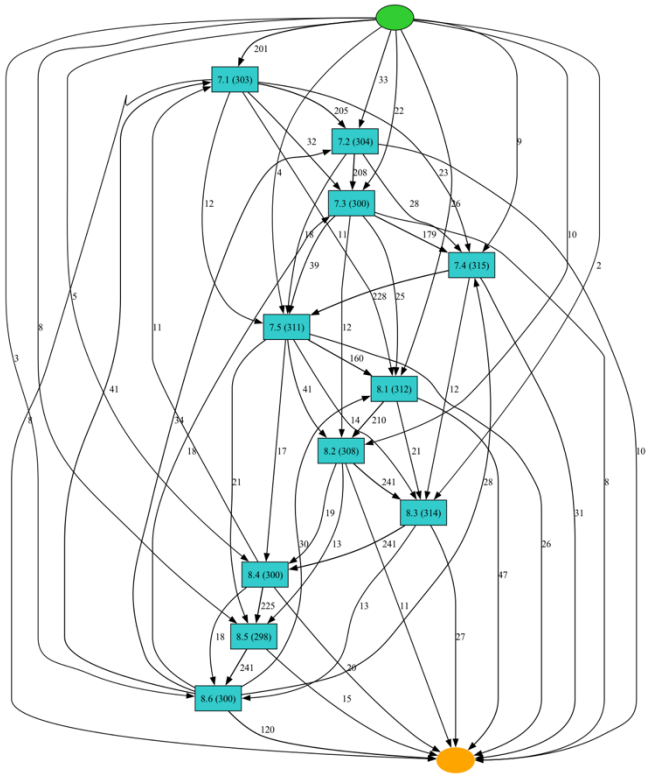

Figure 9. Results heuristic miner external auditors – final analysis

The top ten variants are shown in Table IX. For clarity purposes, the number of occurrences per unique variant is added.

TABLE IX. TOP 10 VARIANTS EXTERNAL AUDITORS – FINAL ANALYSIS

												Number of occurences
Variant 1	7.1	7.2	7.3	7.4	7.5	8.1	8.2	8.3	8.4	8.5	8.6	95
Variant 2	8.1	8.2	8.3	8.4	8.5	8.6	7.1	7.2	7.3	7.4	7.5	6
Variant 3	7.1	7.2	7.3	7.4	7.5	8.2	8.3	8.4	8.5	8.6	8.1	6
Variant 4	7.1	7.3	7.4	7.5	8.1	8.2	8.3	8.4	8.5	8.6	7.2	5
Variant 5	7.1	7.2	7.3	7.5	8.1	8.2	8.3	8.4	8.5	8.6	7.4	5
Variant 6	7.1	7.2	7.3	7.4	7.5	8.5	8.6	8.1	8.2	8.3	8.4	3
Variant 7	8.1	7.4	7.1	7.2	7.3	7.5	8.2	8.3	8.4	8.5	8.6	2
Variant 8	7.2	7.3	7.5	8.1	8.2	8.3	8.4	8.5	8.6	7.1	7.4	2
Variant 9	7.2	7.3	7.4	7.5	8.1	8.2	8.3	8.4	8.5	8.6	7.1	2
Variant 10	7.1	7.5	8.1	8.2	8.3	8.4	8.5	8.6	7.2	7.3	7.4	2

With a frequency of 95 occurrences, variant 1 emerges as the most prevalent. Sequentially, this variant aligns with the order of questions (7.1 to 8.6), showcasing a logical utilization of data analysis types in the expected sequence. It's noteworthy that this pattern applies to only 29.4% of the respondents (n=95). The instances of other variants are dispersed widely, ranging from two to four occurrences for variants two through ten.

D. Summary results

All results, combining initial, subsequent and final analyses, are summarized in Table X.

TABLE X. SUMMARY RESULTS

Analysis	Sample size	Variance (% unique variants)	Number of occurences of anticipated sequence	% of occurences of anticipated sequence
Initial analysis - total	203	65.0%	58	28.6%
Initial analysis - external auditors	111	71.2%	31	27.9%
Subsequent analysis - total	609	58.6%	179	29.4%
Subsequent analysis - external auditors	332	58.7%	105	31.6%
Final analysis - total	592	63.2%	158	26.7%
Final analysis - external auditors	323	61.9%	95	29.4%

The results from both the initial and subsequent analyses exhibit a considerable degree of similarity. The anticipated sequence in the utilization of data analysis is observed in only 28-30% of the respondents. Even after refining the data by excluding 'I don't know' responses in the final analysis, the percentage of the expected sequence remains within the range of 26-30%. Additionally, all analyses indicate a high percentage of variance, exceeding 58%. Despite the increase in variances resulting from the elimination of 'I don't know' responses in the final analysis, the overarching trend remains consistent.

VI. CONCLUSION AND FUTURE WORK

In this article, we aimed to answer the main question: *"How and to what extent is Audit Data Analytics currently used by auditors/accountants?"* With the help of a survey distributed across members of the NBA working group Accounttech, an overview was given of the use (and its extent) of ADA. The insights derived from our study provide a better understanding of how and to which extent ADA is currently used by auditors/accountants and specific external auditors. However, the results in conjunction with the non-chronological order of the data analysis types, indicate the presence of a misinterpretation or possible gap in comprehending the data analysis types utilized in the survey and their appropriate chronological order. This discrepancy raises questions about the competence and understanding of the survey participants in applying these data analysis techniques in a correct and coherent manner. Remarkable are the similar results within the external auditor group, as they are expected to have the most experience regarding audits. Future research could therefore focus on concretizing (and creating an understanding of) the data analysis types. This could be achieved by creating a more practice-oriented survey. Moreover, in future research we would like to follow up on the answers: *'I don't know' or 'Not relevant'* to identify the underlying reasons and expand our results/knowledge.

ACKNOWLEDGEMENTS

We would like to thank Michelle van Wamelen for collecting the data. Moreover, we would like to thank the NBA working group Accounttech for collaborating on this survey.

REFERENCES

[1] L. Verhoeven, E. Mantelaers, and M. Zoet, "Usage of Audit Data Analytics within the Accountancy Sector," in Proc. eKNOW, 2023, pp.14-19.

[2] MCA, "Accountancy Monitoring Committee." Accessed: Mar. 24, 2023. [Online]. Available: https://www.monitoringaccountancy.nl/

[3] Future Accountancy Sector Committee, "Confidence in Control Final Report of the Committee on the Future of the Accountancy Sector | Parliamentary Document | Central Government." [Online]. Available: https://www.rijksoverheid.nl/documenten/kamerstukken/2020/01/30/vertrouwen-op-controle-eindrapport-van-de-commissie-toekomst-accountancysector

[4] AFM, "AFM supervisory agenda 2022," 2022.

[5] AFM, "Research reports on supervision of audit firms | Audit firms | AFM Professionals." Accessed: Mar. 24, 2023. [Online]. Available: https://www.afm.nl/nl-nl/sector/accountantsorganisaties/rapporten-publicaties

[6] D. Brydon, "Assess, assure and inform: improving audit quality and effectiveness," UK Government, 2019.

[7] Future Accountancy Sector Committee, "Reliance on Audit," *Ministerie van Financiën*, 2020.

[8] E. Mantelaers, "An Evaluation of Technologies to Improve Auditing," Open University, 2021.

[9] L. E. DeAngelo, "Auditor Size and Audit Quality," *Journal of Accounting and Economics*, vol. 3, no. 3, pp. 183–199, 1981, doi: https://doi.org/10.1016/0165-4101(81)90002-1.

[10] Government Accountability Office, "Public Accounting Firms: Required Study on the Potential Effects of Mandatory Audit Firm Rotation," Government Printing Office, Washington D.C., 2003.

[11] J. R. Francis, "What do we know about audit quality?," *British Accounting Review*, vol. 36, no. 4. pp. 345–368, 2004. doi: 10.1016/j.bar.2004.09.003.

[12] D. Barr-Pulliam, H. L. Brown-Liburd, and K. A. Sanderson, "The Effects of the internal control opinion and use of audit data analytics on perceptions of audit quality, assurance, and auditor negligence," *A Journal of Practice & Theory (2022)*, vol. 41, no. 1, pp. 25–48, 2022, [Online]. Available: https://doi.org/10.2308/AJPT-19-064

[13] G. Salijeni, A. Samsonova-Tadderu, and S. Turley, "Big Data and changes in audit technology: contemplating a research agenda," *Accounting and Business Research*, vol. 49, no. 1, pp. 95–119, 2019.

[14] M. Cao, R. Chychyla, and T. Stewart, "Big Data analytics in financial statement audits," *Accounting Horizons*, vol. 2, no. 29, pp. 423–429, 2015.

[15] J. van Buuren and W. Wijma, "On quality assurance of data-driven control methodology," *Maandblad Voor Accountancy en Bedrijfseconomie*, vol. 96, no. 1/2, pp. 15–25, 2021.

[16] AFM, "Legislative letter." 2021.

[17] FRC, "The use of technology in the audit of financial statements," 2020.

[18] A. Eilifsen, F. Kinserdal, W. F. Jr. Messier, and T. E. McKee, "An Exploratory Study into the Use of Audit Data Analytics on Audit Engagements," *American Accounting Association*, pp. 1–23, 2020.

[19] M. Jans, P. Soffer, and T. Jouck, "Building a valuable event log for process mining: an experimental exploration of a guided process," *Enterp Inf Syst*, vol. 13, no. 5, pp. 601–630, May 2019, doi: 10.1080/17517575.2019.1587788.

[20] W. M. P. Van Der Aalst, "Process Mining," in *Discovery, Conformance and Enhancement of Business Processess*, 2011, pp. 215–217.

[21] W. van der Aalst, "Process Mining," *ACM Trans Manag Inf Syst*, vol. 3, no. 2, pp. 1–17, Jul. 2012, doi: 10.1145/2229156.2229157.

[22] A. Berti, S. van Zelst, and D. Schuster, "PM4Py: A process mining library for Python," *Software Impacts*, vol. 17, p. 100556, Sep. 2023, doi: 10.1016/j.simpa.2023.100556.

[23] A. J. M. M. Weijters, W. M. P. van der Aalst, and A. K. A. de Medeiros;, "Process Mining with the HeuristicsMiner Algorithm," *Beta working papers*, no. May, 2006.

[24] R. Likert, "A Technique for the Measurement of Attitudes," *rchives of Psychology*, no. 140, pp. 1–55, 1932.

[25] L. H. Kidder, C. M. Judd, and E. R. Smith, *Research methods in social relations*, 5th ed. CBS College Publishing, 1986.

[26] M. Zoet, "VTA-model," 2018. Accessed: Feb. 01, 2023. [Online]. Available: https://martijnzoet.com/2018/10/22/het-value-through-analytics-vta-model/

[27] J. Leek and R. D. Peng, "What is the question?," *Science Magazine*, pp. 1314–1315, 2015.

[28] W. M. P. Van Der Aalst, "Process Mining," in *Discovery, Conformance and Enhancement of Business Processess*, 2011, pp. 215–217.

[29] E. Mantelaers and M. Zoet, "Data-analysis (III)." Accessed: Mar. 27, 2023. [Online]. Available: https://www.accountant.nl/vaktechniek/2021/1/data-analyse-nader-geanalyseerd-iii/

Design Analysis and Fabrication of High Gain Wideband Antipodal Vivaldi Antenna for Satellite Communication Applications

Nitin Muchhal*#, Renato Zea Vintimilla*, Mostafa Elkhouly*, Yaarob Fares*, Shweta Srivastava#
*Fraunhofer Institute for Integrated Circuits IIS, Am Wolfsmantel 33, 91058 Erlangen, Germany
{firstname.lastname@iis.fraunhofer.de}*
#Jaypee Institute of Information Technology Noida, India
{shweta.srivastava@jiit.ac.in}
*#corresponding author e-mail: nmuchhal@gmail.com

***Abstract* — A wideband and high gain corrugated epsilon negative index metamaterial (ENG) Antipodal Vivaldi Antenna (AVA) with gain>12 dBi and working in frequency range from 10 GHz - 25 GHz (for SATCOM applications) is proposed in this paper. The overall performance of the proposed Antipodal Vivaldi Antenna (AVA) is enriched by using a triangular shaped corrugation slots and pi (∏) shaped epsilon negative metamaterial cells. The '∏' shaped metamaterial unit cells are positioned on the upper surface amid both radiators of AVA to emanate the intense electric field in the end-fire direction. The proposed antenna size is 22.6 mm × 15.8 mm x 1.6 mm and it is designed on the FR4 substrate. The proposed antenna is then fabricated using photolithography process and tested for its performances. There is good agreement between simulated and measured results. The measured gain varies from 6.2 – 10.7 dBi.**

Keywords- Metamaterial; Corrugation; Antipodal Vivaldi Antenna (AVA); Gain; SATCOM.

I. INTRODUCTION

Wideband antenna with high gain is the primary requisite for any communication system. Such a high gain wideband antenna is recently proposed in [1]. Furthermore, high data rates and increased quality of service (QoS) for end users are in ever-increasing demand due to the recent improvement and spectacular achievement in the field of wireless communication technology [2], [3]. Wireless communication system designers face a challenging task when designing compact and wideband antenna for high-speed, high-capacity, and secure wireless communications. In contemporary times numerous designs of wideband antennas fulfilling varied objectives have been proposed by various researchers for modern wireless networks [4-6].

To accomplish pervasive connectivity on the globe, SATellite COMmunication (SATCOM) is a crucial constituent of next-generation wireless communications. Also, SATCOM is one of the leading technologies used today for high speed internet communication [7]. Ku-band that is a part of the electromagnetic spectrum, which operates in frequency range from 12 GHz to 18 GHz, is one of prominent and widely used frequency band for satellite communication in the world. It is considered trustworthy for the high-powered satellite services used in digital TV, teleconferences, vehicular communication, entertainment, and international programming [8],[9]. Also, they find huge application in Very Small Aperture Terminal (VSAT) [10] systems on ships, commercial aircraft, etc.

In recent times, a significant amount of research work has been proposed to design various vital components [11-13] for SATCOM applications. The Vivaldi antenna was proposed and designed by Gibson for high-frequency applications [14]. Later, Gazit improved it by giving it an antipodal shape to enhance the bandwidth and gain [15]. By incorporating numerous enhancement methods, e.g., adding parasitic patch, dielectric lens, array and metamaterial, the parameters of the Antipodal Vivaldi Antenna (e.g., directivity, bandwidth, reduction inside lobe level, etc.) can be improved. Agahi et al. [16] proposed a novel scheme for enhancing the performance of AVA by integrating two small parasitic patches inserted adjacent to the conventional flare structure to make the current distribution stronger. The addition of the parasitic patches augment the bandwidth, nonetheless, the gain performance is not much improved. Moosazadeh et al. [17] proposed a high gain AVA. To enhance gain at lower frequencies, first slit edge technique is applied to conventional antipodal Vivaldi antenna (CAVA). Furthermore, a trapezoid dielectric lens is appended to improve the gain and directivity at higher frequencies. The dielectric lens used upsurges the end-fire radiations, but at the cost of a large size. Dixit et al. [18] proposed 1 x 4 AVA array (AVA-A) designed with apertures amid two antenna elements. Further performance of AVA-A is boosted by incorporating corrugations in it. The proposed AVA Array design improves the gain but suffers from augmented mutual coupling due to proximity of antenna elements. A wide-band and compact Antipodal Vivaldi Antenna (AVA) was proposed by Zhang et al. [19] for use in ultra wideband applications. To make the AVA smaller, an arc curve is used in place of the radiator's exponential tapering edge. The AVA also has a "director" and a "convex lens" to increase its gain at high frequencies. The proposed antenna has a small size and operates in the 3.01 to 10.6 GHz frequency range but it has a drawback of complex design and fabrication. Dixit et al. [20] proposed a 1 × 4 AVA array for numerous 5G services. The proposed

antenna has a high gain and works in the frequency bands 24–29 GHz and 30–40 GHz, respectively; nonetheless, it has large size due to multiple array elements. A novel technique was proposed by Nassar et al. [21] to improve the bandwidth and directivity of broad band (2 GHz - 32 GHz) antipodal Vivaldi antenna configuration. The technique is based on adding a parasitic elliptical patch to the aperture to increase field coupling between the arms and create additional radiation in the direction of the end fire, still it has low gain. Emre et al. [22] proposed an UWB Vivaldi antenna array with high gain for Synthetic Aperture Radar applications. First, the single element of antenna is designed for ultra-wide band operation in the X and Ku-band frequency range. Afterward, the proposed antenna is then shielded from surface currents by edge grooves made on the sides of the exponential etched patch surface. Additionally, the parasitized element is supplemented to improve antenna gain still due to ineffective coupling, radiation properties are not good. Cheng et al. [23] proposed a miniaturized Vivaldi Antenna for Ground Penetrating Radar system. In the proposed design, an Artificial Materials Lens (AML) and a Side Lobe Suppressor (SSR) are implanted to enhance the gain and radiation properties of the GPR antenna. The higher frequency of EM waves is affected by AML, whereas the lower frequency of EM wave is affected by SSR but design is quite complex.

Amongst several techniques, the enhancement technique using metamaterial is quite effective without increasing the size of an antenna [24],[25]. After an intensive literature review, it is established that little work is done on AVA with metamaterial for SATCOM applications. This paper presents a compact and enhanced gain AVA with '∏'(pi) shaped metamaterial for SATCOM applications.

The rest of the paper is structured as follows: Section I covers introduction and literature review of Vivaldi antenna. Section II briefly discusses about Vivaldi antenna. Section III elaborates on the design of the proposed conventional AVA. Section IV deals with the design of the corrugated AVA. Section V covers the design and analysis of corrugated AVA with the novel metamaterial unit cells. The simulated results of the proposed AVA are discussed in Section VI. Section VII deals with the fabricated design and measured results. The outcomes of the proposed AVA are concluded in Section VIII followed by references.

II. VIVALDI ANTENNA

Vivaldi antenna is a traditional UWB antenna possessing wide bandwidth, high efficiency and small size. Vivaldi antenna's early design was unveiled by Gibson in 1979 [4]. Figure 1 depicts the generalized structure of microstrip fed taper slot Vivaldi antenna. It is essentially a flared slotline that is fabricated on a single metallization layer reinforced by a dielectric substrate. The tapered profile conventionally has exponential curve that generates a smooth transition from the slotline to the open space.

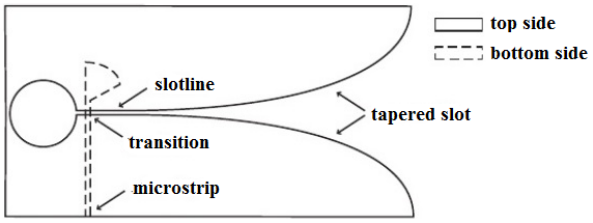

Figure. 1 Tapered slot Vivaldi antenna [26]

The tapered-slot antennas employ a traveling wave propagating along the antenna structure since the phase velocity is less than the velocity of light in free space. Therefore, they create radiation in the endfire direction at the broader end of the slot in preference to other directions [27].

III. DESIGN OF CONVENTIONAL AVA (CAVA)

Antipodal Vivaldi Antenna (AVA) was first proposed by Gazit in 1988. It unveils superior features such as wideband, high gain, stable radiation pattern and easy fabrication and hence it can efficiently gratify the various requirements of SATCOM. It consists of tapered or exponential metallic patches on top and bottom plane with a microstrip feed line matching with the connector, as shown in Figure 2.

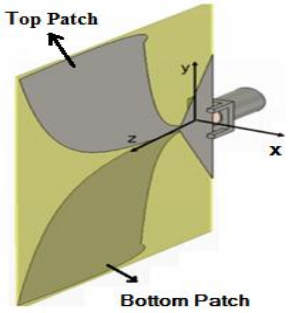

Figure 2. Antipodal Vivaldi Antenna [28]

Figure 3 depicts the geometry of the Conventional Antipodal Vivaldi Antenna (CAVA) simulated in HFSS ver. 13. This antenna consists of two parts: elliptical curved radiation flares and feed line. The top and bottom patches act as radiator and ground, respectively. The antenna is designed on standard and economical substrate FR4 with a dielectric constant of 4.4, tan δ as 0.02 and thickness 1.6 mm and simulated using HFSS ver. 13. As the Antipodal antennas operate as a resonant antenna at the lower end of frequency band, the antenna length L1 and width W1 are determined based on the lowest frequency f_L, relative

dielectric constant ε_r. The antenna dimensions are calculated by using the following equations [28]:

$$L_1 = \frac{C}{f_L}\sqrt{\frac{2}{\varepsilon_r + 1}} \quad (1)$$

$$W1 = \frac{C}{2f_L\sqrt{\varepsilon_r}} \quad (2)$$

The curve equations are given as

$$Y = \pm(R_1 e^{rx} + R_2) \quad (3)$$

where R1 and R2 are given by:

$$R1 = \frac{y2-y1}{e^{rx2}-e^{rx1}} \quad (4)$$

$$R2 = \frac{e^{rx2}y1 - e^{rx1}y2}{e^{rx2}-e^{rx1}} \quad (5)$$

Here, R1 and R2 are constants, 'r' symbolizes the increase rate of an exponential curve and, x1, y1, are the initial points and x2, y2 are the termination points of the exponential curve.

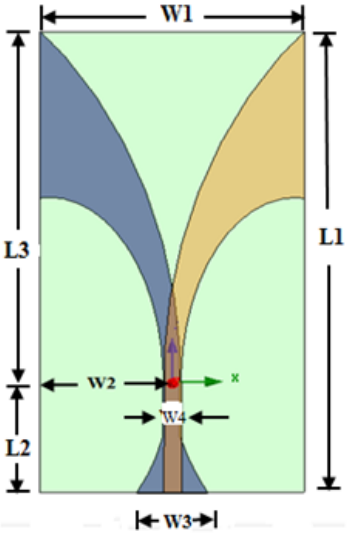

Figure 3. Structure of CAVA

The dimensions of the CAVA are calculated to have an optimized response over the desired bandwidth and they are found to be as follows: L1= 22.60 mm, L2 = 5.50 mm, L3= 17.1 mm, W1= 15.8 mm, W2= 7.2 mm, W3= 4.2 mm. The width of the microstrip feedline (W4) is calculated to match the characteristic impedance of 50 ohm which comes out to be W4= 1.25 mm. The radiating structure of the antenna is formed from the intersection of quarters of two ellipses, as explained in [29].

Figure 4 depicts the S11 response for the CAVA. From the curve, it can be seen that the designed CAVA resonates below -10 dB in the range of 10.8 GHz to more than 25 GHz.

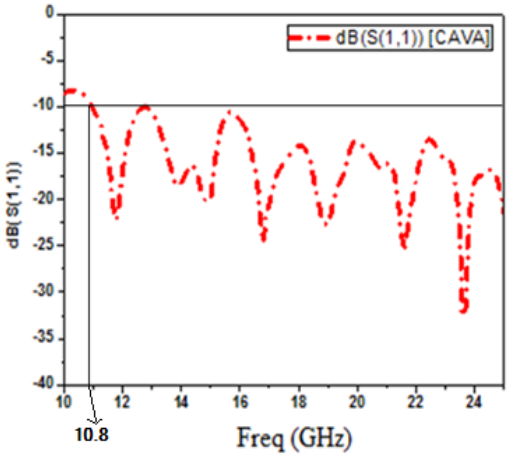

Figure 4. Frequency response of CAVA

Figure 5 shows the gain for the conventional AVA (CAVA). It is evident from Figure 4 that CAVA achieves low values of gain mainly at lower frequencies with maximum gain of 5.8 dBi only towards higher frequency.

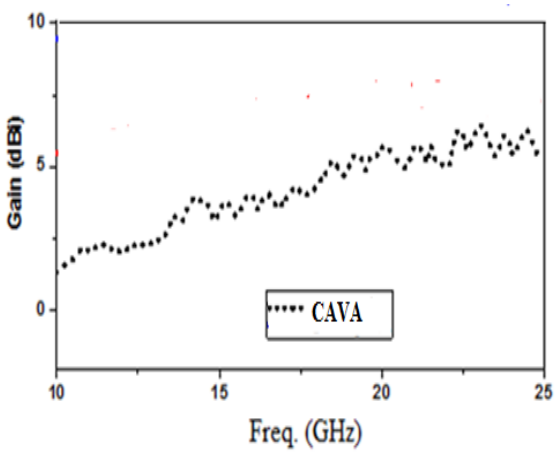

Figure 5. Gain plot of CAVA

Since the proposed CAVA dispenses low gain at lower frequencies, corrugation can be used to overcome this problem [30]. This will be explained in detail in Section IV.

IV. DESIGN OF CORRUGATED AVA

The low frequency performance of an AVA flare is enriched by the corrugation on its outer edges. Figure 6 depicts the design of the equilateral triangular corrugated AVA with slot side length, S = 0.85 mm.

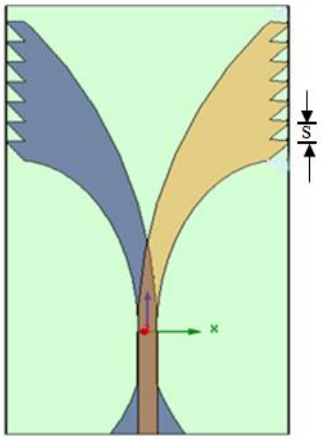

Figure 6. Structure of Corrugated AVA

The simulated S11 response of corrugated AVA is depicted in Figure 11. It can be seen that by adding corrugation, the lower cutoff frequency shifts to 10.3 GHz. The reason behind this shift in frequency is that the slot corrugation facilitates the electrical length of the inner taper profile to be elongated thereby extending the lower end cut-off frequency [31]. Further, the corrugation acts as a high impedance region due to which the maximum surface current remains towards the inner edge of the tapered slot reducing side and backlobe radiation, increasing the gain in boresight direction [32].

To further enhance the gain and improve the radiation characteristics, an array of metamaterial is commonly used on AVA aperture [33]. This will be explained in detail in Section V.

V. DESIGN AND ANALYSIS OF CORRUGATED AVA WITH METAMATERIAL (MTM)

To enhance the gain and characteristics of the proposed Vivaldi antenna, an array of epsilon negative metamaterial (ENG) unit cells is supplemented at its aperture. The proposed 'pi shape (π)' metamaterial is shown in Figure 7. The proposed MTM is placed inside a waveguide with Perfect Magnetic Conductors (PMC) on its top and bottom, Perfect Electric Conductors (PEC) on its side walls and two waveguide ports for excitation [34], as shown in Figure 8. Standard retrieving procedure is followed by using transmission and reflection coefficient of the unit cell, as described in [35], and it is found that the proposed metamaterial unit cell exhibits epsilon negative property, as shown in Figure 9. The optimized dimensions (in mm) of unit cell are as follows: A = 1.6, B= 0.25, C=1.35, D = 0.70.

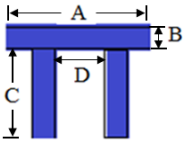

Figure 7. π shape Metamaterial Unit Cell

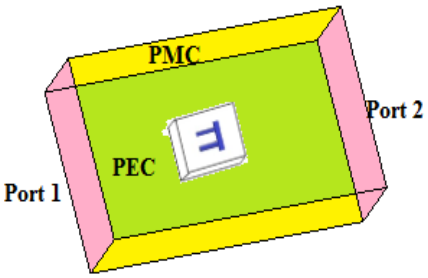

Figure 8. Simulation model of the proposed unit cell

Figure 8 illustrates the ENG behavior of the unit cell with negative relative permittivity property in range of 14 GHz - 18 GHz.

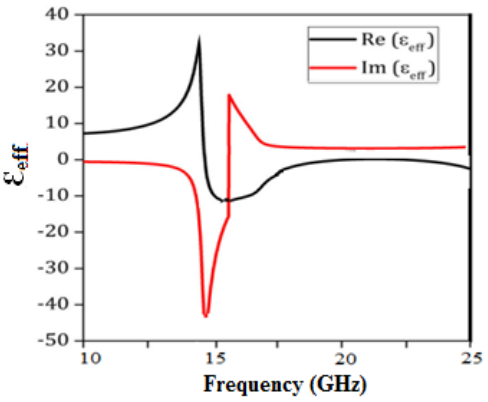

Figure 9. Permittivity graph of ENG unit cell

The MTM array was supplemented to the upper side of the antenna radiating aperture to augment the performance of the corrugated AVA. Using [36] and analyzing by various placements and numbers of the proposed metamaterial cells for the desired frequency range, it was found that the proposed design with six MTM cells at 3-2-1 arrangement (from the top), as shown in Figure 10, attains the preferred bandwidth with better gain radiating maximum energy in the end-fire direction, as will be discussed in Section VI.

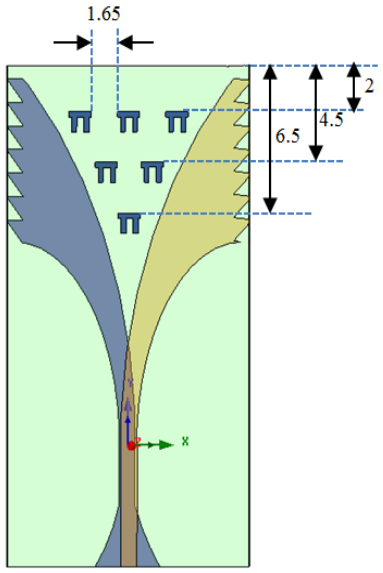

Figure 10. Corrugated AVA with Metamaterial (MTM) unit cells

VI. SIMULATED RESULTS AND DISCUSSION

Figure 11 illustrates the simulated results of reflection coefficient (S11) with frequency for the corrugated AVA and corrugated MTM AVA. As can be noticed from the figure, the reflection coefficient of the corrugated AVA is below -10 dB for the frequency range of 10.3 GHz to 25 GHz. Applying the corrugation technique resulted in extension of the lower end frequency limit due to elongation of inner taper length. The negative index metamaterial further ameliorated the lower cut-off frequency making S11<-10 dB for the entire range from 10 GHz - 25 GHz.

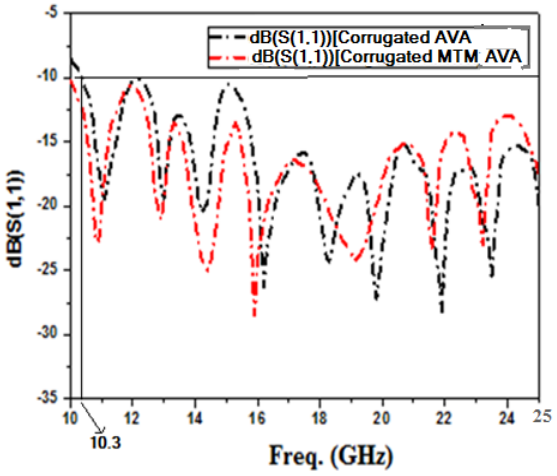

Figure 11. Comparison of Frequency response of Corrugated AVA and Corrugated MTM AVA

Figure 12 depicts the comparison of the gain plot of Corrugated AVA and Corrugated MTM AVA. The Corrugated AVA provides gain in the range of 6.5 dBi - 8.6 dBi, whereas the AVA-M provides the gain in the range of 7.3 dBi – 12.2 dBi with maximum gain achieved at 14.5 GHz. As evident from the gain plot, by integrating corrugation on both side edges of conducting arms, the gain of the proposed antenna increased significantly, especially at the lower end of the operating frequency band. Further, by integrating the metamaterial unit cells structure, the gain enrichment is more pronounced in the mid frequency band. Hence, the peak gain is enhanced by approximately 3.8 dBi in the desired range after inclusion of metamaterial unit cells, which is a significant gain enhancement without changing the antenna size. Also, as observed from Figure 11, the gain is maximum towards the center frequency and drops towards lower and higher frequencies. Since, gain is dependent on the matching, and it is matched at mid-frequency ranges, therefore, it may be getting worse at higher and lower frequency ranges, causing a reduction in gain.

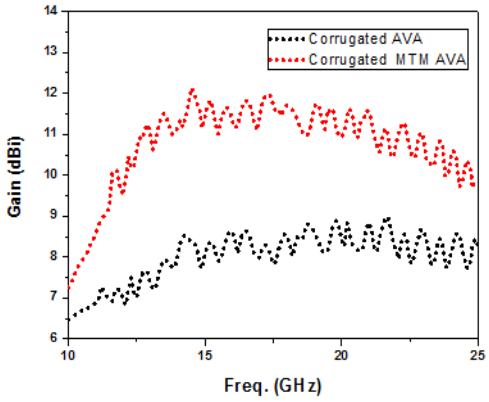

Figure 12. Comparison of Gain of Corrugated AVA and Corrugated MTM AVA

Figure 13 and Figure 14 illustrate the simulated radiation patterns of the corrugated AVA and the proposed MTM antenna on the E-plane and H-plane at 10, 15 and 25 GHz, respectively. It can be seen from the radiation pattern that loaded MTMs result in better directivity with improvement in gain [37] and possess enhanced radiation performance by suppressing the undesired side lobes [38] resulting in low side lobe levels.

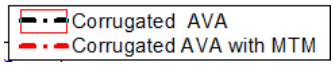

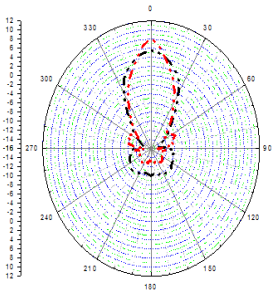

E Plane at 10 GHz

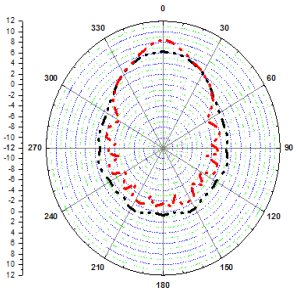

H Plane at 10 GHz

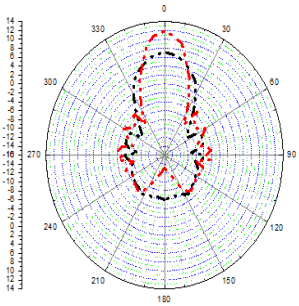

E plane at 15 GHz

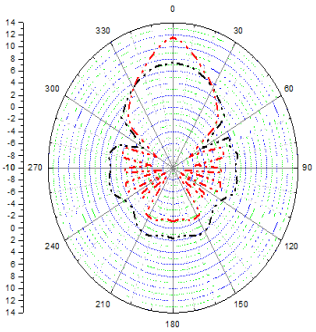

H plane at 15 GHz

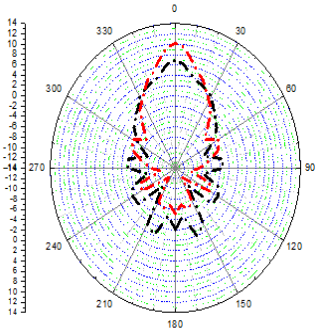

E Plane at 25 GHz

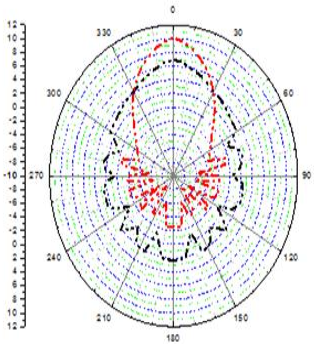

H Plane at 25 GHz

Figure 13. E plane radiation patterns

Figure 14. H plane radiation patterns

Thus, it is evident that the proposed antenna offers higher directivity, but it can be costlier due to the complex fabrication process.

VII. FABRICATION AND MEASURED RESULTS

To substantiate the simulated result as proposed in [1], the antenna is fabricated using substrate material FR4 with the relative dielectric constant of 4.4, tan δ = 0.02, and thickness of 1.6 mm. The antenna is fabricated by photolithographic technique [39]. The fabrication steps for the proposed antenna using photolithography process are briefly summarized: First, a computer aided design of the antenna geometry is made. A negative of this geometry printed on transparent sheet serves as the mask. Thereafter, a negative photo-resist film is laminated to the cleaned and dried copper clad substrate. The masked and photo-resist laminated copper clad substrate is exposed to ultra violet (UV) light. UV exposed photo-resist laminated copper clad substrate is developed. Finally, the developed copper clad substrate is chemically etched by Ferric Chloride FeCl3 solution. Figure 15 (a, b) illustrates the photograph of the top and bottom layer of the fabricated antenna with overall dimensions as 22.60 mm x 15.80 mm.

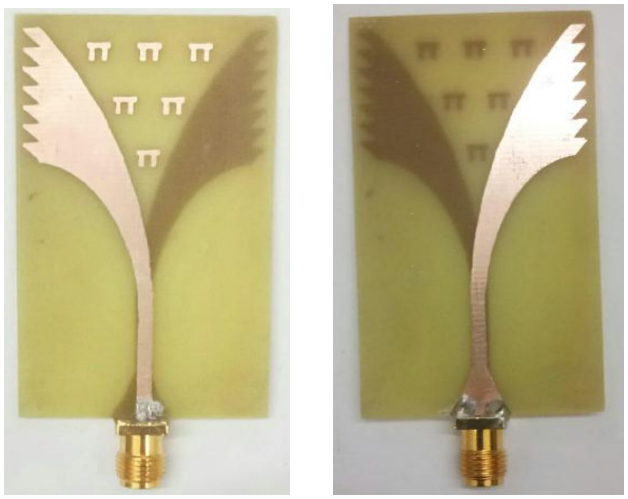

Figure 15. (a) Top (b) Bottom view of the fabricated antenna

Figure 16 depicts the simulated and measured S11 characteristics of the proposed antenna covering the entire band from 10 GHz - 25 GHz. Before carrying the measurement, the VNA (Agilent Fieldfox) was calibrated with a calibration kit with a short, open and loading apparatus, respectively. Subsequently, after the calibration process, the proposed antenna was connected to the VNA, and the S11 parameter results were obtained.

The measured return loss result displays that the proposed fabricated antenna achieves good impedance bandwidth (S11 ≤ −10 dB) from 10 to 25 GHz though there is some decline in measured return loss. The maximum value of S11 lies in mid-range which is -21.4 dB at frequency of 18.2 GHz. The discrepancy between the simulation and measurement may be due to ohmic and substrate loss, surface roughness, and fabrication errors [40] mainly loading of metamaterials that may introduce distortion. Also, insertion loss of SMA connectors may contribute to the discrepancy in simulated and measured result [41]. Also, external disturbances and adjacently placed instruments may also contribute to the error.

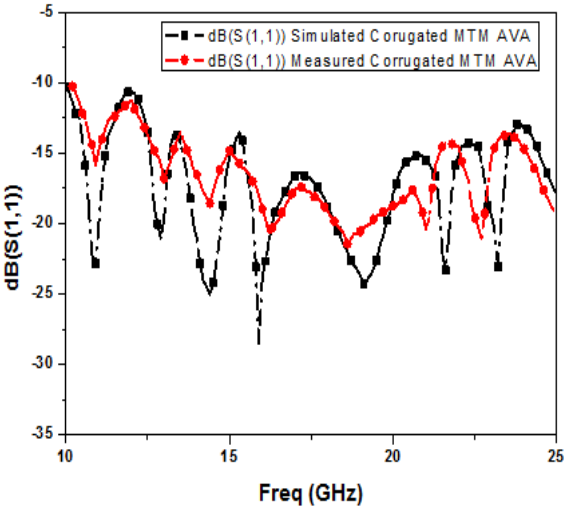

Figure 16. Comparison of Simulated and Measured return loss

Figure 17 depicts the comparison of the simulated and measured gain of the proposed corrugated AVA with novel metamaterial cells. The result shows good matching between the simulated and measured results except some minor loss in the measured result. The gain depends on the impedance matching, and since it is matched at mid frequencies, the match may be getting poorer at the lower and higher frequencies resulting in decline in gain at lower and upper frequency range. The measured gain of the antenna varies between 6.2 dBi – 10.7 dBi over 10 GHz – 25 GHz.

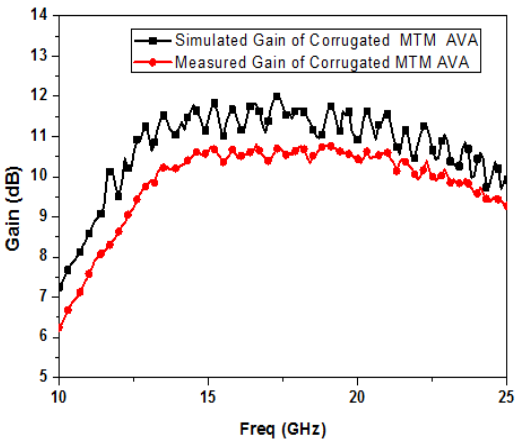

Figure 17. Comparison of simlated and measured Gain

The radiation characteristics of the proposed antenna are measured in the anechoic chamber and are shown in Figure 18. Radiation Patterns [42] are graphical representations of the distribution of radiated energy into space as a function of direction. The radiation pattern has two lobes: the main lobe where the maximum amount of radiated energy exists and the side lobes or minor lobes, where the radiation is distributed in a sideward and backward direction.

.

The AVA antenna which is antenna under test (AUT) and a RF transmitter system are placed at a known distance from the reference antenna. Horn antenna is used as the reference antenna, which is connected to a known receiver. The receiver system is employed to measure the power acquired by the antenna under test. A power meter to calculate the RF power is associated to the test antenna terminals by means of a co-axial cable and connectors. The positioning system is used to adjust the orientation of the AUT. The positioning system rotates the antenna under test and aids in the correct measurement of the AUT radiation pattern as a function of the angle.

Figures 18 and 19 display measured and simulated radiation patterns in the E and H planes at various AVA frequencies (10 GHz, 15 GHz, 25 GHz). As can be observed, the tapered slot's middle axis is where the maximum radiation occurs. Also, for E plane, the gain and HPBW increases with the frequency while for H plane it remains almost similar for various frequencies. As can be seen, the highest gain is in mid frequency range and drops for very low and high frequencies. The figure depicts improved radiation properties of the proposed antenna with high directivity and low sidelobe levels.

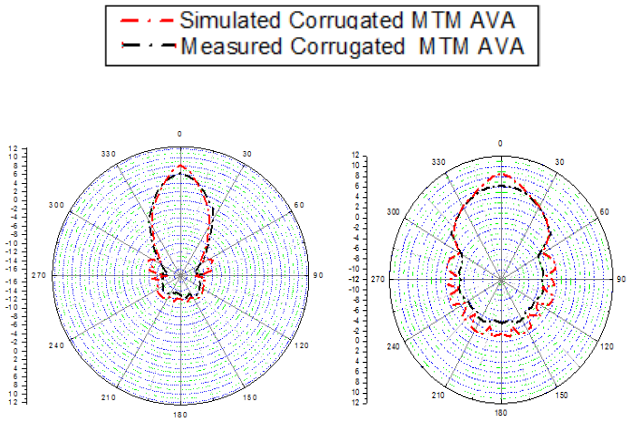

E plane at 10 GHz

H plane at 10 GHz

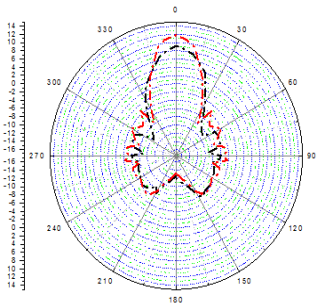

Eplane at 15 GHz

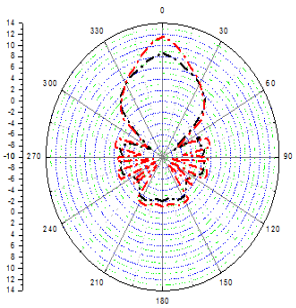

H plane at 15 GHz

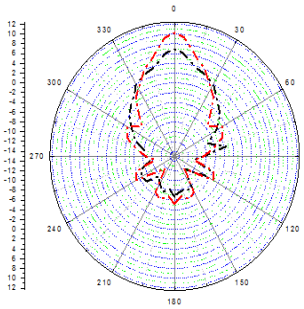

Eplane at 25 GHz

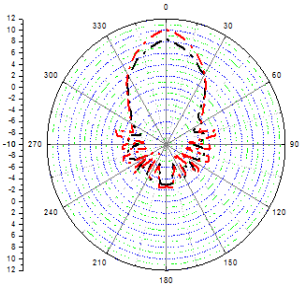

H plane at 25 GHz

Figure 18.Simulated and measured E plane radiation pattern

Figure 19. Simulated and measured H plane radiation patterns

The results from simulation and measurement are in good agreement, except for slight discrepancy at higher frequencies caused by a fabrication error and the influence of the SMA connector on radiation characteristics. Hence, it is evident that the proposed fabricated antenna possesses higher directional properties with high gain.

VIII. CONCLUSION

This paper proposes the analysis design and testing of a high gain corrugated AVA with novel epsilon negative (ENG) metamaterial. The ENG metamaterial enhances the reflection coefficient with a wider bandwidth from 10 to 25 GHz without increasing the size. Further, the proposed corrugated MTM AVA enhances the gain by approximately 3.8 dBi as compared to corrugated AVA in the desired frequency range. In this paper, first a conventional AVA (CAVA) is designed for desired frequency range. Thereafter, triangular corrugation is integrated and corrugated AVA is analyzed. Subsequently, its performance is further enhanced and analyzed by introducing ∏ shaped array of optimally placed metamaterial unit cells. Thereafter, the simulated design is fabricated using photolithography technique and the proposed fabricated antenna is tested for its return loss, gain and radiation pattern. The measured results are then compared with the HFSS simulated results. There is good agreement between simulated and measured results. The maximum gain achieved is approximately 10.7 dBi and antenna possesses high directional properties. As the proposed AVA design provides enhanced gain, improved return loss and compactness, it can be considered as a suitable candidate for satellite transmitter applications.

ACKNOWLEDGMENT

This work was undertaken during the tenure of an "ERCIM (The European Research Consortium for Informatics and Mathematics) Alain Bensoussan Fellowship" programme. Founded in 1988, ERCIM has members from leading European information technology and mathematics research establishments from 18 countries which provide research opportunities to brilliant PhDs from all over the world. Authors would also like to thanks to the microwave laboratory facilities at Fraunhofer Institute of Integrated Circuits (IIS), Germany. Fraunhofer society is the German research organization with 76 institutes spread throughout Germany and is Europe's largest application-oriented research organization.

REFERENCES

[1] N. Muchhal, M. Elkhouly, Y. Fares and R. Z. Vintimilla, "Design of High Gain Corrugated Antipodal Vivaldi Antenna with Π Shaped Metamaterial for SATCOM Applications," in Fifteenth International Conference on Advances in Satellite and Space Communications SPACOMM, April 24 - April 28, 2023, ISBN: 978-1-68558-035-3.

[2] T. Rappaport, "Wireless communications - principles and practice," 2nd Edition., Prentice Hall, 2002, ISBN 10: 0130422320.

[3] A. F. Molisch, “Wireless Communications,” 2nd Edition, John Wiley & Sons Ltd, Wiley-IEEE Press, New York, 2011, ISBN: 978-0-470-74187-0.

[4] M. Donelli, S. Menon and A. Kumar, “Compact Antennas for Modern Communication Systems,” Intl. Journal of Antenna and Propagation, Volume 2020 | Article ID 6903268.

[5] D. Srikar and S. Anuradha, "A Compact Super Wideband Antenna for Wireless Communications," 2018 9th International Conference on Computing, Communication and Networking Technologies (ICCCNT), July 2018, pp. 1-4, DOI: 10.1109/ICCCNT.2018.8494146.

[6] M. S. Elsayed et al., “Compact wide band antenna for millimetric communications,”2021 IOP Conf. Ser.: Mater. Sci. Eng. 1051 012032, DOI : 10.1088/1757-899X/1051/1/012032.

[7] S. H. Son, U. H. Park, S. I. Jeon and C. J. Kim, "Mobile antenna system for Ku-band satellite Internet service," 2005 IEEE 61st Vehicular Technology Conference, Stockholm, Sweden, 2005, pp. 234-237, DOI: 10.1109/VETECS.2005.1543285.

[8] R. D. Gaudenzi, C. E. and R. Viola, "Analysis of satellite broadcasting systems for digital television," in IEEE Journal on Selected Areas in Communications, vol. 11, no. 1, pp. 99-110, Jan. 1993, DOI: 10.1109/49.210548.

[9] S. Vaccaro, F. Tiezzi, M. F. Rúa and C. D. G. De Oro, "Ku-Band Low-Profile Rx-only and Tx-Rx antennas for Mobile Satellite Communications," 2010 IEEE International Symposium on Phased Array Systems and Technology, October 2010, pp. 536-542, DOI: 10.1109/ARRAY.2010.5613316.

[10] S. -Y. Qin and W. -J. Zhang, "Design Objectives of Antenna for Satellite Communication VSAT and USAT Earth Station," 2012 Second International Conference on Instrumentation, Measurement, Computer, Communication and Control, February 2012, pp. 635-637, DOI: 10.1109/IMCCC.2012.155.

[11] K. -X. Li, Z. -J. Guo and Z. -C. Hao, "A Multipolarized Planar Phased Array for LEO SATCOM Applications," in IEEE Antennas and Wireless Propagation Letters, vol. 21, no. 11, pp. 2273-2277, Nov. 2022, DOI: 10.1109/LAWP.2022.3185208.

[12] N. Muchhal, M. Elkhouly, K. Blau and S. Srivastava, “Design of Highly Selective Band-pass Filter with Wide Stop-band using Open Stubs and Spurlines for Satellite Communication (SATCOM) Applications,” The Fourteenth International Conference on Advances in Satellite and Space Communications, SPACOMM , April 2022, ISBN: 978-1-61208-939-3.

[13] H. Alsuraisry, W. -J. Lin, I. Huang and T. -W. Huang, "Design of Ka-band Transceiver for Satellite Communication," 2019 IEEE Jordan International Joint Conference on Electrical Engineering and Information Technology (JEEIT), April 2019, pp. 307-310, doi: 10.1109/JEEIT.2019.8717521

[14] P. J. Gibson, "The Vivaldi Aerial," 9th European Microwave Conference, September 1979, pp. 101-105, DOI: 10.1109/EUMA.1979.332681

[15] E. Gazit, “Improved design of the Vivaldi antenna,” IEE Proceedings H-Microwaves, Antennas and Propagation, vol. 135(2), pp. 89–92, 1988, DOI: 10.1049/ip-h-2.1988.0020.

[16] M. Agahi, H. Abiri, and F. Mohajeri, “Investigation of a new idea for antipodal Vivaldi antenna design, ” Int. J. Computer Elec. Eng., vol. 3, no. 2, 2011.

[17] M. Moosazadeh, S. Kharkovsky, and J. T Case, “Microwave and millimetre wave antipodal Vivaldi antenna with trapezoid-shaped dielectric lens for imaging of construction materials,” IET Microwaves, Antennas & Propagation, 10(3), pp. 1–9, 2015, DOI: 10.1049/iet-map.2015.0374.

[18] A. S. Dixit and S. Kumar, “A miniaturized antipodal Vivaldi antenna for 5G communication applications,” 7th international conference on signal processing and integrated networks (SPIN), February 2020 pp. 800 - 803, DOI**:** 10.1109/SPIN 48934.2020.9071075.

[19] X. Zhang, Y. Chen, M. Tian, Liu J, and H. Liu, “A compact wideband antipodal Vivaldi antenna design,” International Journal of RF and Microwave Computer-Aided Engineering, vol. 29, issue 4, April 2019, https://doi.org/10.1002/mmce.21598.

[20] A. S Dixit, S. Kumar, S. Urooj, and S. A. Malibari, “A Highly Compact Antipodal Vivaldi Antenna Array for 5G Millimeter Wave Applications,” Sensors, vol. 21, 2360, 2021, DOI: 10.3390/s21072360.

[21] T. Nassar and T. M. Weller, "A Novel Method for Improving Antipodal Vivaldi Antenna Performance," in IEEE Transactions on Antennas and Propagation, vol. 63, no. 7, pp. 3321-3324, 2015, DOI: 10.1109/TAP.2015.2429749.

[22] H. Emre and A. M. Emre, “High Gain Ultrawide Band Vivaldi Antenna Design for Mini/Micro Satellite Synthetic Aperture Radar Applications,” IEEE 2019 9th International Conference on Recent Advances in Space Technologies (RAST), July 2019, pp. 491-495, DOI: 10.1109/RAST.2019.8767888.

[23] H. Cheng, H. Yang, Y. Li and Y. Chen, "A Compact Vivaldi Antenna with Artificial Material Lens and Sidelobe Suppressor for GPR Applications," IEEE Access, vol. 8, pp. 64056-64063, 2020, DOI: 10.1109/ACCESS.2020.2984010.

[24] H. Sakli, C. Abdelhamid, C. Essid and N. Sakli, "Metamaterial-Based Antenna Performance Enhancement for MIMO System Applications," in IEEE Access, vol. 9, pp. 38546-38556, 2021, DOI: 10.1109/ACCESS.2021.3063630.

[25] H. Attia, O. Siddiqui, L. Yousefi and O. M. Ramahi, "Metamaterial for gain enhancement of printed antennas: Theory, measurements and optimization," 2011 Saudi International Electronics, Communications and Photonics Conference (SIECPC), April 2011, pp. 1-6, DOI: 10.1109/SIECPC.2011.5876888.

[26] J. Shan, A. Xu and J. Lin, "A parametric study of microstrip-fed Vivaldi antenna," 2017 3rd IEEE International Conference on Computer and Communications (ICCC), December 2017, pp. 1099-1103, DOI: 10.1109/CompComm.2017.8322713.

[27] D. H. Schaubert, "Endfire tapered slot antenna characteristics," 1989 Sixth International Conference on Antennas and Propagation, ICAP 89, April 1989, pp. 432-436 INSPEC Accession Number: 3416994.

[28] S. Wang, X. D. Chen and C. G. Parini, "Analysis of Ultra Wideband Antipodal Vivaldi Antenna Design," Loughborough Antennas and Propagation Conference, April 2007, pp. 129-132, DOI: 10.1109/LAPC.2007.367448.

[29] A. M. Abbosh, H. K. Kan, and M.E Bialkowski, “Design of compact directive ultra-wideband antipodal antenna,” Microwave and Optical Technology Letters, vol. 48, issue 12, pp. 2448-2450, Dec. 2006, DOI: 10.1002/mop.21955.

[30] A. S. Dixit and S. Kumar, "A Survey of Performance Enhancement Techniques of Antipodal Vivaldi Antenna," in IEEE Access, vol. 8, pp. 45774-45796, 2020, DOI: 10.1109/ACCESS.2020.2977167.

[31] J. Bai, S. Shi, and D.W. Prather, “Modified compact antipodal Vivaldi antenna for 4–50 GHz UWB application,” IEEE Trans. Microw. Theory Tech, vol. 59(4), pp. 1051–1057, 2011, DOI: 10.1109/TMTT.2011.2113970.

[32] G. K. Pandey and M. K. Meshram, "A printed high gain UWB Vivaldi antenna design using tapered corrugation and grating elements," International Journal of RF and Microwave Computer-Aided Engineering, vol. 25 (7), pp. 610-618, September 2015, DOI: 10.1002/mmce.20899.

[33] A. S. Dixit and S. Kumar, "The enhanced gain and cost-effective antipodal Vivaldi antenna for 5G communication applications," Microwave and Optical Technology Letters, vol. 62 (6), pp. 2365-2374, 2020, DOI: 10.1002/mop.32335.

[34] N. Muchhal, and S. Srivastava, "Compact Substrate Integrated Waveguide Bandpass Filter with S-Shaped Broadside-Coupled Complementary Split Ring Resonators (BC-CSRR)," International Journal of Microwave and Optical Technology (IJMOT), vol. 15, No. 5, pp. 440-448, Sept. 2020, DOI: IJMOT-2020-5-21976.

[35] N. Muchhal, S. Srivastava, and M. Elkhouly, "Analysis and Design of Miniaturized Substrate Integrated Waveguide CSRR Bandpass Filters for Wireless Communication," in Recent Microwave Technologies. London, United Kingdom: IntechOpen, 2022, DOI: 10.5772/intechopen.104733.

[36] M. Guo, R. Qian, Q. Zhang, L. Guo, Z. Yang, and Z.Wang, "High-gain antipodal Vivaldi antenna with metamaterial covers," IET Microwaves, Antennas & Propagation , vol. 13, issue 15, pp. 2654-2660, Sept. 2019, DOI: 10.1049/iet-map.2019.0449.

[37] L Chen, Z Lei, R Yang, J Fan, X Shi. "A broadband artificial material for gain enhancement of antipodal tapered slot antenna," IEEE Trans. Antennas Propag. , vol. 63(1), pp. 395-400, Oct. 2015, DOI: 10.1109/TAP.2014.2365044.

.

[38] M. C. Johnson, S. L. Brunton, N. B. Kundtz and J. N. Kutz, "Sidelobe Canceling for Reconfigurable Holographic Metamaterial Antenna," in IEEE Transactions on Antennas and Propagation, vol. 63, no. 4, pp. 1881-1886, April 2015, DOI: 10.1109/TAP.2015.2399937.

[39] G. K. Reddy, G. U. Bhargava and P. Sridhar, "Fabrication of patch antenna with circular polarization for wireless LAN applications," International Conference on Electrical, Electronics, Communication, Computer, and Optimization Techniques (ICEECCOT), December 2017, pp. 98-102, DOI: 10.1109/ICEECCOT.2017.8284647.

[40] K. Y. Yazdandoost and K. Sato, "Fabrication error in resonant frequency of microstrip antenna," Proceedings of 2001 International Symposium on Micromechatronics and Human Science (Cat. No.01TH8583), September 2001, pp. 41-44, DOI: 10.1109/MHS.2001.965219.

[41] S. K. Dhar, M. S. Sharawi and F. M. Ghannouchi, "Microwave Connector De-Embedding and Antenna Characterization [Education Corner]," in IEEE Antennas and Propagation Magazine, vol. 60, no. 3, pp. 110-117, June 2018, DOI: 10.1109/MAP.2018.2818002.

[42] C. A Balanis, "Antenna theory: Analysis and design," 4th ed. Wiley and Sons (USA), 2016, ISBN: 978-1-118-64206-1.

Finite Memory Arithmetic and the Number Representations on Computing Machines

Pavel Loskot
ZJU-UIUC Institute
Haining, China
e-mail: *pavelloskot@intl.zju.edu.cn*

***Abstract*—Numerical values on computing machines are normally represented as finite-memory data objects. Such values can be mapped to a finite set of integers, so the computing machines effectively perform only the integer arithmetic operations. Consequently, all programs and algorithms implemented on the computing machines can be modeled by Diophantine equations. This is also true for the computations that are performed by analog computers with a limited resolution. In order to study the Diophantine systems, this paper introduces a dual modulo operator to select the subsets of digits in the string representations of machine numbers, which is also useful when the number equality is replaced by a modulo equivalence. Moreover, it is shown that the solutions of Diophantine equations such as the Fermat Last Theorem can be obtained in the domain of integers that are offset by the same constant real value. The Fermat metric is newly introduced to define the distances between integers and other discrete sets of numbers. Finally, a two-dimensional quantization is devised for mixed arithmetic operations to allow the computations to be equivalently performed either between discrete analog values, or between the integer indices. The key claim of this paper is that all practical computing problems can be exactly and completely represented by an integer arithmetic.**

***Keywords*—dual modulo arithmetic; Fermat last theorem; Fermat metric; natural numbers.**

I. Introduction

Numbers are abstract mathematical objects that can also carry a semantic meaning of quantity. The former leads to rich axiomatic algebraic systems, and the latter enables performing arithmetic operations on computing machines. Numerical algorithms generate and transform numerical values by performing various arithmetic and non-arithmetic operations. Since the computing machines have limited resources, they must execute numerical algorithms in a time and memory efficient manner. The computed numerical values are stored as the precisely defined finite size objects in software and hardware, usually referred to as data structures. Consequently, these values cannot directly represent unconstrained real numbers in a mathematical sense, but it requires specifying a mapping from an infinite set of real numbers that are assumed in the definitions of computing problems into a finite set of selected discrete values that can be effectively represented in software and hardware as indicated in Figure 1.

The problem of representing numerical values on computing machines as integers when these values are stored in finite-memory data structures was introduced and examined in [1, SIGNAL'23]. The current paper extends our conference paper by adding more background knowledge, providing more comprehensive literature review as well as by presenting the new results on the quantization of real values and the related mixed arithmetic operations.

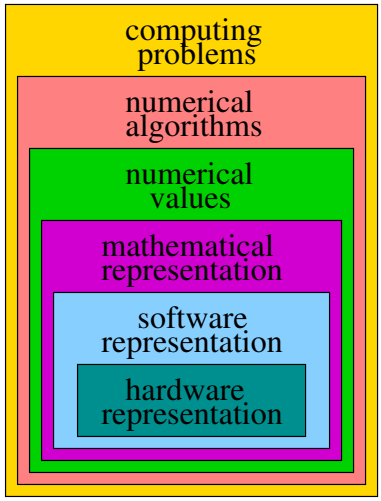

Figure 1. Embedded representations of numbers on computing machines.

Many programming languages used in computing applications such as Fortran, Matlab, Python, Julia and even C define integer and floating point numbers as their native data structures. Some of these languages allow further specifying the number of bytes used for storing the integer values, whether they are stored as signed or unsigned integers, and whether floating point numbers are stored with single or double precision. Furthermore, since the total number of unique values that can be represented by finite size data structures is finite, it limits the largest and the smallest numerical values as well as the precision that can be considered in any given computing application. For example, in Matlab, the functions, realmin, realmax, intmin, intmax and eps can be used to explore what numerical values are actually available to perform the computations.

Majority of real numbers are not computable [2], i.e., there is no algorithm that can express these numbers explicitly with an arbitrary precision (note that the constant π and $\sqrt{2}$ are both computable). On the other hand, a set of integers is said to be computably enumerable, if there exists an algorithm that

eventually lists all the elements in this set, even though such an algorithm may never halt.

Any algorithm described or implemented in any programming language can only compute numbers from a finite set, $\mathcal{N} = \{N_1 < N_2 < \ldots\}$, such that,

$$\forall i: \ -\infty < \inf(\mathcal{N}) \leq N_i \leq \sup(\mathcal{N}) < \infty. \tag{1}$$

Thus, the machine numbers, N_i, and, N_j, can be compared, i.e., ordered, and their smallest difference, $\min_{i\neq j}|N_i - N_j| = \varepsilon_0$, defines the precision. Moreover, the set, $\mathcal{N}$, is necessarily computable [3].

Most computing machines use floating point and fixed point number representations. These representations including the basic arithmetic operations are precisely defined by the IEEE 754 standard [4]. They enable efficient utilization of hardware and software resources to achieve time and space efficiency in implementing and executing the computing algorithms. Universal numbers (unums) were recently introduced as a superset of the IEEE-754 standard. However, their latest version known as posits is no longer the IEEE-754 format compatible, as they were primarily designed to mitigate the hardware constraints in representing the floating point numbers [5]. These modern number representations enable variable-width storage, support the interval (posit) arithmetic, and they also guarantee that the exact result of arithmetic operations is within the defined bounds.

The interval arithmetic assumes that numbers are represented by open or closed intervals rather than typical point values [6]. It then induces corresponding arithmetic operations between such intervals. For instance, if the two numbers have their values within the intervals, $[x_1, x_2]$, and, $[y_1, y_2]$, then their addition and multiplication is defined, respectively, as [7],

$$\begin{aligned} [x_1,x_2] + [y_1,y_2] &= [x_1+y_1, x_2+y_2] \\ [x_1,x_2] \cdot [y_1,y_2] &= [\min(x_1y_1, x_1y_2, x_2y_1, x_2y_2), \\ &\qquad \max(x_1y_1, x_1y_2, x_2y_1, x_2y_2)]. \end{aligned} \tag{2}$$

Similarly, the univariate function values of interval numbers are computed as,

$$f([x_1,x_2]) = [\min(f(x_1), f(x_2)), \max(f(x_1), f(x_2))]. \tag{3}$$

However, the interval arithmetic is not consider further in this paper, although it is an interesting and relevant topic for future investigations.

The multi-precision arithmetic can be implemented recursively by tracking a small number of the most recent digits of the arithmetic operands. Some languages (e.g., Python) support infinite-precision integer arithmetic, or perform the computations at the user-defined precision (e.g., Mathematica). The GNU library [8] is a popular and efficient implementation of the multi-precision arithmetic for integer and floating-point numbers in C programming language. This library is also used in several commercial software products (e.g., Mathematica and Maple). There is another the GNU library that is intended for multiple-precision floating point numbers [9], and another similar library for multiple-precision complex numbers [10]. Both these libraries are supported in all major programming languages. They focus on implementing the basic but fast arithmetic operations involving univariate polynomials and interpolations, however, without controlling the rounding of the results. The smallest and the largest integers and single and double precision floating point numbers are defined in the Matlab toolbox Elementary Matrices, and in the C standard libraries limits.h and float.h.

In general, the algorithms described in various programming languages represent the numbers as strings of digits in a given basis. In particular, the number, $N \in \mathcal{N}$, in basis, B, is represented as,

$$\begin{aligned} N &= \sum_{i=i_{\min}}^{i_{\max}} D_i \times B^i \\ &\leftrightarrow \quad D_{i_{\max}} D_{i_{\max}-1} \cdots D_1 D_0 \,.\, D_{-1} \cdots D_{i_{\min}} \end{aligned} \tag{4}$$

where the digits, $D_i \in \{0, 1, \ldots, 9, \mathrm{A}, \mathrm{B}, \mathrm{C}, \ldots B-1\}$, and the orders, $i_{\min} \leq 0 \leq i_{\max}$. Furthermore, it is customary to place a decimal point between the digits, D_0, and, D_{-1}, which divides the digits into an integral and a fractional part, respectively. More importantly, the decimal point has a purely syntactical meaning to align the numbers in the arithmetic operations and comparisons.

In programming and computing applications, the most common bases are decimal ($B = 10$), hexadecimal ($B = 16$), and binary ($B = 2$). However, internally, the numbers are stored much more efficiently in a byte-size oriented basis, i.e., $B = 2^{8\times\#\text{bytes}-1}$, with one bit reserved for a sign to indicate whether the number is negative. The total number of bytes used for each numerical value is usually fixed for different classes (types) of numbers including short and long integers, and single and double precision floating point numbers. The conversions between the string notation and the internal representation are performed automatically by the compiler.

The textbook [4] provides a comprehensive overview of the number systems that are used on computers. The computability of functions of natural numbers is established in [11]. The mismatch between the exact mathematical description and practical implementation of algorithms using the approximate number representations has been studied in [12] including the methods how to mitigate the discrepancies. A construction of the large-scale real numbers, which are suitable for software implementation is considered in [13]. The binary approximations of real-numbers are investigated in [14]. Other representations of real numbers such as binary expansions, Dedekind cuts and Cauchy sequences are compared in [3]. The p-adic number systems allow defining real-numbers as the arithmetic of rational numbers [15]. The logical statements involving comparisons of real-numbers are studied with the help of satisfiability modulo theories in [16]. The article [17] argues that finite precision is often sufficient in many practical engineering applications. The most important number-theoretic theorems and conjectures can be found in [18].

In this paper, it is argued that the number systems commonly used on computers can be assumed to be integer-valued,

which also includes single and double precision floating point numbers and the corresponding arithmetic operations. Consequently, the computing machines are inherently governed by integer algebras and arithmetic. The paper contributions are formulated as three claims, a proposition and several lemmas. In particular, in Section II, dual modulo operator is introduced to select or to discard the digits in the string representations of numbers. It can be exploited to define equivalences between numbers in integer arithmetic. In addition, it is proposed that natural numbers can be offset by a real-valued constant, and still be considered as being integers. The Fermat last theorem (FLT) is studied in Section III as an example of Diophantine equation involving integers. The Fermat metric is newly defined, which is then used to compute the distances between natural numbers, and to cluster natural numbers into subsets. A new Section IV has been added to devise a quantization scheme that supports arithmetic operations. Discussion is provided in Section V, and the paper is concluded in Section VI.

II. Machine Integers and Arithmetic

The key observation is that finite-size data structures can only represent a finite set of numerical values. Constraining machine computations to the numbers, $\mathcal{N}$, has several fundamental consequences. First, the results of arithmetic operations can overflow the limits, $\inf(\mathcal{N})$, or, $\sup(\mathcal{N})$. Second, the results of arithmetic operations can underflow the precision, ε_0, so the results may have to be truncated, rounded, or otherwise approximated. Third, the decimal point to align the numbers can be arbitrarily placed in-between any digits as long as the placement is consistent in the number system and the arithmetic considered. This is formalized in the following claim.

Claim 1. *The machine numbers that are allocated a finite memory space can be uniquely represented by a set, $\mathcal{N}$, which is isomorphic to a finite ordered subset of integers, $\mathcal{Z} \subseteq \mathbb{Z}$.*

The important consequence is that (without a formal proof) any machine arithmetic is isomorphic to the integer arithmetic. However, implementing such a integer arithmetic at large scale and precision to be efficient and also error-free is non-trivial. It raises important questions about how to optimally represent mathematical models on computers under the number representation constraints as well as how to model the underlying computations.

The memory allocated by the compilers of programming languages allows adding only a finite number of digits before and after the decimal point. If the numbers are padded by zero-digits from both ends, the numbers are represented by the strings of the same length, and the decimal point becomes a hypothetical construct. The non-zero digits at the right end of the number string represent the precision (resolution), whereas the first non-zero digits from the left represent the scale.

The algorithms usually contain many logical statements (predicates). These statements involve comparisons of numerical values. Even analog computers can compare numerical values, e.g., against a threshold, only with a certain resolution. In general, any two numerical values can only be compared reliably, if they are represented with an infinite precision. On the other hand, two integers are said to be exactly equal, provided that all digits in their string representations are the same. The exact comparison can be rather restrictive in some applications, where the differences in scale and precision could be or must be tolerated. Specifically, if the differences are tolerated in precision (the right-end sub-strings), it is equivalent to comparing the quantized values. On the other hand, if the differences are tolerated at scale (the left-end sub-strings), it induces the periodicity, and it is equivalent to comparing the periodically repeated values.

Mathematically, removing the right-end or the left-end sub-strings from the string representation of a number can be expressed by a canonical modulo operator. In particular, for any integer a, and any positive integer b, let, $(a \bmod b) = (|a| \bmod b) \in \{0,1,\ldots,b-1\}$, be a reminder after the integer division of a by b. Note that this can be readily extended to the real numbers as, $0 \leq (a \bmod b) = (|a| \bmod b) < b$, assuming the real division of, $a \in \mathcal{R}$, by an integer, b. Then, the numbers, a_1, and, a_2, are said to be equivalent in the sense of congruence, provided that, $a_1 \equiv a_2 \ (\bmod b)$. Both equality (indicated by the symbol, $=$) and equivalence (indicated by the symbol, $\equiv$) satisfy the axiomatic properties of reflexivity, symmetry, and transitivity, and the equality implies the equivalence. Moreover, if the two numbers are not congruent after comparing their modulo values, then these numbers are not equal even without using modulo operator.

If the machine numbers, $N_i = \sum_{i=0}^{L-1} D_i B^i$, are represented by the strings of L digits in some basis B, then the first L_1 digits and the last L_2 digits, $(L_1 + L_2) < L$, can be zeroed by applying a dual modulo operator, which is introduced next.

Definition 1. *The dual modulo operator has two parameters, m_1, and, m_2, and it is defined as the difference,*

$$\begin{aligned} N_i \ \mathrm{Mod}(m_1, m_2) &= (N_i \bmod m_1) - (N_i \bmod m_2) \\ &= \underbrace{0\cdots0}_{L_1} D_{L-L_1-1} \cdots D_{L_2+1} D_{L_2} \underbrace{0\cdots0}_{L_2}. \end{aligned} \tag{5}$$

where $m_1 = B^{L-L_1}$, and $m_2 = B^{L_2}$.

It should be noted that representing the numbers in different bases does not change their semantic meaning. There is a one-to-one mapping between different representations, so they are mathematically equivalent. However, they are not equivalent in the string operations.

The modular arithmetic with dual modulo operator has similar properties as the arithmetic involving canonical modulo operator. In particular, given the integers, a, b, m_1, and m_2, then,

$$\begin{aligned} a \ \mathrm{Mod}(0, m_2) &= a - (a \bmod m_2) \\ a \ \mathrm{Mod}(m_1, 1) &= a \bmod m_1 \\ a \ \mathrm{Mod}(m_1, m_1) &= 0. \end{aligned} \tag{6}$$

Furthermore, it is straightforward to prove that,

$$\begin{aligned} a+b &\equiv a \text{ Mod}(m_1,m_2)+b \text{ Mod}(m_1,m_2) \text{ (Mod}(m_1,m_2)) \\ a-b &\equiv a \text{ Mod}(m_1,m_2)-b \text{ Mod}(m_1,m_2) \text{ (Mod}(m_1,m_2)) \\ a\cdot b &\equiv a \text{ Mod}(m_1,m_2)\cdot b \text{ Mod}(m_1,m_2) \text{ (Mod}(m_1,m_2)). \end{aligned} \tag{7}$$

However, in general, assuming the integer division with a reminder, one has,

$$a/b \not\equiv a \text{ Mod}(m_1,m_2)/b \text{ Mod}(m_1,m_2) \text{ (Mod}(m_1,m_2)). \tag{8}$$

The Chinese reminder theorem [18] can be restated for the dual modulo operator as follows. If m_{11} and m_{12} are co-prime, and,

$$\begin{aligned} N_i &\equiv a_1 \text{ (Mod}(m_{11},m_2)) \\ N_i &\equiv a_2 \text{ (Mod}(m_{12},m_2)) \end{aligned} \tag{9}$$

for some integers, N_i, and, m_2, then there is a unique integer, a, such that,

$$N_i \equiv a \text{ (Mod}(m_{11}m_{12},m_2)). \tag{10}$$

The proof is based on the property that, if $N_i \equiv a \pmod{m_1}$, then also, $N_i \equiv a$ (Mod(m_1,m_2)).

It is useful to consider how the machine integers used in algorithms are the approximations of infinite precision real-numbers that are normally obtained from the mathematical analysis. The dual modulo operator defined in (5) produces a finite-length integer, x Mod(m_1,m_2), from a real number, $x \in \mathcal{R}$. This introduces a periodicity due to truncation from the left (specified by the parameter, m_1), and the quantization due to truncation from the right (specified by the parameter, m_2).

Furthermore, define countably infinite integer sets,

$$\tilde{\mathbb{N}}_x = \{x, x+1, x+2, \ldots\} \tag{11}$$

which are parameterized by a finite real-valued constant, $x \in \mathcal{R}$, so that, $\tilde{\mathbb{N}}_0$, is the set of natural numbers. Such integer sets can provide the exact solutions to some integer (Diophantine) problems, which otherwise do not have any such a solution. More importantly, for all finite x, the integers, $\tilde{\mathbb{N}}_x$, satisfy Peano axioms except the first one, i.e., that the first element in the integer set represents a zero [18]. Peano arithmetic includes both addition and multiplication, and it is known to be incomplete and undecidable whilst its consistency cannot be proven as can be shown by the Gödel's incompleteness theorems. However, when multiplication is dropped, Peano arithmetic becomes Presburger arithmetic, which is consistent, complete and decidable. More importantly, both Peano as well as much weaker Presburger arithmetic can be used to define the set of natural integers.

III. Case Study: FLT Problems

The FLT is the most famous special case of a Diophantine equation. It is considered here for illustration of the effects of the number representations used on computing machines. The FLT states that there are no positive integers a, b, c, and $n > 2$, such that,

$$a^n + b^n = c^n. \tag{12}$$

This has been first verified numerically on computers for very large exponents until a formal mathematical proof was established only recently [18]. It is straightforward to show that the case of coefficients, a, b, and c being rational numbers (i.e., they are expressed as the integer fractions) is only a special case of the more general FLT. This is also the case when the exponent, n, is a rational number, and so neither this special case have any solution among the integer coefficients. Specifically, if $n = m/(m+k)$, where m and k are integers, $k \neq -m$, we get, $a^k + b^k = (ab/c)^k$, i.e., a special case of the FLT. Interestingly, the FLT can be equivalently rewritten as a condition for the arithmetic average of the integer products, i.e.,

$$a^n b^n c^n = \frac{1}{2}\left((a^n+1)(b^n+1)(c^n-1)+(a^n-1)(b^n-1)(c^n+1)\right). \tag{13}$$

Another equivalent formulation of the FLT involves the infinite sets, $S_1 = \{a^n + b^n : \ a,b \in \mathbb{N}_0\}$, and, $S_2 = \{c^n : \ c \in \mathbb{N}_0\}$; the FLT then states that the intersection, $S_1 \cap S_2 = \emptyset$ (empty set), for all the exponents, $n > 2$.

In addition, constraining the maximum difference as, $|a^n + b^n - c^n| \leq 1$, has a trivial solution, $a = 1$, and, $b = c$, for $\forall n \geq 1$. Note also that the Fermat Number Transform (FNT) resembles the Discrete Fourier Transform (DFT), however, the former assumes the sums modulo a prime [19].

More importantly, the original formulation of the FLT can be modified as follows to allow the solutions to exist.

Claim 2. *For every n, there exist infinitely many natural integers a, b, c, m_1 and m_2 satisfying the congruence,*

$$a^n + b^n \equiv c^n \text{ (Mod}(m_1,m_2)). \tag{14}$$

For example, assuming the first 100 natural numbers represented as the strings of $l = 9$ digits in the basis, $B = 8$, and, $B = 10$, respectively, the total number of solutions, n_l, and, n_r, of (14), for the first l_1 digits, and for the last $l_2 = l - l_1$ digits is given in Table I. We can observe that, always, $n_\text{l} > n_\text{r}$, since the number strings often contain zeros at the left end in order to make up the given string width, l.

TABLE I. The number of solutions of (14) among the first 100 integers

	$B=8$				$B=10$			
	$n=3$		$n=4$		$n=3$		$n=4$	
(l_1,l_2)	(3,6)	(4,5)	(3,6)	(4,5)	(3,6)	(4,5)	(3,6)	(4,5)
n_l	69627	22278	5505	2318	1284	44532	10666	3622
n_r	212	644	730	2076	198	207	230	596

The following FLT formulation utilizes the integers with a fixed offset that were defined in (11).

Claim 3. *For any integer exponent, $n \geq 1$, the equation,*

$$a^n + b^n = c^n \tag{15}$$

has infinitely many solutions among the integers, $a,b,c \in \cup_x \tilde{\mathbb{N}}_x$, for specific real-values, $x > 0$.

Proof. Let $c = y \in \mathcal{R}$, $a = y - d_1$, and, $b = y - d_2$, where d_1 and d_2 are the arbitrarily chosen positive natural integers. Then, for any n, the polynomial (15) has at least one real-valued solution, $y > \max(d_1, d_2)$. Let $d_0 = \lfloor y \rfloor$ (floor function), so that $x = (y - d_0) < 1$. This defines the positive integer solution, $c = d_0 + x$, $a = d_0 - d_1 + x$, and $b = d_0 - d_2 + x$, from the integer set, $\tilde{\mathbb{N}}_x$. ■

The Euler's conjecture from the year 1769 states that the n-th power of a positive integer cannot be expressed as a sum of a fewer than n, n-th powers of other integers. This has been disproved in 1966 by finding the counterexample, $27^5 + 84^5 + 110^5 + 133^5 = 144^5$, using a computer search [20]. Another counterexample, $2682440^4 + 15365639^4 + 18796760^4 = 20615673^4$, was obtained in [21] using theoretical methods. More precise formulation of determining the number of m-th power summands is known as the Waring's problem [22]. The further generalization of the Euler-Fermat equation was examined in [23] by assuming a weighted sum of the m-th power summands with the integer weights. Another variation of the Euler's sum was recently considered in [24].

A weaker form of the Euler's conjecture can be stated as follows.

Proposition 1. *For any natural integer, n, there exists an integer, $m \geq n$, such that the expression,*

$$\sum_{i=1}^{m} a_i^n = b^n \tag{16}$$

is satisfied for a set of natural integers, $\{a_1, a_2, \ldots, a_m\} \cup \{b\}$.

The proof of Proposition 1 appears to be rather non-trivial, except when $n = 1$ and $n = 2$ (Pythagorean theorem); the interested readers are referred to [21]–[24] for more in-depth investigations of this problem. However, it is easy to find examples among the smallest integers satisfying expression (16), i.e.,

$$\begin{aligned} 3^2 + 4^2 &= 5^2 \ \ (m = n = 2) \\ 3^3 + 4^3 + 5^3 &= 6^3 \ \ (m = n = 3) \\ 2^4 + 2^4 + 3^4 + 4^4 + 4^4 &= 5^4 \ \ (m = n + 1 = 5) \\ 19^5 + 43^5 + 46^5 + 47^5 + 67^5 &= 72^5 \ \ (m = n = 5). \end{aligned} \tag{17}$$

In general, the sequence, $a^n + b^n$, obtained by enumerating all natural integers, a, and, b, becomes rapidly very sparse as the exponent, n, is increased. Moreover, given n, it is easy to show that the best approximation of $(a^n + b^n)$ by c^n is obtained for, $c = \lfloor (a^n + b^n)^{1/n} \rceil$ (rounding function). It motivates the following distance metric for the pairs of natural integers.

Definition 2. *The Fermat metric for positive numbers, a, and, b, is computed as,*

$$\mathcal{F}_n(a,b) = a^n + b^n - \lfloor (a^n + b^n)^{1/n} \rceil^n \tag{18}$$

where $n = 2, 3, \ldots$ is a natural number, and, $\mathcal{F}_1(a,b) = 0$, for any a and b. The Fermat distance between the numbers, a, and, b, is then the absolute value of the Fermat metric, i.e.,

$$D_n(a,b) = |\mathcal{F}_n(a,b)|. \tag{19}$$

Note that rounding in (18) can be replaced with the floor function or the ceil function to obtain the Fermat metric values that are always positive or always negative, respectively. The floor and ceil functions can be also used to find the largest integer, $c_{\max}$, and the smallest integer, $c_{\min}$, respectively, that are bounded as, $c_{\max}^n < a^n + b^n < c_{\min}^n$, for $n > 2$.

The distributions of the Fermat metric values by enumerating all pairs of natural integers up to 10^5 are shown in Figure 2, for $n = 2$ and $n = 3$, respectively. It can be observed that the Fermat metric values are spread much more evenly for $n = 2$, and these distributions have no obvious symmetry.

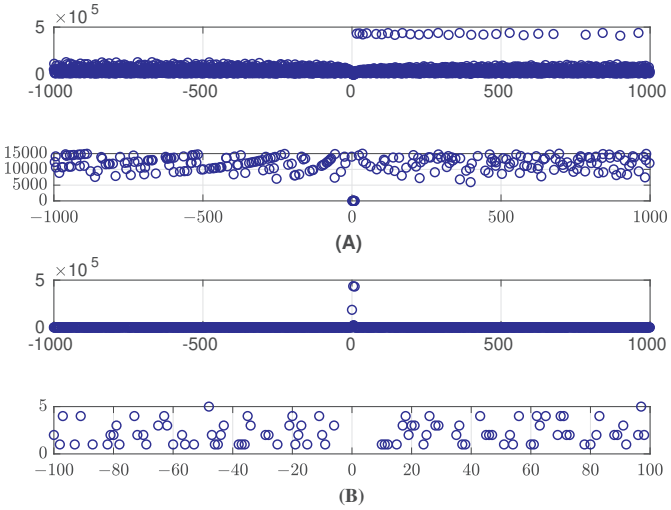

Figure 2. The counts of the Fermat distance values for all pairs of natural integers up to 10^5, and the exponent $n = 2$ (A), and $n = 3$ (B).

The Fermat distance can be used to cluster natural integers into subsets. Figure 3 shows a dendrogram of the Fermat distances, $\mathcal{F}_2(a,b)$. The corresponding assignment of the first 50 natural numbers into the four subsets based on the distances, D_2, D_3, D_4, and D_5 are then shown in Figure 4.

IV. Case Study: Mixed Arithmetic Aided Quantization

The unconstrained real-valued numbers that are used in mathematically defined computing models must be eventually represented as numerical values that are constrained by the representations in software and hardware. As discussed above, the numerical values that are represented as finite-memory data objects can be equivalently considered to represent finite sets of integers. The process of approximating continuous real values by discrete values is referred to as quantization. The normally assumed equidistant quantization levels may become problematic, when the number of quantization levels that can be represented by the finite-size data structures is relatively small. A common solution is to scale-down the real values,

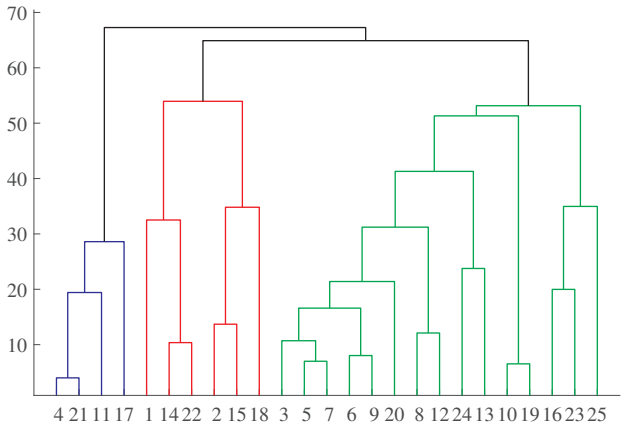

Figure 3. The dendrogram of natural numbers constructed assuming the Fermat distance, $D_2(a,b)$, defined in (19).

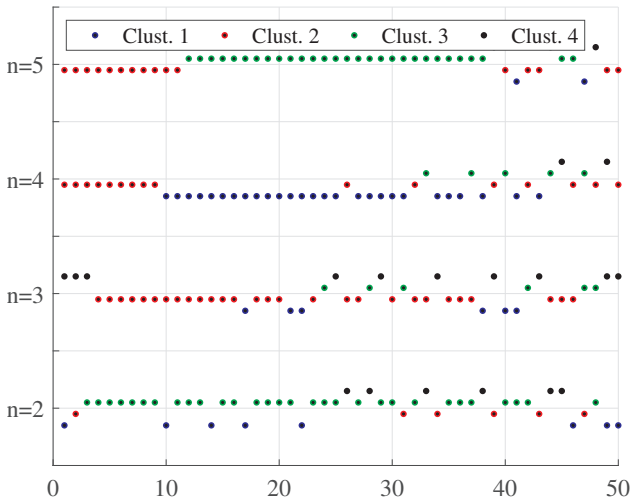

Figure 4. The first 50 natural numbers partitioned into four clusters (subsets) using the Fermat distances, $D_n(a,b)$, for $n = 2,3,4$, and 5.

and to limit these values to a finite-length interval prior to quantization. However, this reduces the resolution as well as the dynamic range that can be represented by the quantized values. Here, we consider designing a quantization scheme that is constrained by the modular and mixed arithmetic in order to obtain a non-uniform quantization with more effective mapping of real numbers to unique positive integers.

In particular, any real number, $v \in \mathcal{R}$, can be expressed as,

$$\begin{aligned} v &= q \cdot w + r, \\ r &= v \bmod w \end{aligned} \tag{20}$$

where the quotient, $q \in \mathbb{Z}$, and, $-w < r < w$, denotes the reminder for the chosen real positive parameter, $w \in \mathcal{R}^+$. Since q can be stored as a signed integer, or it can be completely dropped in some applications, our task is to define the quantization function as the mapping,

$$Q: \ [-w,w] \mapsto \{r_0, r_1, \ldots, r_K\} \tag{21}$$

which maps the reminder, r, to a unique value from the set of $(K+1)$ values, such that,

$$-w \le r_0 < r_1 < \cdots < r_K \le w. \tag{22}$$

It is customary to select the quantized values that minimize the Euclidean distance to the input sample, r, i.e.,

$$r_k = \text{argmin}_{0 \le k \le K} \|r - r_k\|. \tag{23}$$

The quantization levels, r_k, should be defined as an increasing function of the quantization labels, k, i.e., $r_{k_1} < r_{k_2}$, if and only if, $k_1 < k_2$. Furthermore, it is desirable to control the non-uniformity of the quantization levels, and to also compute the index, k, from the quantized value, r_k. These requirements can be satisfied by an n-th order polynomial having a single root with multiplicity, n. Hence, define,

$$r_k = \mathcal{J}_{a,z,n}(k) = a(k+z)^n \tag{24}$$

where $a > 0$ and $z \in \mathcal{R}$ are the real constants. Note that the function, $\mathcal{J}_{a,z,n}(k)$, has an even symmetry about the vertical axis at the point, $k = -z$, if k is even, and it has an odd symmetry about the point, $k = -z$, if k is odd. Moreover, for any n, the minimum of $|\mathcal{J}_{a,z,n}|$ occurs at $k = -z$.

In addition, function (24) is invertible, i.e.,

$$k = \mathcal{J}^{(-1)}_{a,z,n}(r_k) = \begin{cases} \pm\sqrt[n]{r_k/a} - z, & r_k > 0, \ n - \text{even} \\ \sqrt[n]{r_k/a} - z, & n - \text{odd}. \end{cases} \tag{25}$$

More importantly, the quantization can be further constrained to achieve the equivalence between the arithmetic of real quantization values, r_k, and the arithmetic of corresponding quantization indices, k. In particular, provided that,

$$r_{k_1} \bigcirc r_{k_2} = r_{k_3} \tag{26}$$

where $\bigcirc$ denotes a binary arithmetic operation, such as addition, subtraction, multiplication or division, it is required that the corresponding quantization indices satisfy another arithmetic relation (in general, different from the one used for quantization values above), i.e.,

$$k_1 \ \square \ k_2 = k_3. \tag{27}$$

For instance, assuming binary addition for both the quantized values and the corresponding quantization indices, it is required that,

$$\begin{aligned} r_{k_1} + r_{k_2} &= r_{k_3} \\ \mathcal{J}_{a,z,n}(k_1) + \mathcal{J}_{a,z,n}(k_2) &= \mathcal{J}_{a,z,n}(k_3) \\ a(k_1+z)^n + a(k_2+z)^n &= a(k_3+z)^n. \end{aligned} \tag{28}$$

The solution of (28) is formalized by the following lemma.

Lemma 1. *For any integers, $k_1, k_2, k_3 \in \mathbb{Z}$, eq. (28) has exactly one real solution in z, if n is odd, and there are exactly two real solutions, when n is even.*

Proof. For addition, the multiplicative constant, $a > 0$, can be eliminated, and we need to solve, $(k_1+z)^n + (k_2+z)^n = (k_3+z)^n$, for z. The function, $\mathcal{J}_{a,z,n}(k)$, defined in (24) is strictly convex for n being even, and non-negative for any k and z. The

sum of convex functions remains convex [25]. The minimum of the left-hand side addition occurs for $z = -(k_1 + k_2)/2$, which is independent of n. It is then straightforward to show that any two convex functions, which have an unlimited support intersect at exactly two points. On the other hand, the function, $\mathcal{J}_{a,z,n}(k)$, for n-odd, is strictly increasing everywhere, and there is exactly one point where two such functions with an infinite support intersect. The solution can be obtained in a closed form for $n \leq 3$, otherwise it can be computed numerically. ■

Note that the scaling by a used in (28) affects numerical accuracy of the solution, especially for larger values of n. Moreover, $z = -k_2$ is the solution of (28), if and only if, $k_1 = k_3$, for any exponent, n. In addition, provided that the quantization values were defined as, $\mathcal{J}_{a,z,n} = k^n - b$, where $b \in \mathbb{Z}$, then eq. (28) becomes, $k_1^n + k_2^n = k_3^n + b$, and it can be satisfied for any integer coefficients k_1, k_2 and k_3, by appropriate choice of b.

Assuming multiplication instead of summation in (28), we need to solve,

$$a^2(k_1 + z)^n(k_2 + z)^n = a(k_3 + z)^n \tag{29}$$

for z, which is formalized by the next lemma.

Lemma 2. *For any integers, $k_1, k_2, k_3 \in \mathbb{Z}$, eq.* (29) *has exactly two real solutions,*

$$z = \frac{1}{2a}\Big(1 - ak_1 - ak_2 \pm \sqrt{(1 - ak_1 - ak_2)^2 - 4(ak_1ak_2 - ak_3)}\Big) \tag{30}$$

provided that, $(1 - ak_1 - ak_2)^2 > 4(ak_1ak_2 - ak_3)$, and n is odd. If n is even, there are two more solutions,

$$z = \frac{-1}{2a}\Big(1 + ak_1 + ak_2 \pm \sqrt{(1 + ak_1 + ak_2)^2 - 4(ak_1ak_2 + ak_3)}\Big) \tag{31}$$

provided that, $(1 + ak_1 + ak_2)^2 > 4(ak_1ak_2 + ak_3)$.

Proof. Eq. (29) can be converted to a quadratic equation, for which the solution is well known. ■

The properties stated in Lemma 1 and Lemma 2 can be exploited to define the mixed arithmetic, such that binary computations between analog quantized values can be equivalently performed as binary computations between the corresponding discrete indices as illustrated in Figure 5. It may be desirable, but not necessary to assume that the same binary operation is used in both the analog and the digital domains. For example, the quantization levels can be defined, so that the sum, $r_1 + r_2 = r_3$, in the analog domain is fully equivalent to computing the sum, $k_1 + k_2 = k_3$, in the discrete domain. This is formalized by the following lemma.

Lemma 3. *Consider a binary arithmetic operation, $k_3 = k_1 \square\ k_2$, such as addition, subtraction, multiplication, or division. Then, for any two integers k_1 and k_2 from the set, $\{0, 1, 2, \ldots, K\}$, and a given exponent, n, there exist, $z \in \mathcal{R}$, and, $a \in \mathcal{R}^+$, so that, a binary computation, $\mathcal{J}_{a,z,n}(k_1) \bigcirc \mathcal{J}_{a,z,n}(k_2) = \mathcal{J}_{a,z,n}(k_3)$, is exact, where the function, $\mathcal{J}_{a,z,n}$, has been defined in* (24).

Proof. The key result for addition and multiplication has been proven in Lemma 1 and Lemma 2, respectively. However, now, the proof is further constrained by requiring that $k_3 = k_1 \square\ k_2$. The cases of subtraction and division can be converted to addition and multiplication, respectively; for the latter, one should consider, $k_3 = k_1/(1 + k_2)$, in order to avoid division by zero, when $k_2 = 0$. ■

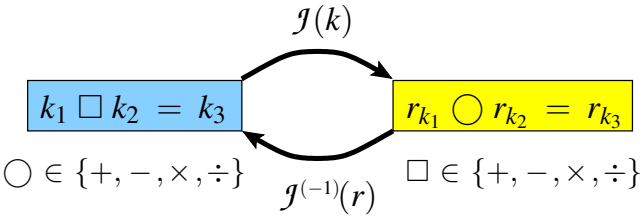

Figure 5. Binary computations for discrete indices (on the left) can be uniquely mapped to binary computations between the corresponding quantized values (on the right).

In practice, it is useful to compute a look-up table of z values that are indexed by the integer tuples, (k_1, k_2) as shown in Table II and Table III assuming binary operations of addition and multiplication, respectively. For example, if $k_1 = 1$ and $k_2 = 3$, then $k_3 = 1 + 3 = 4$, and we can numerically compute, $z \doteq 5.01$; then, $a(k_1 + z)^3 \doteq 435.78$, $a(k_2 + z)^3 \doteq 1030.72$, and $a(k_3 + z)^3 \doteq 1466.50 = 435.78 + 1030.72$. This calculation can be verified for all other rows in Table II and Table III.

More importantly, the quantization levels generated by function (24) are symmetric as shown in the next lemma. This can be used to calculate the quantized values also for negative indices.

Lemma 4. *The addition of quantized values has the following symmetry:*

$$\mathcal{J}_{a,-z,n}(-k_1) + \mathcal{J}_{a,-z,n}(-k_2) = \begin{cases} \mathcal{J}_{a,z,n}(k_1) + \mathcal{J}_{a,z,n}(k_2), & n - even \\ -\mathcal{J}_{a,z,n}(k_1) - \mathcal{J}_{a,z,n}(k_2), & n - odd. \end{cases} \tag{32}$$

Proof. The property is a direct consequence of the even or odd symmetry of function $\mathcal{J}_{a,z,n}$ defined in (24), for n being even or odd, respectively. ■

It should be emphasized that the calculated values of z are functions of the indices k_1 and k_2 as well as of the binary operations considered. The real-valued offsets, z, of the integer indices in the analog domain are necessary in order to enable a one-to-one mapping between the binary calculations in the discrete and the analog domains, respectively. Consequently, such a mapping defines a two-dimensional non-uniform vector quantization as indicated in Figure 6 assuming the examples

TABLE II. The index addition, $k_1 + k_2$, corresponding to the analog summation, $r_1 + r_2 = \mathcal{J}_z(k_1) + \mathcal{J}_z(k_2)$, for $a = 2.0$ and $n = 3$

k_1	k_2	r_1	r_2	$r_1 + r_2$	z
0	0	0	0	0	0
0	1	0.00	2.00	2.00	0.00
0	2	−0.00	16.00	16.00	−0.00
0	3	−0.00	54.00	54.00	−0.00
1	0	2.00	0.00	2.00	0.00
1	1	113.89	113.89	227.79	2.84
1	2	258.27	443.89	702.16	4.05
1	3	435.78	1030.72	1466.50	5.01
2	0	16.00	−0.00	16.00	−0.00
2	1	443.89	258.27	702.16	4.05
2	2	911.16	911.16	1822.32	5.69
2	3	1453.61	1994.59	3448.20	6.99
3	0	54.00	−0.00	54.00	−0.00
3	1	1030.72	435.78	1466.50	5.01
3	2	1994.59	1453.61	3448.20	6.99
3	3	3075.17	3075.17	6150.34	8.54

TABLE III. The index multiplication, $k_1 \cdot k_2$, corresponding to the analog multiplication, $r_1 \cdot r_2 = \mathcal{J}_z(k_1) \cdot \mathcal{J}_z(k_2)$, when $a = 2.0$ and $n = 3$

k_1	k_2	r_1	r_2	$r_1 \cdot r_2$	z
0	0	1.00	1.00	1.00	+0.79
0	1	−0.01	1.22	−0.01	−0.15
0	2	−0.00	16.00	−0.00	−0.00
0	3	−0.00	54.00	−0.00	−0.00
1	0	1.22	−0.01	−0.01	−0.15
1	1	1.00	1.00	1.00	−0.20
1	2	1.00	11.54	11.54	−0.20
1	3	1.00	43.60	43.60	−0.20
2	0	16.00	−0.00	−0.00	−0.00
2	1	11.54	1.00	11.54	−0.20
2	2	10.13	10.13	102.77	−0.28
2	3	9.51	38.56	366.81	−0.31
3	0	54.00	−0.00	−0.00	−0.00
3	1	43.60	1.00	43.60	−0.20
3	2	38.56	9.51	366.81	−0.31
3	3	35.75	35.75	1278.73	−0.38

in Table II and Table III. For $n = 1$, the quantized values are spaced uniformly, and they become more expanded when n is increased. The quantization values can be also scaled by adjusting the parameter, a.

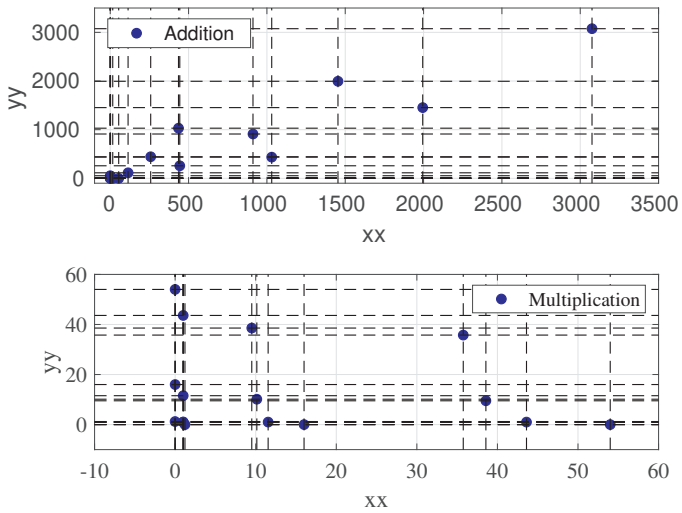

Figure 6. A two-dimensional vector quantization levels for the examples in Table II and Table III.

V. Discussion

The main claim of this paper is that all numerical values that are represented by the finite-memory data structures on any computing machine can be considered to be integers. It is a mathematical property, which is unaffected how the values are actually stored in software and hardware, e.g., using the fixed point or floating point number representations. This has a number of fundamental consequences. In particular, mathematical models on computing machines can be represented by systems of Diophantine equations. These equations have been studied extensively in the literature, and there is a rich mathematical theory available to understand their properties.

It may be claimed that any computer program or algorithm implemented in actual software and hardware can be modeled as a generator of the integer sequences. The integer sequences, in turn, can be generated by multivariate polynomials with the integer coefficients and integer variables. Such integers are then referred to as Diophantine sets; these sets are computably enumerable by Diophantine polynomials (the MRDP theorem). Unfortunately, there is no algorithm that could find the integer roots of general polynomials in several variables with the integer coefficients, or just to determine, if such a solution might even exist. Hence, there is a large gap between mathematical description based on the real analysis, and the actual implementation of algorithms on the computers [12].

Furthermore, once the numbers on computing machines are considered to be integers, the meaning of decimal point becomes mainly syntactical to allow aligning the operands in arithmetic operations. Improving the accuracy of machine numbers by p-adic representations [15] and by Diophantine approximations [26] is impractical, since the corresponding arithmetic operations would require more time and consume more memory. There are several efficient multi-precision arithmetic C-libraries that are available as open-source. Crucially, in many practical applications, the finite accuracy is often sufficient [17]. There are, however, scenarios when the full accuracy is required, for example, in cryptography [27].

The FLT was considered as an example of a Diophantine equation. Several modifications of the FLT were considered to allow the solutions to exist, and to explore how the different number representations affect the solution. Exchanging the numbers equality for their modulo equivalence immediately provides many solutions for the FLT, and likely for other Diophantine problems. The number congruence defined by a newly introduced double modulo operator induces periodicity, when the number is cut-off from the left, and it induces quantization, when the number is cut-off from the right. Whereas quantization problems have been studied extensively, it would be very useful to identify the scenarios where the induced periodicity is not only acceptable, but also useful, for example, to increase the range of the numerical values that can be considered.

Another promising strategy for solving Diophantine equations is to offset all the integers by a constant real value. This strategy can provide a solution for the roots of at lest some

multivariate Diophantine polynomials including the FLT. The proof was presented for the FLT, but it is likely also feasible for more general cases. The caveat is that the offsetted integers break down the validity of arithmetic operations, unless the offset is determined for each pair of numbers involved in the specific arithmetic operation. The offsetted integers can be exploited to define the mixed arithmetic aided quantization, so that arithmetic operations can be performed either in the analog domain, or equivalently, in the discrete domain for the integer indices. This was achieved by assuming a simple exponential function mapping the integer indices to the discrete real values, which can be also used for quantization. Other functions could be considered for other binary arithmetic operations and even more complex computations.

The future work can define and prove other mathematical properties of the machine numbers and the associated integer arithmetic. It can lead to more efficient design of integer-based models and architectures for large-scale computing machines as well as the improved approximations of complex mathematical models. The focus should be on transforming mathematical models using unconstrained numerical values to their constrained representations on the computing machines with limited resources. The interval arithmetic, which was briefly mentioned, but otherwise not considered, could be developed further towards this goal. Moreover, the rich theory involving integer sets including Diophantine equations, ordinal and cardinal arithmetic could be utilized to more formally describe the key characteristics of computing systems as the integer processing machines. There are also many fundamental theoretical results that can be adopted for the integer representations of computer programs, which are provided by Presburger and Peano arithmetic, interval arithmetic, and the Gödel's incompleteness theorems.

VI. Conclusion

The paper investigated the problem of representing the numerical values on computing machines as the finite-memory data objects. Such numbers can be then treated as integers. The other key ideas introduced in the paper were defining the equivalences between the numbers assuming only subsets of digits in their number string representations, and considering the sets of natural numbers offset by the real-valued constants. The dual modulo operator was introduced, which allows removing the most significant and the least significant digits. The basic properties of arithmetic involving the dual modulo operator were presented. The FLT was studied as an example of Diophantine equation. The Fermat metric was introduced to measure the distances between natural numbers as well as to cluster general sets of any numbers. Finally, a two-dimensional non-uniform quantization was introduced to support the mixed arithmetic with binary operations that can be equivalently performed in the analog and the discrete domains.

Acknowledgment

This work was funded by a research grant from Zhejiang University.

References

[1] P. Loskot, "On machine integers and arithmetic," in *Proc. 8th International Conference on Advances in Signal, Image and Video Processing (SIGNAL), Barcelona, Spain*, March 13–17, 2023, pp. 63–66.

[2] T. Rado, "On non-computable functions," *Bell System Technical Journal*, vol. 41, no. 3, pp. 877–884, May 1962.

[3] X. Zheng and R. Rettinger, "Weak computability and representation of reals," *Mathematical Logic Quarterly*, vol. 50, no. 4–5, pp. 431–442, Sep. 2004.

[4] R. T. Kneusel, *Numbers and Computers*, 2nd ed. Springer International Publishing, Cham, Switzerland, 2017.

[5] J. L. Gustafson and I. Yonemoto, "Beating floating point at its own game: Posit arithmetic," *Supercomputing Frontiers and Innovations*, vol. 4, no. 2, pp. 71–86, Jun. 2017.

[6] R. E. Moore, *Methods and Applications of Interval Analysis*. Society for Industrial and Applied Mathematics, Philadelphia, PA, USA, 1979.

[7] T. Hickey, Q. Ju, and M. H. van Emden, "Interval arithmetic: From principles to implementation," *Journal of the ACM*, vol. 48, no. 5, pp. 1038–1068, Sep. 2001.

[8] T. Granlund, "The GNU multiple precision arithmetic library, GNU MP 6.2.1," https://gmplib.org, Jan. 2020, accessed: 2023-01-30.

[9] G. Hanrot, V. Lefévre, P. Pélissier, P. Théveny, and P. Zimmermann, "The GNU floating-point computations with correct rounding library GNU MPFR 4.2.1," https://www.mpfr.org/, Aug. 2023, accessed: 2023-09-30.

[10] A. Enge, M. Gastineau, P. Théveny, and P. Zimmermann, "The GNU multi-precision c library rounding library GNU MPC 1.3.1," https://www.multiprecision.org/mpc/, Dec. 2022, accessed: 2023-09-30.

[11] M. Wrocławski, "Representations of natural numbers and computability of various functions," in *Conference on Computability in Europe*, 2019, pp. 298–309.

[12] R. Krebbers and B. Spitters, "Type classes for efficient exact real arithmetic in Coq," *Logical Methods in Computer Science*, vol. 9, no. 1:01, pp. 1–27, Feb. 2013.

[13] R. O'Connor, "A monadic, functional implementation of real numbers," *Mathematical Structures in Computer Science*, vol. 17, no. 1, pp. 129–159, 2007.

[14] J. van der Hoeven, "Computations with effective real numbers," *Theoretical Computer Science*, vol. 351, pp. 52–60, 2006.

[15] F. Q. Gouvêa, *p-adic Numbers: An Introduction*, 3rd ed. Springer, Cham, Switzerland, 2020.

[16] G. Kremer, F. Corzilius, and E. Ábrahám, "A generalised branch-and-bound approach and its application in SAT modulo nonlinear integer arithmetic," in *Computer Algebra in Scientific Computing*, vol. 9890, 2016, pp. 315–335.

[17] NASA/JPL Edu, "How many decimals of Pi do we really need?" https://www.jpl.nasa.gov/edu/news/2016/3/16/how-many-decimals-of-pi-do-we-really-need, Oct. 2022, accesssed: 2023-01-30.

[18] T. Gowers, J. Barrow-Green, and I. Leader, *The Princeton Companion to Mathematics*. Princeton University Press, Princeton, NJ, USA, 2008.

[19] M. Křížek, , F. Luca, and L. Somer, *17 Lectures on Fermat Numbers: From Number Theory to Geometry*. Springer New York, USA, 2001, ch. Fermat Number Transform and Other Applications, pp. 165–186.

[20] L. J. Lander and T. R. Parkin, "Counterexample to Euler's conjecture on sums of like powers," *Bulletin of AMS*, p. 1079, Nov. 1966.

[21] N. D. Elkies, "On A4+B4+C4=D4," *Mathematics of Computation*, vol. 51, no. 184, pp. 825–835, Oct. 1988.

[22] W. K. Hayman, "Waring's theorem and the super Fermat problem for numbers and functions," *Complex Variables and Elliptic Equations*, vol. 59, pp. 85–90, Jan. 2014.

[23] L. N. Vaserstein and E. R. Wheland, "Vanishing polynomial sums," *Communications in Algebra*, vol. 31, no. 2, pp. 751–772, 2003.

[24] T. Cai and Y. Zhang, "A variety of Euler's sum of powers conjecture," *Czechoslovak Mathematical Journal*, vol. 71, pp. 1099–1113, May 2021.

[25] S. Boyd and L. Vandenberghe, *Convex Optimization*. Cambridge University Press, Cambridge, UK, 2004.

[26] B. Church, "Diophantine approximation and transcendence theory," Apr. 2019, Lecture Notes.

[27] J. Hoffstein, J. Pipher, and J. H. Silverman, *An Introduction to Mathematical Cryptography*, 2nd ed. Springer, New York, NY, USA, 2014.